Aging of cerebellar granule neurons *in vitro*

Dissertation
zur Erlangung des Grades eines Doktors
der Naturwissenschaften
der Fakultät für Biologie
und
der Medizinischen Fakultät
der Eberhard-Karls-Universität Tübingen
vorgelegt
von

Ana Pekanovic
aus Sombor, Serbien

Tübingen im November 2006

Tag der mündlichen Prüfung: 27. Februar 2007

Dekan der Fakultät für Biologie: Prof. Dr. Friedrich Schöffl

Dekan der Medizinischen Fakultät: Prof. Dr. Ingo B. Autenrieth

1. Berichterstatter: Prof./PD Dr. Jörg B. Schulz

2. Berichterstatter: Prof./PD Dr. Ralf Dringen

Prüfungskommission:

Prof./PD Dr. Andreas Luft

Prof./PD Dr. Simone Di Giovanni

Prof./PD Dr. Rejko Krüger

Stipanu i Olgi

DJEVOJČICI UMJESTO IGRAČKE

Ljerko, srce moje, ti si lutka mala,
Pa ne slutiš smisla žalosnih soneta,
Kesteni pred kućom duhu tvom su meta
Još je deset karnevala do tvog bala.

Ti se čudiš, dušo. Smijat si se stala
Ovoj ludoj priči. Tvoja duša sveta
Još ne sniva kako zbore zrela ljeta.
Gledaš me k'o grle. Misliš - to je šala.

Al će doći veče kad ćes, ko Elvira,
Don Huana sita i lažnih kavalira,
Sjetiti se sjetno nježne ove strofe.

Moje će ti ime šapnut moja muza,
A u modrom oku jecati će suza
Ko za mrtvim klovnom iza katastrofe.

Antun Gustav Matoš

Acknowledgements

My years at the Laboratory for Neurodegenerative and Neurorestorative Research have given me a remarkable opportunity to work with and learn from a range of bright and interesting people. This thesis draws upon that background not just for technical issues, but as a standard to live up to.

I would like to thank, first and foremost, my advisor, Prof. Jörg B. Schulz, who let me join his group in the beginning to "learn new techniques and gain skills at the bench" and then as a PhD student. Thanks for the excellent working conditions, for his guidance, positive critics and encouragement throughout my career and during completion of this thesis. At many stages in the course of this research project I benefited from his advice, particularly so when exploring new ideas and hypotheses.

I am also grateful to the members of my committee, Prof. Ralf Dringen and Prof. Olaf Riess for their input and interest in this research.

I would like to thank Prof. Horst Herbert for giving me opportunity to become a PhD student at the International Max Planck Research School for Neural and Behavioural Sciences and for all the support throughout my studies.

My thanks to Dr. Frank Soldner and Dr. Marc Gleichmann for having devoted time to this project, for being always available and enthusiastic to share their knowledge, and for having useful scientific discussions.

I would also like to thank to Dr. Ellen Gerhardt and Dr. Björn Falkenburger for helping me to enrich my knowledge and for creating a pleasant and joyful atmosphere in the lab.

I am grateful to Cathy Ludwig for critical reading of the manuscript.

I would also like to thank...

...

... Marion Schifmann, Caroline Herrmann, Anette Bennemann, and Christiane Fahlbusch for their excellent technical help.

... Daniele Bano for the valuable work on measurements of intracellular calcium concentration in cerebellar granule neurons.

...Anja Schneider for being my companion throughout many long nights in the lab.

...Katarina Trajkovic for having me "for a while" in Göttingen and for her genuine friendship.

...Katiuska Molina-Luna for providing helpful suggestions for improving this manuscript and for being my friend and soul sister.

I am deeply indebted to my brother, Stipan, and to my parents for their endless love and support over the years.

Last but not the least I am grateful to Dietmar for understanding and help to see beyond bad days.

Table of contents

Abbreviations

°C	degree centigrade
ab	antibody
AMPA	a-amino-3-hydroxy -5-methyl-4isoxazole propionic acid
APS	ammonium persulfate
AraC	cytosine arabinoside
BME	Eagle's basal medium
bp	base pairs
BSA	bovine serum albumin
CAD	caspase-activated deoxyribonuclease
CGN	cerebellar granule neurons
CHAPS	3[(3-Cholamidopropyl)dimethylammonio]-propanesulfonic acid
CI1	calpain inhibitor 1
CNS	central nervous system
CSS	control salt solution
ctrl	control
Ac-DEVD-amc	acetyl-Asp-Glu-Val-Asp-amino-4-methylcoumarin
DIV	days *in vitro*
DMSO	dimethylsulfoxide
DNP-hydrazine	2.4-dinitrophenylhydrazine
DTT	dithiothreitol
ECL	enhanced chemiluminescence
EDTA	ethylene diamine tetraacetic acid
FCS	fetal calf serum
FDA	fluorescein diacetate
GAPDH	glyceraldehyde-3-phosphate dehydrogenase
GFAP	glial fibrillary acidic protein
h	hour
HEPES	N-2-hydroxyethylpiperazin-N'-2-ethansulfonic acid
HRP	horseradish peroxidase
KA	kaininc acid
kDa	kilo Dalton
Suc-LLVY-AMC	Succinyl-Leu-Leu-Val-Tyr-7-amido-4-methylcoumarin
M	marker
MW	molecular weight
NBQX	6-nitro 7-sulphamobenzo[f]quinoxaline-2,3-dione
o/n	over night

PAGE	polyacrylamide gel electrophoresis
PARP	poly-(ADP-ribose) polymerase
PBS	phosphate-buffered saline
PFA	paraformaldehyde
PLL	poly-L-lysine
PMSF	phenylmethysulfonylfluoride
ROS	reactive oxygene species
RT	room temperature
SDS	sodium dodecylsulfate
TAE	tris-acetate buffer
TCA	trichloroacetic acid
TCEP	tris(2-carboxyethyl)phosphine hydrochloride
UV	ultra violet
X-gal	5-bromo-4-chloro-3-idolyl beta-D-galactoside
z-VAD-fmk	N-benzyloxycarbonyl-Val-Ala-Asp-fluoromethylketone

1 Introduction

1.1 Definition of aging

In last few decades there has been an increased interest in studying the phenomena of aging. The reasons for this seem clear: the quality of living environment caused by development of technology and medicine has increased human life expectancy.

Aging is a phenomenon that occurs in every living organism and can be defined as a decline of normal physiological functions, being a progressive, deleterious and irreversible process, leading ultimately to death.

1.2 Theories of aging

It is not easy to explain the aging process, because even though aging phenomena is universal, it does not affect all living beings in the same way. Why some animals live longer than others and show fewer signs of aging is still not known. There are many theories trying to explain this process from different points of view. Some of them try to explain it from the population level and others from the molecular level. All of them contain some truth. For this reason there is no universal definition of aging.

Some of the most commonly applied theories of aging are the programmed and error theories of aging.

Programmed theories of aging propose that aging depends on biological clocks regulating the timetable of lifespan through the stages such as development, growth, maturity, and old age: this regulation would depend on the genes that are switched on and off in order to keep the homeostasis during certain stages of life.

The “error” theories propose that insults that are gradually accumulated during a lifespan induce progressive damage at various levels (molecular, cellular, etc.).

There are also other classifications of theories of aging. These classifications are now described below.

1.2.1 Evolutionary theories

Evolutionary theories argue that aging occurs from a decline in natural selection. Because the primarily goal of evolution is to increase reproductive success, longevity is preferred only if it is beneficial for fitness. Life span may have a large degree of plasticity within an individual species as well as among species. The evolutionary theory of aging stems from the observation by J.B.S. Haldane in the 1940s that Huntington's disease (dominant lethal mutation) remained in the population even though it should be strongly selected against. Because this disease has late onset, it allows the carrier to reproduce before developing the symptoms and in this way avoid natural selection. Haldane asked the question: If the Huntington mutation stayed in the population because there is no natural selection for it, what happens with other mutations that occur after the reproductive period of life? The power of natural selection must be very weak. A few theories emerged from this: the mutation accumulation theory, the pleiotropy or trade-off theory and the disposable soma theory. The first predicts that mutations will enter the population according to their mutation rate, and selection will remove them with decreasing efficacy the later their age of onset. The second proposes that the same mutations that are beneficial early in life and later increase the rate of aging are under the effect of natural selection for the beneficial effect, because natural selection affects only the reproductive period of life (Partridge et al., 2002). The disposable soma theory proposes that somatic cells are maintained only to ensure continued reproductive success; after reproduction, soma becomes disposable.

1.2.2 Molecular theories

The gene regulation theory of aging proposes that aging is caused by changes in the expression of genes that regulate both development and aging. Dozens of genes extend adult longevity. Many of these genes are

involved with normal hormone signals, and both these genes and their endocrine systems are conserved among eukaryotes. Thus, insulin-like peptides, insulin-like growth factor (IGF), lipophilic signalling molecules, and sterols are all candidate effectors of aging in organisms as diverse as the nematode *Caenorhabditis elegans*, the fly *Drosophila melanogaster*, and the mouse *Mus musculus*. Suppression of these hormones or their receptors can increase life-span and delay age-dependent functional decline (Tatar et al., 2003).

Codon restriction theory proposes that the accuracy of mRNA translation impairs due to an inability of ribosomes to accurately decode codons in mRNA. Reduced translational activity is an observed age-associated biochemical change in cells **(**Ballesteros et al., 2001**).** Although there is a considerable variability among different tissues and cell types in the extent of decline, the fact is that the bulk protein synthesis slows down during aging (Shikama et al., 1994). The consequences of slower rates of protein synthesis are manifold in the context of aging and age-related pathology. These include decreased availability of enzymes, inefficient removal of intracellular damaged products, inefficient intracellular and intercellular communication, decreased production of hormones and growth factors, decreased production of antibodies, and altered nature of the extracellular matrix. Eukaryotic protein synthesis is a highly complex process which requires a large number of components to function effectively and accurately in order to translate one mRNA molecule while using large quantities of cellular energy. Since the error frequency of amino acid misincorporation in aged organisms is generally considered to be quite high (10^{-3} to 10^{-4}) compared with nucleotide misincorporation, the role of protein error feedback in aging has been a widely discussed issue.

The somatic mutation theory of aging postulates that aging results from the accumulation of mutations in somatic cells, resulting in a failure of the cells either to survive, to proliferate, or to function at complete efficiency (Morley, 1998). The accumulation of mutations, and thus aging, is therefore a stochastic process, although its rate of accumulation can

obviously be influenced by genetic or environmental factors. The theory also conceives that aging is a secondary but inevitable consequence of the more fundamental biological process of mutagenesis.

The error catastrophe theory was proposed by Leslie Orgel in 1963. His hypothesis was that if an error was made in the molecular copying processes (transcription or translation) that result in the synthesis of a given protein(s), the faulty protein could then set off a chain of flawed events which would result in an „error crisis"— a cascade of altered biochemical processes that impair cellular functioning, such as that which occurs in aging. This theory differs from the somatic mutation theory in that it postulates an error in information transfer which occurs at some site other than in the DNA. Generally, errors occurring in proteins are lost by natural turnover and simply replaced with error-free molecules. Error-containing molecules which are involved in the protein-synthesizing machinery, however, would introduce errors into the molecules that they produce. This could result in such an amplification that the subsequent rapid accumulation of error-containing molecules would be an "error-catastrophe" incompatible with normal function and life.

1.2.3 Cellular theories

Wear and tear theory, developed by August Weismann (1834–1914), suggests that the body is damaged by continual use and abuse. It states that toxins in our environment and diet such as excess sugar, caffeine and alcohol, and also physical and emotional stresses cause a degeneration of the organs, tissues and cells of our bodies. The old nineteenth century explanation for aging - the wear and tear that normal living inflicts on us - still sounds perfectly reasonable to many people even today, because this is what happens to most familiar things around them. It seems natural that our body's parts will deteriorate with use.

1.2.3.1 Senescence/telomere theory

Replicative senescence is the progressive decline of the ability of cells to proliferate as an intrinsic property of most normal somatic cell populations

(Campisi, 2001). It is limited to the cells that have ability to divide *in vivo*, and for that reason does not apply to postmitotic cells such as mature muscle cells or neurons. During replicative senescence, cells sense the number of divisions they have completed, not the chronological time. The number of divisions at which a cell population senesces varies depending on the cell type, donor species, age and genotype.

How do cells keep track of the number of doublings they have completed? It is now clear that that telomere shortening is a major mechanism by which cells from humans (Chiu and Harley, 1997) sense their senescence. However, cells from some species, such as mice (they have very long telomeres) probably do not undergo replicative senescence as a consequence of telomere shortening (Wright and Shay, 2000).

Telomeres are special functional complexes at the ends of eukaryotic chromosomes. Linear DNA molecules, such as eukaryotic chromosomal DNAs, require mechanisms besides the conventional DNA polymerases to complete the replication of their ends. This is achieved by the ribonucleoprotein enzyme telomerase, which balances terminal DNA losses by lengthening the ends of eukaryotic telomeric DNA through RNA-templated addition of tandemly repeated telomeric sequences (Blackburn, 2000). Germ cells, immortalized cells and transformed cells express telomerase, which prevents shortening of the telomeres. (Sugihara et al., 1996). With each cell division a small amount of telomeres is lost on each chromosome and if telomerase is not efficient, the cell stops dividing at some point and goes into senescence.

There are other mechanisms that lead cells into senescence, such as oxidative stress, double DNA breaks, expression of certain oncogenes (e.g. activated RAS or RAF), modifications in chromatin structure or changes in energy metabolism (Campisi, 2001).

1.2.3.2 The free radical theory of aging

In 1956, Harman suggested that free radicals produced during respiration cause cumulative oxidative damage, resulting in aging and death. The central nervous system (CNS) is especially sensitive to oxidative stress.

One reason for this is that in humans the brain accounts for twenty percent of the body's oxygen consumption (not proportional to its size compared to other body parts). Another reason is that the brain has less capacity for cellular regeneration than other organs.

Free radicals are highly reactive molecules or atoms that have an unpaired electron in an outer orbital that does not contribute to molecular bonding. Atoms or small molecules that are free radicals tend to be the most unstable, because larger molecules can have the capacity to form resonance structures. Under normal physiological O_2 levels, 1-2% of the O_2 consumed is converted to reactive oxygen species (ROS): for biological systems, oxygen free radicals are the most important, in particular superoxide ($^{\cdot}O_2^-$), nitric oxide ($^{\cdot}NO$) and the hydroxyl radical ($^{\cdot}OH$).

What are the targets of endogenous oxidants? The macromolecules such as nucleic acids, lipids, sugars, and proteins are susceptible to free radical attack. Nucleic acids can get additional base or sugar group, break in a single- and double-strand fashion in the backbone and cross link to other molecules. The most prominent oxidative modification of DNA and RNA bases is formation of 8-hydroxydeoxyguanosine (Sohal et al., 1994a). Lipids form peroxides and aldehydes under oxidative stress conditions, which further affect membrane fluidity and disrupt membrane bound proteins. Protein targets for free radicals are peptide bonds or sidechains. ROS are responsible for deamidation, racemization, and isomerization of protein residues as well as formation of carbonyl groups. These chemical modifications result in protein cleavage, aggregation and/or loss of catalytic and structural function by distorting the proteins secondary and tertiary structure.

In cases of neurodegenerative diseases such as Alzheimer's disease (AD), Parkinson's disease (PD) and amyotrophic lateral sclerosis (ALS), various indices of ROS have been reported within the specific brain region that undergoes selective neurodegeneration. Markers for lipid peroxidation, such as 4-hydroxynonenal (4-HNE) and malondialdehyde (MDA), have been identified in the cortex and hippocampus of patients

with AD, the substantia nigra of patients with PD and in spinal fluid from patients with ALS (Butterfield et al., 2002; Dexter et al., 1989; Pedersen et al., 1998). Protein nitration, a marker of protein oxidation was shown to appear in hippocampus and neocortex in individuals with AD, in Lewy bodies in PD and in motor neurons in ALS patients (Smith et al., 1997; Good et al., 1998; Aoyama et al., 2000).

1.2.3.2.1 Repair of damage

If the production of ROS was the major reason for aging, having better antioxidants and enzymes involved in antioxidative defense (e.g., super oxide dismutase (SOD), catalase (CAT), glutathione peroxidase) should slowdown the aging process and increase life span. However, levels of antioxidants and antioxienzymes in different mammalian species appear to be constant. This relationship has been explained by considering the concentrations of antioxidants and antioxienzymes relative to specific metabolic rate rather than absolute concentrations (Cutler, 1985). Nevertheless, the antioxidant systems display reduced activity in the regions of the brain affected by AD, for example (Pappolla et al., 1992).

In order to rid itself of modified proteins, the cell has a powerful machinery to recognize these proteins, then destroy and recycle them. All intracellular proteins undergo continuous synthesis and degradation. The rates at which different proteins are synthesized and degraded inside cells change in response to different stimuli or under different conditions. Proper protein degradation is essential for cell survival under conditions resulting in extensive cellular damage. Damaged proteins are first recognized by molecular chaperones, which try to repair/refold the protein. If the damage is too extensive, the proteins are targeted for degradation. Two major proteolytic systems are responsible for intracellular protein turnover: the lysosomal system and the ubiquitin proteasome system (Goldberg, 2003). Lysosomes are single membrane organelles, which contain large assortment of hydrolases and are able to degrade all kinds of macromolecules from inside and outside the cell. The lysosomal system

undergoes big changes as a cell ages (increase in lysosome volume, decrease in stability and activity, changes in pH, accumulation of lipofuscin) (Terman and Brunk, 2004). The functional consequence of these changes is a decrease in the rate of degradation of damaged macromolecules, which means more instability for the cell.

The ubiquitin-proteasome machinery is a multicatalitic protease that degrades proteins into small oligopeptides. Degradation occurs after recognition of tagged substrates by ubiquitin, contributing to the maintenance of cellular homeostasis. It has been shown that the ubiquitin-proteasome system may decrease in function as a cell ages, though not always (Zeng et al., 2005). Studies in human fibroblasts have revealed no changes with age in levels of ubiquitin and different ligases (E1, E2, and E3), which tag ubiquitin to proteins predisposed to degradation. Consequently, the accumulation of ubiquitin conjugates increases in aged tissue and is likely a result from a decrease in proteasomal efficiency to remove it (Carrard, et al., 2002). Changes in the oxidative state of the proteasome subunits (oxidation, glycation and conjugation with peroxodozed lipid products) increase with age and are likely to result in changes in proteasomal regulation (Carrard et al., 2002). In addition, oxidized proteins and crosslinked proteins can directly inhibit the proteasome (Terman and Brunk, 2004).

1.3 Brain aging

Aging could be considered as process where reparative mechanisms are declining in ability and efficiency, but it should be distinguished from a state of disease. There are people that live for one century and enjoy a well functioning brain for their whole life. Then again many elderly people who do not manifest clinical symptoms of a certain age-related disorder may exhibit physiologically disease-related alterations that represent preclinical stages of such diseases. Knowing that is possible for elderly people to have a properly functioning brain should make it the major goal of the neurobiology of aging to identify ways to facilitate successful brain

aging. Studying neurodegenerative diseases or creating and studying aging model systems should help towards this goal.

It has been shown that during brain aging increased oxidative stress and the accumulation of damaged molecules promote dysfunction of different metabolic and signalling pathways (LeBel and Bondy, 1992) as well as energy deficits. Signalling mechanisms such as gene transcription (Lee et al., 2000), calcium homeostasis (Mattson, 1992), protein folding and degradation, phosphorylation and dephosphorylation (Jin and Saitoh, 1995) are some of the processes that change during brain aging.

Some neurological diseases are considered to be at high risk with increasing age, for example Alzheimer's disease and Parkinson's disease, both very common. Thus far there are no treatments to halt or cure these diseases. Better understanding of molecular basis of the processes involved in their pathology and their relation to aging (not absolute, but remarkable) should change this in future.

1.3.1 Alzheimer's disease

More then 12 million people worldwide have AD, and it accounts for the majority of cases of dementia diagnosed in patients over the age of 60 (Citron, 2004). The pathogenesis of this disease involves altered proteolytic processing of the β-amyloid precursor protein (APP) resulting in increased production of a long (42 amino acid) form of the amyloid β (Aβ) peptide, which in turn aggregates and forms insoluble plaques in the brain. These aggregates generate ROS which in turn disrupt cellular ion homeostasis, energy metabolism (Mattson, 1997) and neuronal synapses and makes cells more prone to apoptosis or excitotoxicity. Neurofibrillary tangles are another hallmark of AD. These tangles accumulate inside cells and have hyperphosphorylated tau protein as their main constituent.

The link between tau and amyloid pathology in AD is not yet clear, nor is the link between age-related accumulation of tau or amyloid and their contribution to AD. Research on multiple transgenic mice combining

abnormalities in amyloid and tau (Oddo et al., 2004) should give some answers to these questions.

Oxidative stress is implied as a causal factor of AD. Diets enriched in antioxidants show an improved learning and memory and a reduction of plaque load in aged canines (Milgram et al., 2004). Antioxidants are one potential therapeutical treatment, others being antiamyloid agents, anti-inflammatory drugs, compounds that limit the phosphorylation of tau protein, antiapoptotic agents, and glutamatergic antagonists.

Current therapies for patients with Alzheimer's disease only ease symptoms, providing temporary improvement and slowing the reduction rate of cognitive decline. Progress in identifying molecular mechanisms of AD should help in future to delay onset or modify the progression of this disease.

1.3.2 Parkinson's disease

Parkinson's disease is a progressive neurodegenerative disorder, which is characterized by motor symptoms such as tremor, postural imbalance, and slowness in movements. As it progresses, it can lead to psychiatric and cognitive dysfunctions such as anxiety, depression and dementia. It affects at least 1% of population over 65 and 4-5% of those over 85 years of age (Lang and Lozano, 1998). The main hallmark of this disorder is a loss of dopaminergic neurons in the *substancia nigra pars compacta*, which results in depletion of dopamine in the striatum, to which these neurons project. The cellular pathological hallmarks of PD are round eosinophilic intracytoplasmatic protein-containing inclusions – Lewy bodies and dystrophic neurites (Forno, 1996).

What causes this disease? So far, PD has been shown to be sporadic in the majority of cases and has been linked to environmental risk factors (toxins, oxidative stress, mitochondrial dysfunction). On the other hand hereditary PD has been linked to mutations in α-synuclein, parkin (Polymeropoulos et al., 1997; Kitada et al., 1998), then PINK1 (Valente et al., 2004), DJ-1 (Bonifati et al., 2002), and LRRK2 (Zimprich et al., 2004).

Sporadic PD is usually associated with impairment in mitochondrial complex I which leads to generation of ROS, and makes neurons vulnerable to glutamate toxicity (Sherer et al., 2002). The prototypical mitochondrial complex I inhibitor 1-methyl-4-phenyl-1,2,3,6-tetrahydropyridine (MPTP) replicates most features of sporadic PD in humans and is used as a model system for this disease (primates, mice). Its major limitation is that in most cases it causes acute degeneration, whereas PD is a chronic, slowly progressive neurodegenerative disorder. α-synuclein was the first gene identified whose mutation was linked to PD. The physiological role is still largely unknown, but its localization at presynaptic terminals and some functional studies indicate a possible role in synaptic plasticity and vesicular transport. Several animal models for α-synucleinopathy-induced neurodegeneration have been developed in mice and *Drosophila* (Dawson et al., 2002). Parkin is involved in the ubiquitin dependent degradation of intracellular misfolded, unassembled, or damaged proteins by the proteasome. It is an E3 ligase responsible for the attachment of ubiquitin to substrates. However, its specific substrates and specifically those that are affected by its loss of function are not known. Mutation in parkin leads to impaired protein degradation (Dawson and Dawson, 2003).

There are many different approaches to experimentally fight PD, which might be separated into neuroprotective and neurorestorative therapies (Dawson and Dawson, 2002). Neuroprotective therapies concentrate on pathways involved in MPTP toxicity and strategies against α-synuclein toxicity and loss of parkin function. Neurorestorative therapies include therapeutic deliveries of growth factors which enhance survival and promote recovery of cells (Kordower et al., 2000). Other potential restorative therapies include cell replacement strategies, for example with stem cells (Kim et al., 2002).

Understanding more about the almost absolute dependence of PD on aging, the mutations that cause familial PD, and the circumstances which

increase the risk of developing PD will help to provide therapeutic approaches for this serious disease.

1.4 Cell death in neurodegenerative diseases and aging

The underlying causes of the various neurodegenerative diseases are not clear; death of neurons and loss of neuronal synapses are key pathological features. Explaining molecular events that control neuronal cell death is critical for the development of new strategies in helping to prevent and treat neurodegenerative diseases and aging.

Neuronal tissues are not proliferative and are not replaced by new ones for the lifetime in most brain regions except in regions such as the olfactory bulb and dentate gyrus of the hippocampus, where there is a constant replacement of neurons from a pool of progenitor (stem) cells (Gage, 2000, Rao and Mattson, 2001). However, even for these cells there is clear evidence that their replacement function is limited. During development there is an excess number of neurons which die in order to match the number of neurons with the size of their projection areas. This process is dependent on neurotrophins and conduction of action potentials as a marker of synaptic activity (Oppenheim, 1991). Neuronal death (apoptotic or necrotic) later in life means injury and disease. For example, loss of hippocampal and cortical neurons results in symptoms of Alzheimer´s disease; death of midbrain neurons that use dopamine as a neurotransmitter causes Parkinson´s disease; loss of striatal neurons is the hallmark Huntington´s disease; and death of lower motor neurons cause symptoms of amyotrophic lateral sclerosis.

Cell death occurs by necrosis or apoptosis (Kanduc et al., 2002; Hengartner, 2000). These two mechanisms have distinct molecular and biochemical mechanisms. In apoptosis, a stimulus activates a cascade of events where there is orchestrated destruction of the cell. In necrosis, by contrast, the stimulus (e.g., ischemia) is itself often the direct cause of the demise of the cell. Necrosis is considered as a pathological process in

contrast to apoptosis which is part of normal development, but the former also occurs in a variety of diseases.

For tissues that proliferate in order to keep their appropriate size and function, old cells die by apoptosis and are replaced by young ones. This kind of death involves changes that don't influence other cells in the neighbourhood, so there is no harm for the cells in which this pathway has not been activated. Dysregulation of the mechanisms of apoptosis may lead to resistance of cells to die which then leads to different types of cancer. During apoptosis a biochemical cascade activates proteases that destroy molecules required for the physiological function and survival of cells. The morphologic features of apoptosis include nuclear and cytoplasmic condensation, internucleosomal DNA cleavage and packaging of the cell into apoptotic bodies that are engulfed by phagocytes, preventing release of intracellular components (Hengartner, 2001). Neuronal apoptosis usually occurs because of mitochondrial damage, hypoxia, UV-rays, increased ROS, etc. and it leads to cytochrome *c* release into the cytosol, with subsequent formation of apoptosome and the activation of effector caspases (caspase-3, -7). This is frequently referred to as the 'intrinsic pathway'. The 'extrinsic pathway' is executed by ligand binding to death receptors of the tumour necrosis factor family inducing the activation of effector caspases through the c-Jun-N-terminal kinase. Activation of caspase-8 (Micheau and Tschopp, 2003) results in cleavage of BID and release of cytochrome *c*. Caspase-8 activation can directly activate effector caspases (Cryns and Yuan, 1998).

In contrast to apoptosis, necrosis is not a developmentally programmed type of cell death. It occurs by dysregulation of normal cellular activities when cells are exposed to extreme stress conditions. Necrosis is morphologically characterised by vacuolisation of the cytoplasm, mitochondrial swelling, dilatation of endoplasmatic reticulum, and rupture of plasma membrane (Artal-Sanz and Tavernarakis, 2005). The cell is lysed without formation of vesicles. Cellular contents are liberated into the intracellular space, evoking damage to neighbouring cells and

inflammation (Leist and Jaattela, 2001). Necrosis is most likely to be mediated by increase of intracellular Ca^{2+}, is independent of caspases, but involves calpains and lysosomal cathepsins. Energy depletion is one potent trigger of necrosis. Membrane potential is not sustained due to shortage of energy and depolarization occurs, resulting in a massive release of excitatory glutamate at the synaptic clefts. Overstimulation of glutamate receptors leads to Ca^{2+} and Na^{+} overload in postsynaptic neurons (Choi, 1992). This phenomenon is called excitotoxicity and primarily involves the elevation of intraneuronal calcium concentration. Calcium activates a family of calcium-dependent cysteine proteases that perform cleavage of a variety of cellular substrates (Goll et al., 2003). There are two ubiquitous isoforms of calpains, namely μ-calpain and m-calpain, that are activated by micro- and mili-molar concentrations of Ca^{2+} in vitro, respectively. Disruption of calcium homeostasis plays a key role in neurodegeneration. Elucidating these mechanisms would be of great importance for treatment of these diseases.

1.5 Caloric restriction (CR) – one way to slow down aging

Research on caloric restriction and aging began with experiments of McCay in 1935 who first argued that caloric restriction (CR) may reduce the rate of aging and increase the lifespan of rats. CR refers to a dietary regimen low in calories without undernutrition. The longevity results from the limitation of total calories derived from fats, proteins, carbohydrates to a level of 25%-60% below that of control animals fed *ab libitum* (Weindruch et al., 1986). CR extends life span in a remarkable range of organisms, including yeast, rotifers, spiders, worms, fish, mice, and rats. How does CR work? It has been documented that oxidative stress is reduced in caloric restricted animals (Li et al., 2003). That does not simply mean that the metabolic rate is reduced, but rather there might be more efficient transport of electrons through the respiratory chain (Duffy et al., 1989). Another hypothesis is that CR animals have an increased ability to detoxify ROS or products such as abnormal proteins by speeding up

protein turnover (Sohal and Weindruch, 1996). As the body runs out of fat during CR, it may trigger the degradation of proteins, thereby increasing their turnover (Koubova and Guarente, 2003).

In addition, CR has direct beneficial effects on the brain. It increases the production of neurotrophic factors such as brain-derived neurotrophic factor (Duan et al., 2001), which can enhance learning and memory, protect neurons against oxidative stress and metabolic insults, and can stimulate neurogenesis. Dietary restriction also induces production of protein chaperones, such as heat-shock protein 70 and glucose regulated protein 78, which are known to protect cells from various insults (Duan and Mattson, 1999). Therefore, it seems that dietary restriction promotes neuronal survival, plasticity, and even neurogenesis by inducing mild stress response that involves activation of genes that encode proteins designed to promote neuronal growth and survival (Mattson, 2003).

1.6 Cell culture as a model for aging

Traditional animal models used in aging research are chosen partially because of their short life spans. That means, they die within several weeks (*C. elegans*) or several months (*Drosophila*) or several years (mice and rats), even though living in a protected environment. There are some long-term experiments ongoing with squirrels and rhesus monkeys (Roth et al., 1999), whose life span is a few decades. The use of short-lived animals for aging research assumes that there is relevance to the much longer human life span and a hope that fundamental aging processes are conserved between species.

The complexity of organisms led scientists to invent simpler model systems in order to obtain some answers and understand organic mechanisms at the cellular and molecular levels. Cell culture approaches make it possible to study tissue-specific and cell-specific aging.

In the beginning of twentieth century (1907) the first neuronal cell culture method was described by Harrison, who combined fragments of embryonic tadpole tissue with clotted lymph from adult frogs. The cultures

were viable for several weeks. In the forties, techniques were developed where neural tissues were removed from chick embryos and used for electrophysiological recordings. A need for single cells in culture led to the development of dissociated neural cell cultures. Many protocols exist for either using lytical enzymes to lose connections between cells or mechanical techniques in order to get a suspension of dissociated neural cells that will grow as a monolayer in culture dishes or flasks.

The first aging experiments using cell cultures were carried out very early in the twentieth century. Carrell (1912) performed a series of experiments where he dissociated cells from chicks, placed them in culture, and showed by subculturing that the cells were seemingly capable of proliferating indefinitely. The conclusion was that organismal mortality (and aging) was a consequence of multicellularity. The logic behind this equivalence, however, was faulty.

Hayflick and Moorehead (1961) documented the fact that normal fibroblasts have only a limited capacity for proliferation in culture. The process that limits cell division has been termed replicative senescence. Replicative senescence is limited to cells that have the ability to divide *in vivo*, and hence does not apply to postmitotic cells such as mature neurons or muscle.

Aging of neuronal cells *in vitro* was not described until the end of the twentieth century (Aksenova et al., 1999, Lesuisse and Martin, 2002, Toescu and Verkhratsky, 2000). Providing the optimal conditions over long period of time was the biggest obstacle. Hippocampal and cortical neurons but not cerebellar granule neurons (CGN) have been described as being able to survive up to 60 days in culture (Aksenova, 1999, Lesuisse and Martin, 2002)

CGN constitute the largest homogenous neuronal population of mammalian brain. Due to the feasibility of the well characterized primary cells *in vitro* cultures, CGN are an interesting model to study cellular and molecular correlates of mechanisms of survival/apoptosis and neurodegeneration/neuroprotection (Contestabile, 2002).

First experiments *in vitro* with CGN were carried out more then twenty years ago, in order to find out which neurotransmitter is secreted by these cells (Gallo et al., 1982) and since then CGN cell cultures have become a very popular model to study development, function and neuropathology.
CGN survive and differentiate in vitro in the presence of depolarizing concentrations of KCl (25 mM) and serum without additional need for neurotrophic factors. After removal of serum and lowering of extracellular potassium from 25 to 5 mM, 50% of granule cells undergo rapid apoptotic cell death within 24 h (D'Mello et al., 1990). This model of apoptotic cell death presumably mimics the naturally occurring death of 20-30% of granule cells, which is important for matching the number of granule cells with Purkinje cells between the third and fifth week postnatally (Williams and Herrup, 1988).
Primary CGN cultures have around 90% cerebellar granule neurons (Schulz et al., 1996; Nicoletti et al., 1986). The remaining cells are mainly astrocytes and olygodendrocytes. When making a decision about having an absolute pure neuronal culture or a co-culture with glial cells (astrocytes), one has to take into account that astrocytes secrete a variety of growth factors which are essential for survival and differentiation of neurons. Astrocytes play a key role in the protection of neurons from excitotoxicity by taking up excess glutamate and converting it to glutamine via the enzyme glutamine synthetase (Huang and O´Banion, 1998).
First aging experiments with cerebellar granule cells *in vitro* were carried out by Ishitani et al., 1996. These experiments showed that CGN can only survive up to 17 DIV. They died abruptly after this time by up-regulating a 38-kDa protein which was identified to be glyceraldehyde-3-phosphate dehydrogenase (GAPDH).

We wanted to test why CGN die after 17 DIV and to find out more about aging of cerebellar granule neurons *in vitro*.
Text.

2 Aims

There has been abundant amount of work done in order to understand the aging phenomena and age-associated degenerative diseases. Nevertheless, the causes of diseases such as Parkinson's or Alzheimer's are still unanswered. Data from *in vivo* studies suggest that neuronal loss observed in these pathologies may occur by apoptosis.

The aim of this study is to investigate the molecular changes that occur during neuronal aging. To address this issue we constructed an *in vitro* model of aging of cerebellar granule neurons of rats. We explored whether molecular machinery that executes cell death changes due to age. The observation that young and old CGN have different cell death pathways prompted us to characterize the possible molecular mechanisms involved. Therefore we characterized the common execution and signalling pathways of neuronal cell death and their contribution to the degenerative processes caused by *in vitr*o aging of cerebellar granule neurons.

3 Material and Methods

3.1 Instruments

Table 1

Autoclave	Steam sterilizator	Sauter, Switzerland
Camera systems	ECL-Camera LAS-1000 Cooled CCD-Camera, model CCD300ETRCX 12 bit cooled CCD-Camera SensiCam	Fujifilm, USA DAGE-MTI, USA PCO, Kelheim
Cell-counting chamber	Neubauer cell chamber	Hecht Assistant, Sondheim/Rhön
Centrifuges and Rotors	Biofuge Fresco with rotor 3325 Biofuge Pico with rotor 3324 Megafuge 1.0R with rotor 2252 Sorvall® RC 5C plus with rotors SLA-3000 and SLA-600 TC	Heraeus, Hanau Heraeus, Hanau Heraeus, Hanau Kendro, Langenselbold
Developing machine	X-OMAT M35	Kodak, Stuttgart
Electrophoresis chambers for agarose gels	Mini Sub Cell GT	Bio-Rad, München
Gel documentation	Kaiser RS1 with UV-table	Kaiser, Buchen MWG Biotech, Ebersberg
Heat blocks	Thermofixer comfort	Eppendorf, Hamburg

	Heatblock QBT4	Grant, UK
Incubators	Function Line, Type BB16, B6420	Heraeus, Hanau
Microscops	Axioplan 2 Leica DMIRBe Wilowert A	Zeiss, Göttingen Leica, Bensheim Hund, Wetzlar
pH meter	CG843/14pH	Schott, Mainz
Photometers	Ultrospec 3000 ELISA-*Reader*- MRX Spectrafluor Fluorescence Spectrophotometer	Amersham Biosciences, Freiburg Dynatech Laboratories, USA Tecan, Crailsheim
Pipets	Gilson Pipetman (10, 20, 200, 1000 µl) Eppendorf Reference (10, 20, 200, 1000 µl)	Gilson, USA Eppendorf, Hamburg
Power supplies	Power-Pac 300 Power-Pac 3000	Bio-Rad, München Bio-Rad, München
SDS-PAGE- and Blotting-Apparatus	Mini-PROTEAN® II-Electrophoresis-System PROTEAN® II xi-Electrophoresis-System	Bio-Rad, München Bio-Rad, München
Shakers	Roller RM5 KS250 basic	Hecht Assistant, Sondenheim/Rhön Kika Labortechnik, Staufen

Sterile bench	Tecnoflow 3F120-II GS	Integra Biosciences, Switzerland
Thermocycler	Primus 96 plus PTC-200 MX3000P™	MWG_Biotech, Ebersberg MJ Research, USA Stratagene, USA
Weighing-instruments	MC1 Laboratory LC420 Micro, Type M5P	Sartorius, Göttingen Sartorius, Göttingen
Vortex	Vortex- Genie 2	Scientific Industries, Inc., USA

3.1.1 Additional material

Table 2

Gel blotting paper	Type GB3000	Schleier and Schuell, Dassel
Transfer membrane	PROTRAN® Nitrocellulose transfer membrane	Schleier and Schuell, Dassel
Cell culture dishes	6-/24-/48-/96-*well* cell culture plates 35 x 10 mm; 60 x 15 mm cell culture plates Costar® cell culture bottles, 25 cm^2; 75 cm^2	BD Falcon, Heidelberg BD Falcon, Heidelberg Corning, USA

3.2 Chemicals

Table 3

6-Carboxyfluorescein Diacetate	Sigma, Taufkirchen
Ac-DEVD-AMC	Bachem, Heidelberg
Acetic acid, glacial	Merck, Darmstadt
Acrylamide 2K-Solution (30%, Mix Acrylamide:Bisacrylamide; 37.5:1)	AppliChem, Darmstadt
Adenosin-5'-triphosphat (ATP)-dipotassiumsalt	Sigma, Taufkirchen
Alamar Blue	Biosource, USA
Albumin	Sigma, Taufkirchen
Ammoniumpersulfate (APS)	Sigma, Taufkirchen
AMPA	Tocris, UK
Ampicillin	Sigma, Taufkirchen
BenchMark® Prestained Protein Ladder	Invitrogen, Karlsruhe
Bromphenolblue	Merck, Darmstadt
BSA	Sigma, Taufkirchen
Calpeptin	Tocris, UK
CHAPS	Sigma, Taufkirchen
Chloroform	Sigma, Taufkirchen
Complete® Proteases-Inhibitor-Cocktail	Roche, Mannheim
Cytosine 1-bD-arabinofuranoside	Sigma, Taufkirchen
Desoxynucleosid-5'-triphosphate (dNTPs) for the PCR	Invitrogen, Karlsruhe
Dimethylsulfoxide (DMSO)	Sigma, Taufkirchen
Dithiothreitol (DTT)	AppliChem, Darmstadt
EDTA-solution (0,5 M)	BioWhittaker, USA
Ethanol, absolute extra pure	Merck, Darmstadt
Ethidiumbromide	Sigma, Taufkirchen
GeneRuler® 1 kb-DNA-Ladder	Fermentas, St. Leon-Rot

GeneRuler® 100 bp-DNA-Ladder	Fermentas, St. Leon-Rot
Glucose-6-Phosphat	Sigma, Taufkirchen
L-Glutamic acid	Tocris,UK
Glycine	AppliChem, Darmstadt
HEPES	Fluka, Neu-Ulm
Hoechst 33258	Molecular Probes, USA
Immu-Mount	Shandon, USA
Immun-star HRP substrate	Biorad, München
Kainic acid	Tocris, UK
Kanamycinsulphate	Fluka, Neu-Ulm
Lactacystin	Calbiochem, Darmstadt
Magnesium chloride hexahydrate	Fluka, Neu-Ulm
Magnesium Sulphate	Fluka, Neu-Ulm
MG132 (Z-LLL-al)	Sigma, Taufkirchen
MK 801 maleate	Tocris, UK
N,N,N',N'-Tetramethylethylendiamin (TEMED)	Roth, Karlsruhe
Natriumazide	Merck, Darmstadt
Natriumdodecylsulphate (SDS)	AppliChem, Darmstadt
Naturaflor® Milk powder	Töpfer, Dietmannsried
NBQX	Tocris, UK
Oligo (dT)-Primer	Roche, Mannheim
Paraformaldehyde (PFA)	Riedel-deHaën, Seelze
Penicillin/Streptomycin	PAN Biotech, Aidenbach
peqGOLD® Universal-Agarose	Peqlab, Erlangen
Phenol red	Sigma, Taufkirchen
Poly-L-Lysine	Sigma, Taufkirchen
Ponceau S	Sigma, Taufkirchen
Potassium chloride	Roth,Karlruhe
Potassium dihydrogen phosphate	Fluka, Neu-Ulm

Prestained SDS-PAGE Standard (Broad Range)	Bio-Rad, München
RNasin® (Ribonuklease-Inhibitor)	Promega, Mannheim
Staurosporine	Sigma, Taufkirchen
Suc-LLVY-AMC	Sigma, Taufkirchen
Sulfosalicylic acid	Sigma, Taufkirchen
TALON® Metal Affinity Resin	BD Clontech, USA
Trichloracetic acid	Merck, Darmstadt
Tris (hydroxymethylaminomethane)	AppliChem, Darmstadt
Triton X-100	Sigma, Taufkirchen
Trizol	Invitrogen, Karlsruhe
Trypsin	Invitrogen, Karlsruhe
Trypsin inhibitor	Sigma, Taufkirchen
Tween® 20	Roth, Karlsruhe
Urea	Invitrogen, Karlsruhe
Xylencyanol	Fluka, Neu-Ulm
z-VAD-FMK	Bachem, Heidelberg
ß-Mercaptoethanol	Fluka, Neu-Ulm

- All chemicals that have not been mentioned in the list were purchased from the following companies: Amersham Pharmacia Biotech (Freiburg), Boehringer (Ingelheim), Merck (Darmstadt), Roth (Karlsruhe), or Sigma (Taufkirchen).

3.3 Kits

- Absolute QPCR SYBR® green mixes, ABgene,UK
- ATP bioluminescence assay kit HS II, Roche, Mannheim
- BCA™ protein assay kit, Pierce, USA
- Calpain activity assay kit, Calbiochem, Darmstadt
- iScript cDNA synthesis kit, Bio-rad, München
- OxyBlot protein oxidation detection kit, Intergen, USA
- QIAEX II gel extraction kit, QIAGEN, Hilden

3.4 Cell culture medium

BME (Basal Medium Eagle), with 2, 2 mg/ml $NaHCO_3$, without L-glutamine (Biochrom, Berlin)

Table 4

Formulation (in mg/l)

	Earle's salts	Earle's diploid-salts	Hanks' salts
NaCl	6800	6800	8000
KCl	400	400	400
$Na_2HPO_4 \cdot 2H_2O$	140	140	60
$NaH_2PO_4 \cdot H_2O$	200	200	60
KH_2PO_4	200	200	200
$MgSO_4 \cdot 7H_2O$	1000	1000	140
$MgCl_2 \cdot 6H_2O$	10	10	1000
$CaCl_2$	2200	2200	10
D-glucose			350
Phenol red			
$NaHCO_3$			

The following chemicals were additionaly used for preparation of CGN:

Table 5

Gentamycine	20 µg/ml
Ara-C	10µM
Potassium chloride	25mM (5mM)
$CaCl_2$	1.2% stock
$MgSO_4$	3.82% stock
10 x Krebs buffer; pH 7,4:	
NaCl	7.25%
KCl	0.4%
NaH_2PO_4 x H_2O	1.4%
D-glucose-monohydrate	2.8%
Phenolred	0.001%
HEPES	5.9%

Trypsine inhibitor	0.52 mg/ml
Trypsine	0.25 mg/ml
Albumine	0.3%
Fetal calf serum (FCS), inactive	10%
L-Glutamine	2 mM
DNAse	1.2 mg
Poly-L-Lysine	0.1 mg/ml
SES synthetical serum A SES synthetical serum B	1000x stock 1000x stock

3.5 Animals

Primary cerebellar granule neuronal cultures were prepared from Sprague Dawley rats, purchased from Charles River Laboratories. All experiments were performed in accordance with international guidelines to minimise pain and discomfort (NIH-guidelines and European Community Council Directive 86/609/EEC).

3.6 Buffers and solutions

3.6.1 Agarose gel electrophoresis

- TAE, 40 mM Tris/Acetat; 1 mM EDTA; pH 8
- 6x TAE loading buffer, 30% (v/v) glycerol
  0.25% (w/v) Bromophenol blue
  0.25% (w/v) xylenol cyanol
- Agarose gel, 1% - 2% Agarose in TAE
  0.001% Ethidiumbromide

3.6.2 PCR

- Taq-Polymerase, Fermentas, USA
- $MgCl_2$, Fermentas, USA
- dNTPs, Fermentas, USA
- 10x Buffer, Fermentas, USA

3.6.3 RNA extraction for RT PCR

- Trizol
- Chloroform
- Isopropanol
- Ethanol, 75%; 100%
- EDTA, 25mM
- DNAse I, 10x reaction buffer

3.6.4 SDS-Polyacrylamide gel electrophoresis

Table 6

Stacking gel buffer	1 M Tris/HCl; 0.8%SDS; pH 6.8
Running gel buffer	1.5 M Tris/HCl; 0.4% SDS; pH 8.8
TEMED N´,N´,N´,N´- Tetramethylethylendiamine	
Acrylamide solution	30% Acrylamide 0.8% N´,N´- Methylenbisacrylamide
Ammonium persulfate solution Ammoniumsulperoxidisulphate (APS)	10%
10x Running buffer	250 mM Tris/HCl; 1.92 M Glycine; 2% SDS; pH 8.3
10x Transfer buffer	250 mM Tris/HCl, 1.92 M Glycine, pH 8.3
5x Lämmli buffer	10% Glycerol 20% SDS (10% (w/v)) 12.5% 0.5 M Tris-Cl, pH 6.8 5% 2-Mercaptoethanol 5% Bromphenol blue (1% (w/v))

3.6.5 Immunoblot

Table 7

Ponceau-S Solution	0.1% (w/v) Ponceau S 5% (w/v) acetic acid
Blocking solution	5% Skim milk 0.02 % NaN_3
Washing buffer: (1x PBS (phosphate buffered saline) + 0, 01% Tween 20) **10x PBS**: Tween 20	 1.4 M NaCl 27 mM KCl 100 mM Na_2HPO_4 18 mM KH_2PO_4; pH 7.4 0.005% - 0.01%
Stripping buffer	0.2 M glycine 0.5 M NaCl; pH 2.8

Table 8

Antibody, primary	**Dilution and the type**	**Company**
Actin (I-19):sc-1616	1:3000, goat polyclonal	Santa Cruz Biotechnology, Inc., USA
Alpha-Synuclein, #610786	1:500, mouse monoclonal	BD Transduction Lab, USA
Anti-GAPDH, #mab374	1:1000, mouse monoclonal	Chemicon International, USA
Anti-MnSOD, #06-984	1:1000, rabbit polyclonal	Upstate, Lake Placid, NY, USA
Anti-Spectrin (Nonerythroid) monoclonal	1:2000, mouse monoclonal	Chemicon International, USA

antibody, #MAB1622		
Bax (N-20):sc-493	1:200, rabbit polyclonal	Santa Cruz Biotechnology, Inc., USA
Bcl-2 (N-19):sc-492	1:500, rabbit polyclonal	Santa Cruz Biotechnology, Inc., USA
Bcl-$x_{S/L}$ (S-18):sc-634	1:500, rabbit polyclonal	Santa Cruz Biotechnology, Inc., USA
Caspase-3 antibody, #9662	1:100, rabbit polyclonal	Cell Signaling Technology, UK
Cleaved caspase-3 (Asp175), #9661	1:100, rabbit polyclonal	Cell Signaling Technology, UK
Cytochrome C, 6H2.B4	1:1000, mouse monoclonal	Pharmingen, USA
GAP-43 (c-19): sc-7457	1:1000, goat polyclonal	Santa Cruz Biotechnology, Inc., USA
Glial fibrillary acidic protein, clone 6F2, #M 0761	1:5000, mouse monoclonal	DakoCytomation, Denmark
Monoclonal Anti-β-Actin, clone AC-15	1:10000, mouse monoclonal	Sigma, Taufkirchen, Germany
Mouse anti-Ubiquitin, #13-1600	1:1000, mouse monoclonal	Zymed® Laboratories Inc., USA
Mouse monoclonal antibody to 20S proteasome α subunits, #PW8195	1:1000, mouse monoclonal	Biotrend, Köln
P44/42 MAP kinase	1:1000, rabbit	Cell Signaling

antibody, #9102	polyclonal	Technology, UK
PathScan™ Multiplex Western Cocktail I #7100	1:100, rabbit polyclonal	Cell Signaling Technology, UK
Phospho-p42/44 MAPK (Thr202/Tyr204) (E10), #5120	1:2000, mouse monoclonal	Cell Signaling Technology, UK

Anti-NCX3 antibody was kindly provided by Prof. K.D. Philipson (Philipson and Nicoll, 2000).

Anti-Tau antibodies (AT8, PHF1, and K9JA) were kindly provided by Anja Schneider, E.-M. Mandelkow, and E. Mandelkow.

3.6.5.1 Secondary antibodies:

- **Donkey anti-goat IgG HRP**, #sc-2020; 1:10000; Santa Cruz Biotechnology, USA
- **Anti-mouse Ig, HRP linked whole antibody (from sheep) GPR**, #NXA931; 1:5000; Amersham Pharmacia Biotech, USA
- **ECL™ anti-rabbit IgG, HRP linked whole antibody (from donkey)**, #NA934V; 1:5000; Amersham Pharmacia Biotech, USA

3.7 Primers

All primers were used for Real Time PCR

Table 9

3-hydroxy-methyl-coenzyme-A reductase	For 5´AACCTGCTGCCATAAACTGGAT´3 Rev 5´ACCACCTTGGCTGGAATGAC´3
BAX	For 5´GCTTTAGGGATTCCGCAGT´3 Rev 5´TCGCCAATTCGCCTGAGA´3
Calcium sensing receptor	For 5´AACCTGCTGCCATAAACTGGAT´3 Rev 5´TTGGATCACTTCGACCACCTG´3

Calcium sensing receptor	For 5´TTGCAGCTGATGACGACTATGG´3 Rev 5´TTGGATCACTTCGACCACCTG´3
Calpastatin	For 5´AGATTCACTGGGCACCCG´3 Rev´TTTGCCTCTTTGACTTGTTTGG´3
Ddit3	For 5´CTGAGGAGCCAGGGCCA´3 Rev 5´TGACTGGAATCTGGAGAGCGA´3
GAPDH	For 5´ACATCTTCCTCAACGTGGTCCA´3 Rev 5´ATGGCGACCTCCTTGGTATCA´3
KA2	For 5´TCTTGGGCTTTTCCATGTTCA´3 Rev 5´ATGTTGAGGCTGCGCACAA´3
Lifeguard	For 5´CATCCTCCTGCCCTTCCAAT´3 Rev 5´CACACCCGCTCCTAGCACA´3
Somatostatin	For 5´CAGAGAACGATGCCCTGGAG´3 Rev 5´CAGCCTCATCTCGTCCTGC´3
Vesicle associated calmoduline binding protein	For 5´GAGCAAGACCAGCGGATCA´3 Rev 5´TGCATTGCCAGAAATCCATTC´3

3.8 Primary cerebellar granule neurons in culture

3.8.1 Preparation of the primary cell culture

The preparation of cerebellar granule cells was based on a previously described method (Schulz et al., 1996). Seven-day-old rats were sacrificed by decapitation and cerebella were isolated and placed in the Krebs buffer where, carefully were cleaned from blood vessels and other tissues that were not part of cerebellum. After that, cerebella were mechanically disrupted with scissors, and placed in the same buffer supplemented with trypsine and DNAse I for 20 minutes on 37°C. The reaction was stopped adding trypsine inhibitor. Cells were centrifuged for 5 minutes on 1200 rpm and supernatant was discarded. In order to get as many granule neurons as possible, cells were resuspended in a small volume of Krebs buffer and using a Pasteurs pipet, solution was taken in and out with the pipette for

mechanical dissociation until it had no visible cell clumps. This step was repeated two times and after every step cells were resuspended in a larger volume of Krebs buffer and left for at least 20 minutes to sediment. The supernatant contained granule neurons. Supernatant was collected, centrifuged as every time for 5 minutes at 1200 rpm and resuspended in BME medium supplemented with 10 % fetal calf serum which was previously inactivated by heat, 2 mM glutamine, 20 µM gentamycine and 25 mM KCl. Plates were coated with poly-L-lysine (MW > 300 kDa; 150 µg/ml for plastic, 250 µg/ml for glass surfaces) in order for CGN to firmly attach and uniformly spread over the plate. Cells were seeded at a density of 2 x 10^5 cells/cm^2. Cytosine arabinoside was added at a concentration of 10 µM after 18-24 h to prevent growth of non neuronal cells. Contamination with glial cells was less then 5% (Schulz et al., 1996). Cells were left for seven days to differentiate and all the experiments were performed starting day 7 *in vitro* (DIV).

3.8.1.1 Long term culturing

Cerebellar granule cells were kept over the period of 60 days in culture. In order to keep similar conditions part of the media was exchanged starting at the second week in culture. After DIV 7 media was supplemented with 5 mM glucose and 2 mM glutamine two times per week. After DIV 14, one third of media was exchanged two times per week. Fresh media contained synthetic serum and glutamine. This procedure was performed until the cells were kept in the culture, continuously over the whole period of time up to 60 days.

3.8.2 Treatment of cells

Table 10

AMPA	100 µM
Calpeptin	5 µM
Kainic acid	100 µM
KCl	5 mM and 25 mM

Lactacystine	5 µM
L-Glutamic acid	100 µM
MG132	1 µM
MK801	10 µM
NBQX	20 µM
NMDA	500 µM
Staurosporine	1 µM
U0126	5 µM
z-VAD-fmk	100 µM

Treatment of primary cerebellar granule neurons was always accompanied was suitable controls consisting of the cells treated with vehicles (medium, water, DMSO, ethanol).

In all experiments, neurons were cultured in 25 mM K^+ (HK) and 10% fetal calf serum during the differentiation period *in vitro* (7 days). For studies of K^+ deprivation, medium was replaced by serum-free basal modified Eagle´s medium containing 5 mM K^+ (LK) or 25 mM K^+ (HK) and supplemented with glutamine and gentamycine as indicated above.

3.9 Protein analysis

3.9.1 Preparation of protein lysates

Medium was aspired from culture dishes and cells were washed with ice cold PBS. Cells were scraped in PBS with Complete protease inhibitor cocktail (Roche). In order to decrease the volume, cells were centrifuged for 15 min at 13000 rpm on 4°C. Pellet was resuspended in lysis buffer (500 mM Tris/HCl pH 8.0; 120 mM NaCl, 5 mM EDTA; 0.5% NP 40) with Complete protease inhibitor cocktail and left on ice for 30 min for lysis to occur. For performing immunoblot analysis with phosphorylated protein forms, phosphatase inhibitors (25 mM NaF, 1 mM Na_3VO_4) were added to lysis buffer to inhibit dephosphorylation. After centrifugation for 20 min at 13,000 rpm on 4°C supernatant was taken for protein determination and

pellet was discarded. For preservation of proteins over a longer period of time aliquots were frozen and kept at -20°C.

3.9.2 Determination of protein concentration

In order to determine protein concentration Bradford Assay (Bio-Rad) and BCA™ Protein Assay (Pierce) were used.

The Bradford dye assay is based on the equilibrium between the three forms of Coomassie Blue G dye. Under strongly acid conditions, the dye is most stable as a doubly-protonated red form. Upon binding to protein, however, it is most stable as an unprotonated, blue form. The stock solution contains 0.5 mg/ml Coomassie Blue G, 25% methanol, and 42.5% H_3PO_4. The assay reagent is prepared by diluting 1 volume of the dye stock with 4 volumes of distilled H_2O. Protein standards were prepared in the same substance as the samples that were assayed (water). A standard curve was made using bovine serum albumine (BSA) with concentrations of 0, 1, 2, 4, 6, 8, 10, 12 µg/µl. Triplets of known protein concentrations were added into 96-well plates (50 µl) together with samples of unknown concentrations (49 µl of distilled H_2O and 1 µl of protein lysate). The assay reagent was added to the final volume of 200 µl. Absorbance was read at 595 nm without any prior incubation.

The BCA protein assay is a detergent-compatible formulation based on bicinchoninic acid (BCA) for the colorimetric detection and quantification of total protein. BCA serves to react with complexes between copper ions and peptide bonds to produce a purple end product. Protein concentrations are determined with reference to standards of a common protein such as BSA. A series of dilutions of known concentrations are prepared from the protein and assayed alongside the unknowns before the concentration of each unknown is determined based on the standard curve.

Two solutions (A and B) are provided by kit and should be mixed in 50:1 ratio giving the working reagent (WR). Working reagent is then mixed with the sample in 20:1 ratio and incubated for 30 min at 37°C. The

absorbance is read at 562 nm. Standard curve is prepared by plotting the average for each BSA standard vs. its concentration in µg/ml. The standard curve is used to determine the concentration of each unknown protein.

3.9.3 Immunoblot analysis

For SDS-PAGE the Protean III mini-gel system (BIO-RAD) was used. Running gel components were mixed at the percentage of acryl amide requested according to the table 11. The poured gels were overlaid with 70% ethanol, which was removed after polymerization. Stacking gel was poured and comb inserted immediately. Samples in 5 x Lämmli buffer containing 10-40 µg of protein were boiled for 5 min on 95°C and cooled down on ice immediately after incubation on 95°C preventing renaturation of proteins. After brief centrifugation samples were loaded on gel. As a protein standard, prestained markers were used (Kaledioscope, Bio-Rad). Running conditions: 150 V constant voltage.

3.9.3.1 Running gel

Table 11

All volumes in ml	**8%**	**10%**	**12%**	**15%**
30% Acrylamide	1.3	1.7	2	2.5
1,5 M Tris/HCl pH 8.8	1.3	1.3	1.3	1.3
10% SDS	0.05	0.05	0.05	0.05
10% APS	0.05	0.05	0.05	0.05
TEMED	0.002	0.002	0.002	0.002
H_2O	2.3	2	1.7	1.2

3.9.3.2 Stacking gel

Table 12

4%	**All volumes in ml**
30% Acrylamide	0.33
0.5 M Tris/HCl pH 6.8	0.5

10% SDS	0.02
10% APS	0.02
TEMED	0.002
H_2O	1.25

3.9.3.3 Protein transfer

Separated proteins on SDS-PAGE were transferred to a nitrocellulose membrane (Hybond, Amersham). Nitrocellulose membrane, Whatmann paper and foam pads were first soaked in 1 x Transfer buffer (25 mM Tris, 192 mM Glycine, 20% Methanol). For a transfer a sandwich was built up on the cathode containing 1 x foam pad, 1 x 3 mm paper, gel, PVDF membrane, 1 x 3 mm paper, 1 x foam pad. The anode was fitted and the transfer performed for 1 h at constant voltage (100 V). The transfer was checked by dying the membrane with Ponceau-S solution (0.1% Ponceau-s in 5% Acetic acid).

3.9.3.4 Western blot analysis

After transfer the membrane was placed for 1 h in blocking solution (PBS; 0.1% (v/v) Tween-20; 5% (w/v) skim milk) on the room temperature. Subsequently membranes were incubated with the primary antibody (Ab) at different concentrations, depending on the antibody with 0.5% skim milk at 4°C over night. Membranes were washed with PBS/Tween (3 x 5 min) before incubation with secondary antibody. Incubation with secondary Ab was performed for 1 h at room temperature. Membranes were washed again (3 x 5 min) and incubated with “Enhanced Chemi-Luminescence” (ECL, Amersham) for 1 min. Membrane was placed in transparent foil and exposed to ECL-film (Kodak) for different time periods.

3.10 Viability measurement

3.10.1 Fluoresceine diacetate staining (FDA)

Neurons plated in 24-well and 48-well plates were used for assessment of viability. Viability was measured by the capability of the cells to diesterify and retain fluorescein diacetate or carboxy-FDA in their cytoplasm. Medium was removed from neuronal cultures, and cells were incubated at 37°C for 5 min (young cultures) or 15 min (old cultures) with Locke´s solution (154 mM NaCl; 5.6 mM KCl; 2.3 mM $CaCl_2$; 1 mM $MgCl_2$; 3.6 mM $NaHCO_3$; 5 mM HEPES; and 20 mM glucose) with 5 µg/ml FDA or carboxy-FDA. Cultures were washed once with Locke´s solution and examined under fluorescent light microscopy. Cell numbers were determined in that way that three random fields were chosen from each well and digitized by a CCd camera connected to an image processor (MCID-V; Imaging Research, St. Catherines, Canada). Images were filtered, and total number of stained cells was counted automatically by MCID-C computer software.

3.11 DNA fragmentation

QIAquick gel extraction kit was used for visualisation of DNA fragmentation. Cells were scraped in PBS and transferred into an eppendorf tube. Buffer QG was added in three time bigger volume and cells were homogenized with a syringe (18 gauge) for five times. One volume of isopropanol was added to the sample. In order to bind DNA, sample was applied to QIAquick column and centrifuged for 1 min. Flow-through was discarded and column was placed back into the same collection tube. To wash, PE buffer was added to the column and again centrifuged for 1 min. Flow-through was discarded again and column was placed into a clean collection tube. To elute DNA 20 µl of EB buffer was added to the column and centrifuged for 1 min. The same volumes of samples were loaded on 1% agarose gels and visualised by ethidium bromide staining.

3.12 Protein carbonylation

Amounts of oxidized proteins containing carbonyl groups were measured using an OxyBlot kit (Intergen, USA). Briefly, 10 µg/sample of protein were treated with 2.4-dinitrophenylhydrazine (DNP-hydrazine), in order to derivatize the carbonyl groups to 2.4-dinitrophenylhydrazone (DNP-hydrazone) for 15-30 min, followed by neutralization with neutralization solution. These samples were electrophoresed on a 12% SDS-PAGE gel, transferred, and blocked. The blot was incubated overnight with a rabbit anti-DNPH antibody (1:150) at 4°C, followed by incubation with goat anti-rabbit secondary antibody (1:300) for 1 hr at room temperature. Bands were visualized using ECL detection system.

3.13 Proteasomal activity

The protocol to measure proteasomal activity was performed according to Canu et al. (2000) with some changes. To measure proteasomal activity, media was aspirated from the CGN and cells were washed with ice cold PBS. Cells were scraped and lysed on ice for 30 min in sample buffer (20 mM Tris/HCl, pH 7.2, 0.1 mM EDTA, 1 mM 2-mercaptoethanol, 5 mM ATP, 20% (v/v) glycerol, and 0.04% (v/v) Nonidet P-40). After centrifugation for 15 min at 13,000 rpm on 4°C, supernatant was used to determine protein concentration. Lysates (10 µg) of cerebellar granule neurons were incubated at 37°C with the fluorogenic substrate Suc-LLVY-AMC (100 µM) in 100 µl of 50 mM HEPES, pH 8, 5 mM EGTA. As a control, lactacystin (50 µM) or MG132 (50 µM) were used to inhibit proteasomal activity. Activity was measured every 30 min at excitation 380 nm and 460 nm emission using a spectrafluor fluorescence spectrophotometer (Tecan, Crailsheim).

3.14 Caspase-3 activity

Cells grown in 96-well plates were used for this assay. At the appropriate time, medium was aspirated, and the neurons were lysed in 50 µl of buffer A (10 mM HEPES, pH 7.4, 42 mM KCl, 5 mM $MgCl_2$, 1 mM PMSF, 0.1 mM

EDTA, 0.1 mM EGTA, 1 mM DTT, 0.5% CHAPS plus cocktail of protease inhibitors (Complete, Roche)). DEVD-amc was added to a final concentration of 10 µM in 150 µl of buffer B (25 mM HEPES, 1 mM EDTA, 0.1% CHAPS, 10% sucrose, 3 mM DTT, pH 7.5). Fluorescent amc production was measured at exctitation 360 nm, emission 460 nm. Experiments were performed in triplicate, and the results were expressed as specific activities (relative fluorescence units/mg protein/minute). For experiments examining the ability of zVAD-fmk to inhibit the production of DEVD-amc cleaving activity, neurons were washed three times with 200 µl PBS to remove residual inhibitor before cell lysis.

3.15 Calpain activity

This assay was used to determine the activity of calpain-1 and calpain-2 in cell cultures using the synthetic calpain substrate in the presence of Ca^{2+} and reducing agent TCEP.

For this assay 35 mm dishes were used in triplicates for each condition. Cells were scraped in ice cold PBS, centrifuged shortly and the pellet was mixed with lysis buffer and left on ice for 30 min. Lysate was vortexed and centrifuged at 14 000 g at 4°C and supernatant was collected. Protein concentration was determined using BCA protein assay. To 96-well plates 100 µl of activation buffer was added for each sample that was measured as well as 100 µl of inhibition buffer in separate wells (as a negative control). Samples were added (50 µl – adjusted for the same concentration of protein) as well as substrate – Suc-LLVY-AMC (50 µl). After incubation for 15 min at room temperature the fluorescence was read using a fluorescence plate reader at an excitation wavelength of 360-380 nm and an emission wavelength of 440-460 nm.

The fluorescence value was calculated by subtracting the value of the blank and of the inhibition buffer for each sample from duplicate readings. The values were displayed as relative fluorescence units.

3.16 ATP bioluminescence assay

The ATP bioluminescence assay kit HS II uses the ATP dependency of the light emitting luciferase catalyzed oxidation of luciferin for the measurement of low concentrations of ATP:

Cells were scraped in PBS, spinned down and resuspended in 50 µl of dilution buffer. In parallel, ATP standard was diluted by serial dilutions in the range of 10^{-10} to 10^{-16} moles ATP (10^{-6} - 10^{-12} M). Samples and ATP standards were added to the same volume of cell lysis reagent and incubated for 5 min at room temperature. Volume of 50 µl was transferred into 96-well plate. Luciferase reagent (50 µl) was added automatically and measurements were performed 1 sec after the injections of substrate. The blank was subtracted from the raw data and ATP concentrations were calculated from a log-log plot of the standard curve data and normalized for the same concentration of protein.

3.17 ß-Galactosidase associated cell senescence

ß-galactosidase associated senescence was assayed at pH 6.0 according to the method of Dimri et al. (1995). Medium was discarded and cells were washed with PBS for three times. After that cells were fixed by 3% formaldehyde for 5 min, washed with PBS, and then incubated in freshly prepared staining of 40 mM citrate-phosphate buffer, pH 6.0, containing 1 mg/ml of 5-bromo-4-chloro-3-indolyl-ß-D-galactopyranoside (X-gal), 5 mM potassium ferrocyanide, 5 mM potassium ferricyanide, 150 mM NaCl, and 2 mM $MgCl_2$. Stain was visible 12 h after incubation at 37°C. Beta-galactosidase activity was detected by phase contrast microscopy.

3.18 Autofluorescence of the primary cultures

Autofluorescence was assessed under excitation ranging from 360 to 600 nm (UV-blue light) and visualised by Leica microscope (DMIRBe).

3.19 DNA microarray

For microarray analysis triplicates of 10 cm dishes with CGN were grown for DIV 7 and DIV 40 in order to extract and later analyze RNA expression of these two time points. Microarray analysis was perfromed using Affymetrix Rat Genome Array 34A in collaboration with the Institute for Human Genetics (of the University of Tübingen). The expression of some genes was checked once more using real time PCR.

3.20 Real-Time PCR

3.20.1 RNA extraction

Cells were scraped in PBS, spinned down and placed in Trizol reagent. In this reagent they were homogenized with syringe (18, 22, 25 gauge). Chloroform was added to the cells with Trizol to get rid of the protein content and after centrifugation supernatant was collected and mixed with isopropanol to precipitate RNA. After centrifugation the pellet was mixed with 75% ethanol and centrifuged again. The pellet, which contained RNA and DNA, was diluted in water and left with DNAse I on 37°C for half an hour. Reaction was stopped by addition of EDTA. The whole procedure was repeated one more time. In the end after washing step with ethanol and centrifugation, RNA was diluted in RNAse free water and the concentration was measured.

3.20.2 cDNA synthesis

In order to synthesise cDNA, iScript cDNA synthesis kit was used. For the reaction 1 µM of RNA was mixed with 5x reaction mixture and water in a volume of 20 µl.

The protocol for the cycler was as follows:

- 5 min at 25°C
- 32 min at 42°C
- 5 min at 85°C

- cool to 4°C

For real time PCR reactions, 1 µl of cDNA was used per reaction.

3.20.3 Real Time PCR protocol

PCR mix per reaction

Table 13

Forward primer	1.2 µl
Reverse primer	1.2 µl
H_20	2.4 µl
Syber green mix	10 µl
cDNA	5 µl

The protocol for the cycler:

- 10 min at 95°C
- 45x:

15 sec at 95°C

1 min at 60°C

1 min at 95°C

- 30 sec at 55°C
- 30 sec at 95°C

3.20.3.1 Real Time PCR calculations

Relative gene expression was determined based on the threshold cycles (Ct) of the gene of interest and of internal reference gene (actin or GAPDH).

3.21 Intracellular free Ca^{2+} concentration measurements

Ca^{2+} changes were measured in individual CGN by fluorescent microscopy using the Ca^{2+} -indicator Fura-2-AM. Neuronal cells loaded with 2 µM Fura-2-AM for 20 min at 37°C in CSS-5 buffer (120 mM NaCl, 5 mM KCl, 1.8 mM CaCl2, 15 mM glucose, and 25 mM HEPES (pH 7.4)

supplemented with 10 µM glycine and 2 mM Mg^{2+}. The measurement was performed at 37°C using a Nikon microscope with a 40x oil immersion lens. Fura-2-AM was excited at a wavelength of 340 and 380 nm, and emitted fluorescence was collected via a 510 nm band pass filter using a cooled CCD camera.

3.22 Statistics

Data were averaged and presented as mean ± SD. Statistical comparisons were made using Student's, unpaired *t* test. To compare data among groups of treatments, one-way ANOVA followed by Bonferroni's multiple comparison test was taken. Significance was assumed when $P < 0.05$ (prism, GraphPad, San Diego).

4 Results

4.1 Primary cerebellar granule neurons as a long term culture

CGN are viable in culture for 2 months. A first report on long term cultures of cerebellar granule neurons claimed that CGN can survive *in vitro* for 17 days (Ishitani et al., 1996). Later, Toescu and colleagues kept CGN for 23 DIV (days *in vitro*) in order to study changes in Ca^{2+} homeostasis related to aging (Toescu et al., 2000). Ishitani and colleagues reported that after 17 days in culture CGN rapidly and synchronously underwent glyceraldehyde-3-phosphate dehydrogenase-dependent apoptosis. In order to test this hypothesis we prepared cultures, left them aging, and checked every day if there were any changes. We splitted cultures into two groups: one that got no additives and the other one which got after DIV 7 every third day 5 mM glucose supplement. Cells with no additional nutrient died in the period of DIV 17-19, and the cells with glucose addition did not. To ensure that the addition of glucose was the reason for the survival of neurons we prepaired three groups of cultures with a different density of neurons (1×10^6 cells/cm^2, 1.5×10^6 cells/cm^2, 2×10^6 cells/cm^2) and separated them again into two groups: with or without 5 mM glucose addition every third day (Figure 1). The cultures with the highest number of cells showed the shortest life-span that was extended by the addition of glucose, indicating that the availability of glucose was the limiting factor.

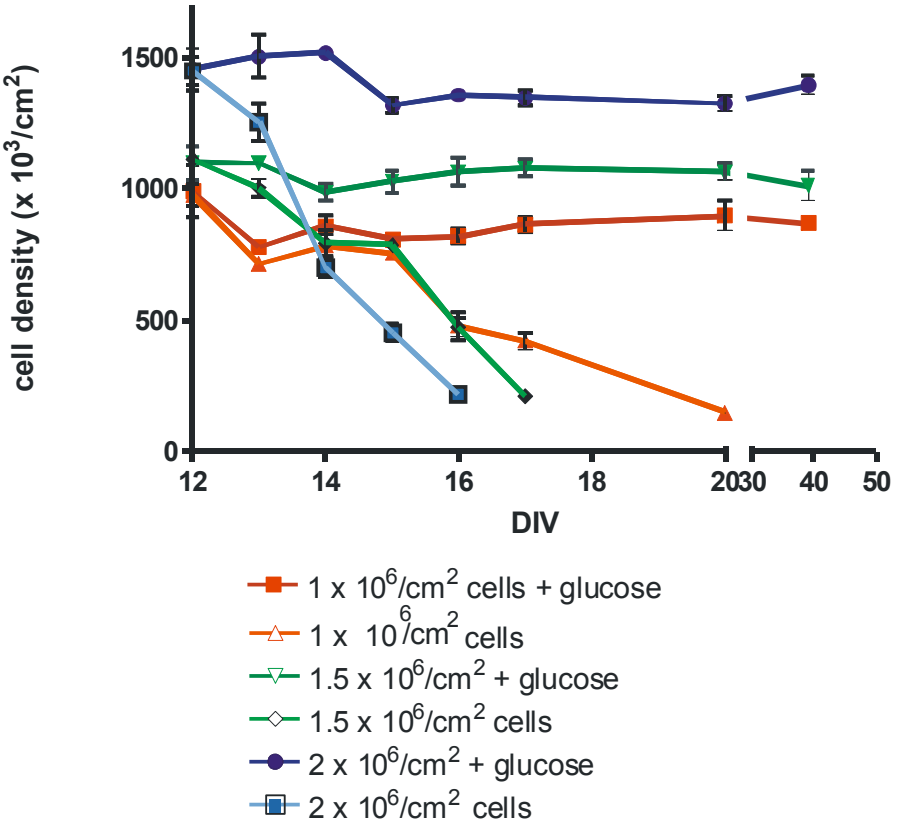

Figure 1: Viability of cerebellar granule neurons depending on the availability of nutrients from the medium. CGN were seeded in three different densities (1 x 10^6/cm^2, 1.5 x 10^6/cm^2, and 2 x 10^6/cm^2 and were cultured with or without regular glucose replenishment (5 µM, every three days). Viability was measured by FDA staining.

The next step was to test how long CGN cultures would survive if only glucose was replenished. CGN survived up to sixty days just with 5 mM regular glucose supplement every three days. We then asked whether the acidification of the medium was a limiting factor, because cell culture medium during this time became acidic (~ pH 6). Complete medium change is toxic for differentiated CGN in culture (Schramm et al., 1990), therefore we replaced only 25% of media starting at DIV 14 and kept changing it two times per week, adding once per week extra 10 µM AraC. Furthermore, for replacement we used synthetic serum instead of fetal calf serum. There was no proliferation of astrocytes, but they increased in size during the first 14 days (Figure 2). Under these conditions CGN kept their

usual morphology with abundant neurites for a period of two months (Figure 3).

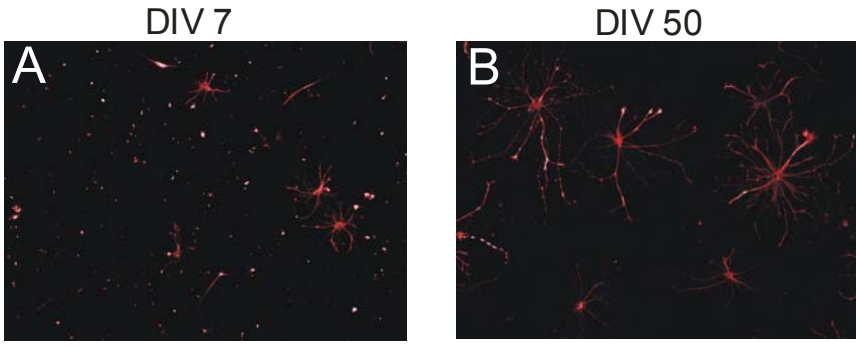

Figure 2: Astroglial contamination of neuronal cultures. (A) DIV 7 and (B) DIV 50 cultures were immunofluorescently labelled using polyclonal anti-GFAP primary antibody. Astrocytes were visualized using Cy3-conjugated anti-rabbit antibody.

Until DIV 45 to 55 cultures were healthy without significant death of CGN. After this time neurons started dying, but not synchronously. Within the next two weeks, cultures were depleted from neurons alive.

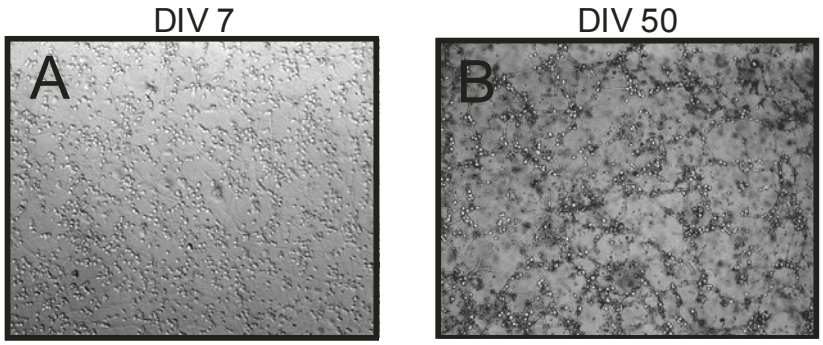

Figure 3: Morphology of CGN after 7 days (A) and 50 days (B) *in vitro*: Phase-contrast microscopy shows the same culture at DIV 7 and DIV 50. At DIV 50 the number of cells is lower in old cultures (B), but the remaining neurons have abundant synaptic contacts and normal morphology.

4.2 Markers of cellular aging

4.2.1 β–Galactosidase activity and autofluorescence as markers of aging

To characterize this model and to study whether there are any similarities to known changes during physiological aging *in vivo* we investigated established markers of aging in CGN *in vitro*.

β–Galactosidase (β-gal) activity increases during replicative senescence of fibroblasts in culture and has been widely used as a marker of cellular senescence (Dimri et al., 1995). Detectable at a pH of 6, senescence associated β-gal activity may result from increased lysosome activities in senescent cells. Evidence points to a rise in the activity of β-gal in senescent cells correlating with a rise in the level of the lysosomal enzyme (Kurz et al., 2000). Old astrocytes (Figure 4B) showed increased β-gal activity compared with astrocytes in young cultures (Figure 4A). However, neurons showed no β-gal activity at any time point (Figure 4A,B)

A typical marker of cellular aging is accumulation of undegradable pigment in the cytoplasm. Lipofuscin (age pigment) is a brown-yellow, electron-dense, autofluorescent material that accumulates progressively over time in lysosomes of postmitotic cells. We investigated accumulation of it by its autofluorescence. The autofluorescent granules were noticeable in the cytoplasm of old astrocytes, but we were not able to detect it in old neurons (Figure 4C-F).

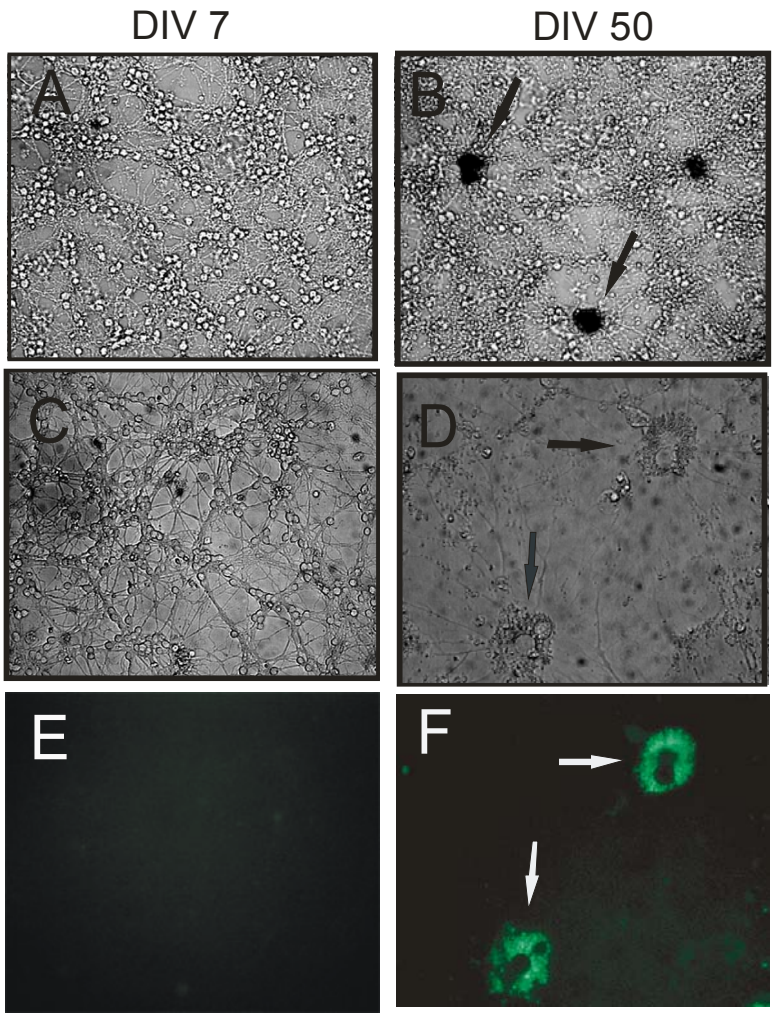

Figure 4: Comparison of senescence associated β-gal activity and autofluorescence in young and old CGN. β-Galactosidase activity was assessed by cytochemistry at pH 6 (A,B) showing senescencent astrocytes in old cultures (B) in opposite to young CGN, in which no staining was noticed (A). Phase contrast (C,D) and fluorescence microscopy (DAPI filter) (E,F) showed autofluorescence of astrocytes at DIV 50 (D,F), which is not present at DIV 7 (C,E).

4.2.2 Increased oxidative stress markers

To test whether there was increased oxidative stress to proteins and abberant protein formation we investigated protein carbonylation and ubiquitination in cultures of CGN at different time points (gradually increasing time in culture – DIV 7, 20, 30, 40, and 50).

Lysine, arginine, proline, and threonine residues of proteins are particularly sensitive to metal-catalyzed oxidation, leading to the formation of carbonyl

derivatives (Amici et al., 1989). Protein carbonyl content in cultured human dermal fibroblasts has been shown to increase exponentially with the age of the fibroblast donor (Stadtman, 1992). Carbonyl formation is irreversible, and thus the only way to eliminate altered proteins is the degradation process (Friguet et al., 2000) As shown for the aging of hippocampal neurons aging *in vitro* (Aksenova et al., 1999), we also found increase in protein carbonylation which gradually increased over the time in culture (Figure 5C).

The proteasome is known to be one of the major proteolytic systems involved in the removal of oxidized proteins. Thus, investigations have focused on a possible decline in the proteasome activity with age that may explain the age-related accumulation of oxidized proteins. We first looked at the amount of ubiqitinized proteins and measured proteasomal activity. The steady-state level of oxidized protein reflects the balance between the rate of protein oxidation and the rate of protein degradation. Age-related accumulation of altered protein can be due to an increase of free radical-mediated damage, a loss of proteasomal activity, or the combination of both mechanisms. Protein ubiquitination of high molecular weight proteins increased in old compared with young cultures, whereas the concentration of non-covalently bound ubiquitin decreased over time (Figure 5 A,B).

The proteasome can cleave peptides on the carboxyl side of hydrophobic, basic, and acid residues (Orlowski, 1990). These proteolytic functions commonly referred to as the chymotryptic, tryptic, and postacidic or caspase-like activities can be measured by evaluating the hydrolysis of specific fluorogenic substrates. CGN at DIV 7 and DIV 50 were homogenized in a buffer containing 5 mM ATP and 20% glycerol to preserve the integrity of the 26S proteasome, and their supernatant fractions were tested for the ability to hydrolyze Suc-LLVY-MCA, a substrate for chymotrypsin-like activity. Assays were performed in a buffer (pH 8.0) containing 5 mM EGTA to inhibit lysosomal peptidases and calpains. We found a significant decrease of proteasomal activity in old neuronal cultures (Figure 5D).

To ascertain whether the decline in proteasome activity was due to a decrease in the actual proteasomal content, equal amounts of proteins from both age groups were subjected to SDS-PAGE, and probed with a monoclonal antibody directed against all 20S α-proteasome subunits. As shown in Figure 5E, the intracellular proteasomal concentration remained unchanged through the time indicating that the observed decline in proteasomal activity must be due to another cause.

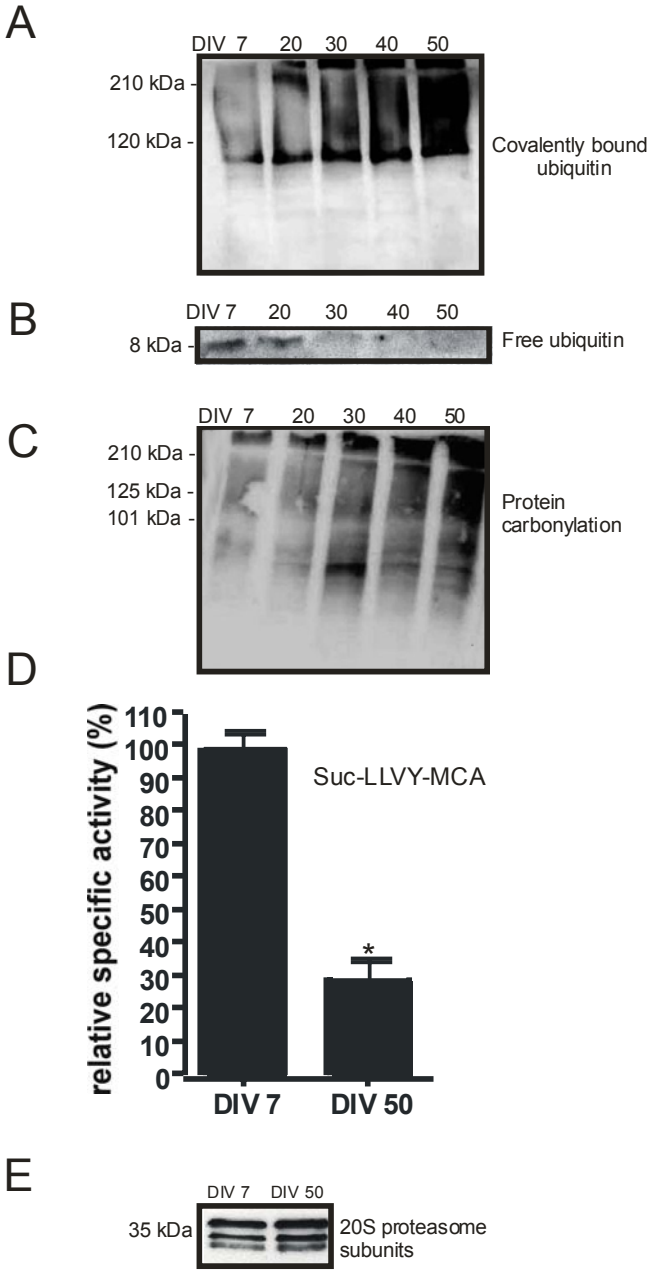

Figure 5: Protein carbonylation, protesomal activity and expression in aging neurons *in vitro*.
(A) Ubiquitination of proteins and (B) free ubiquitin from cells which were cultured *in vitro* for the time indicated. Cell lysates were incubated with monoclonal antibody which recognises conjugated and free form of ubiquitin. (C) Protein lysates incubated with 2,4-dinitrophenylhydrazine, denaturated with 12% SDS, neutralized with neutralization solution (Oxyblot kit) and immunobloted against anti-DNP antibody in order to visualise protein carbonylation. (D) Protein lysates (10 µg) were incubated with substrate specific for chymotrypsin-like activity (Suc-LLVY-MCA) for 6 h. The specific activity is expressed as the percentage of activities of young cells, which have been set to 100%. *p<0.0001, Student´s t-test. (E) Western blot analysis of proteasome content in 20 µg protein of whole cell extracts, from DIV 7 and DIV 50, performed with a monoclonal antibody against the α-subunits of the 20S proteasome.

4.3 Gene expression profiling

In order to examine the molecular events associated with aging of cerebellar granule neurons in vitro (DIV 7 vs. DIV 40) we used The Rat Genome U34A Array which contains probe sets representing all full-length or annotated genes, as well as thousands of EST clusters (8799 transcripts). For our probes we used three independent preparations of primary cell cultures which we divided into two groups. First half we used at DIV 7, and the other half at DIV 40 for RNA isolation and microarray analysis.

For normalization of results we used the normalization ArrayAssist 3.3 software. We statistically analyzed data using *t*-test with unequal variance. When setting the p-value to 0.05 and the signal log ratio to 1 or more we got 373 genes that were differentially regulated when young and old neuronal cultures were compared (Figure 6). Using more stringent conditions, with the p-value being 0.01, we got 211 genes that were significantly regulated between the two conditions. For further analysis of data we used Ingenuity Systems pathway analysis software 3.0 in order to get a better insight into complex changes in gene expression. Out of the 373 genes, only 216 genes were eligible for analysis, because on a rat array the nature of many genes is still unknown (EST clusters).

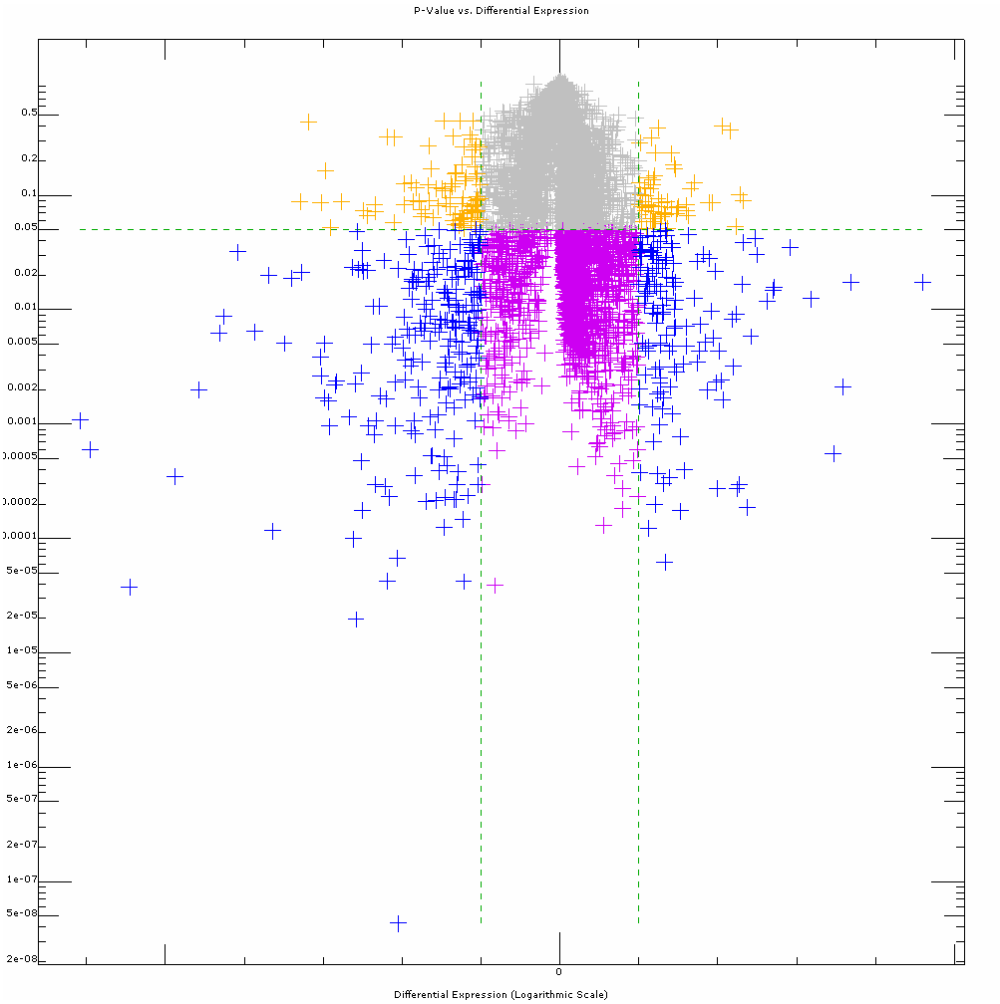

Figure 6: Gene expression projecting p-value vs. differential gene expression. Blue crosses represent significantly up- or downregulated transcripts (p< 0.05, signal log ratio of 1 - two times regulated or more). Not statisticaly significant but two or more times up- or downregulated: yellow crosses, not statistically significant and less then two times up- or downregulated: purple crosses, statistically significant but less then two times up- or downregulated: grey crosses.

We found that aging of CGN *in vitro* resulted in differential expression pattern indicative of a marked stress response, and differential expression of metabolic, biosynthetic, structural proteins, as well as plasma membrane receptors and channels. (Table 13-18).

Table 13: Transcription

Down-regulated genes (values in blue) are indicated by a minus sign in the fold column, whereas positive values represent up-regulated genes (in red).

Unigene	GeneID	Fold	p-value	Title	Gene Symbol
Rn.11134	AF055884_s_at	-2,01	0,002	DEAF-1 related transcriptional regulator (NUDR)	Deaf1
Rn.9909	AB012230_g_at	-2,04	0,004	nuclear factor I/B	Nfib
Rn.56776	AB012234_g_at	-2,45	0,010	nuclear factor I/X	Nfix
Rn.7544	AF054586_at	-3,42	0,002	germinal histone H4 gene	H1ft
Rn.2874	D84418_s_at	-3,52	0,017	high mobility group box 2	Hmgb2
Rn.9981	U92564_at	-6,36	0,001	Olf-1/EBF associated Zn finger protein Roaz	Roaz
Rn.44289	D82074_at	-2,63	0,011	neurogenic differentiation 1	Neurod1
Rn.3306	D28557_s_at	-2,55	0,008	cold shock domain protein A	Csda
Rn.20403	D28560_g_at	-2,17	0,035	ectonucleotide pyrophosphatase/phosphodiesterase 2	Enpp2
Rn.86410	AB002406_at	2,37	0,009	RuvB-like protein 1	Ruvbl1

Table 14: Metabolism

Unigene	GeneID	Fold	p-value	Title	Gene Symbol
Rn.89705	U83880UTR#1_at	-3,83	0,007	glycerol-3-phosphate dehydrogenase 2	Gpd2
Rn.9437	X55286_at	-2,67	0,005	3-hydroxy-3-methylglutaryl-Coenzyme A reductase	Hmgcr
Rn.6995	M29472_at	-3	0,007	mevalonate kinase	Mvk
Rn.228	AB016800_g_at	-4,64	0,001	7-dehydrocholesterol reductase	Dhcr7
Rn.33239	D37920_at	-3,13	0,001	squalene epoxidase	Sqle
Rn.18983	AB009999_g_at	2,41	0,003	CDP-diacylglycerol synthase (phosphatidate cytidylyltransferase) 1	Cds1
Rn.3561	rc_AA892314_at	-2,34	0,009	isocitrate dehydrogenase 1	Idh1
Rn.9744	rc_AI228110_s_at	-3,64	0,004	UDP-glucuronosyltransferase 8	Ugt8
Rn.2589	rc_AA942685_at	-2,2	0,007	cytosolic cysteine dioxygenase 1	Cdo1
Rn.9756	J05592_at	-2,25	0,007	protein phosphatase 1, regulatory (inhibitor) subunit 1A	Ppp1r1a
Rn.10119	D17809_at	-2,31	0,003	beta-4N-acetylgalactosaminyltransferase	Galgt1
Rn.5106	rc_AI177004_s_at	-2,1	0,008	3-hydroxy-3-methylglutaryl-Coenzyme A synthase 1	Hmgcs1
Rn.32351	X04979_at	-2,05	0,010	apolipoprotein E	Apoe
Rn.3661	U96130_at	4,19	0,002	glycogenin	Gyg
Rn.105862	AB012933_g_at	3,42	0,004	fatty acid Coenzyme A ligase, long chain 5	Facl5
Rn.874	J04792_at	2,74	0,010	ornithine decarboxylase 1	Odc1
Rn.3519	M26594_at	2,19	0,019	malic enzyme 1	Me1
Rn.11094	U32314_g_at	2,02	0,002	Pyruvate carboxylase	Pc
Rn.40123	rc_AI013194_at	2	0,017	eukaryotic initiation factor 5 (eIF-5)	Eif5
Rn.100813	rc_AI230228_at	3,09	0,045	phosphoserine aminotransferase 1	Psat1

Table 15: Structural, adhesion, and synaptic proteins

Unigene	GeneID	Fold	p-value	Title	Gene Symbol
Rn.7652	U75920_at	-2,38	0,003	microtubule-associated protein, RP/EB family, member 1	Mapre1
Rn.2458	rc_AA860030_s_at	-2,51	0,003	tubulin, beta 5	Tubb5
Rn.87540	M60666_s_at	-2,52	0,001	tropomyosin 1, alpha	Tpm1
Rn.8737	rc_AI175935_at	-2,67	0,013	myosin IE	Myo1e
Rn.11247	AB015042_s_at	-2,75	0,001	drebrin 1	Dbn1
Rn.35769	rc_AI009806_at	-2,9	0,000	dynein, cytoplasmic, light chain 1	Pin
Rn.88941	M73049_at	-2,92	0,001	internexin, alpha	Inexa
Rn.1646	U59241_at	-3,06	0,026	tropomodulin 1	Tmod1
Rn.3189	Y00826_at	3,79	0,010	nuclear pore membrane glycoprotein 210	Pom210
Rn.21397	D38492_at	-2,8	0,028	contactin 1	Cntn1
Rn.10075	U16845_at	-2,33	0,000	neurotrimin	RNU16845
Rn.10154	rc_AA859752_at	-3,01	0,036	noggin	Nog
Rn.92337	AB010436_at	4,73	0,009	cadherin 8	Cdh8
Rn.9943	D12519_s_at	-3,58	0,001	syntaxin 1a	Stx1a
Rn.107689	U56261_s_at	-3,25	0,016	synaptosomal-associated protein	Snap25
Rn.2163	M64780_at	-5,36	0,001	agrin	Agrn
Rn.22954	U67139_at	-2,59	0,018	PSD-95/SAP90-associated protein-3	DAP-3
Rn.9923	M27812_at	-2,13	0,018	synapsin 1	Syn1
Rn.31977	M24104_at	2,53	0,013	vesicle-associated membrane protein 1	Vamp1
Rn.10928	L21192_at	-2,63	0,006	growth associated protein 43	Gap43

Table 16: Signal transduction

Unigene	GeneID	Fold	p-value	Title	Gene Symbol
Rn.11243	J03806_at	-2,12	0,006	phospholipase C, gamma 1	Plcg1
Rn.108127	M31788_g_at	2,02	0,001	phosphoglycerate kinase 1	Pgk1
Rn.10251	S66024_at	4,73	0,000	cAMP responsive element modulator	Crem
Rn.64487	rc_AI639196_at	2,97	0,003	collybistin I	Arhgef9
Rn.42890	U78517_at	3,27	0,013	cAMP-regulated guanine nucleotide exchange factor II	Cgef2
Rn.10382	L26986_at	4,84	0,000	adenylyl cyclase 8	Adcy8
Rn.11081	U48596_g_at	-2,1	0,004	mitogen activated protein kinase kinase kinase 1	Map3k1
Rn.9903	AF037071_at	-2,13	0,014	C-terminal PDZ domain ligand of neuronal nitric oxide synthase	Capon
Rn.34915	M99169_at	-2,26	0,003	S6 protein kinase (Rsk-1)	Rps6ka1
Rn.20765	AJ005424_g_at	-2,47	0,000	mitogen-activated protein kinase 7	Mapk7
Rn.87208	J05072_at	-3,13	0,009	calcium/calmodulin-dependent protein kinase II, delta	Camk2d

Rn.14558	AB011528_at	-3,22	0,010	cadherin EGF LAG seven-pass G-type receptor 3	Celsr3
Rn.1840	S49760_g_at	-3,35	0,003	diacylglycerol kinase, alpha (80 kDa)	Dgka
Rn.9958	rc_AI102205_s_at	-8,45	0,001	vesicle-associated calmodulin-binding protein	1G5
Rn.11266	X67108_at	2,27	0,010	brain derived neurotrophic factor	Bdnf
Rn.34418	M25890_at	-8,57	0,002	somatostatin	Sst

Table 17: Receptors and channels

Unigene	GeneID	Fold	p-value	Title	Gene Symbol
Rn.4958	M91808_at	2,04	0,023	sodium channel, voltage-gated, type I, beta polypeptide	Scn1b
Rn.9863	L02315_at	2,07	0,037	calcium channel, voltage-dependent, beta 4 subunit	Cacnb4
Rn.32079	M22253_at	5,36	0,006	sodium channel, voltage-gated, type 1, alpha polypeptide	Scn1a
Rn.10019	U10354_at	3,22	0,002	calcium-sensing receptor	Casr
Rn.87696	Z11548_at	-2,06	0,036	glutamate receptor, ionotropic, kainate 2	Grik2
Rn.91361	M38061_at	-2,16	0,011	glutamate receptor, ionotropic, 2	Gria2
Rn.89046	M90518_at	-2,43	0,008	glutamate receptor, metabotropic 4	Grm4
Rn.10368	X51992_at	-2,63	0,034	gamma-aminobutyric acid A receptor, alpha 5	Gabra5
Rn.81205	S55933_i_at	-3,24	0,001	gamma-aminobutyric acid (GABA-A) receptor, subunit alpha 4	Gabra4
Rn.74042	Z11581_at	-3,39	0,007	glutamate receptor, ionotropic, kainate 5	Grik5
Rn.41715	M92076_at	-3,88	0,004	glutamate receptor, metabotropic 3	Grm3
Rn.9840	U11418_s_at	-3,56	0,001	glutamate receptor, ionotropic, N-methyl D-aspartate 1	Grin1
Rn.4089	D13985_at	1,71	0,003	chloride channel, nucleotide-sensitive, 1A	Clns1a
Rn.2992	M28647_g_at	-1,7	0,005	ATPase, Na+K+ transporting, alpha 1	Atp1a1
Rn.11523	AF051561_s_at	-1,63	0,007	solute carrier family 12, member 2	Slc12a2
Rn.74242	AF021923_at	1,68	0,001	solute carrier family 24 (sodium/potassium/calcium exchanger), member 2	Slc24a2
Rn.6384	D63772_at	-2,24	0,007	solute carrier family 1, member 1	Slc1a1
Rn.5805	M93017_at	-1,77	0,003	ATPase, Ca++-sequestering	Atp2c1
Rn.87329	M28648_s_at	-3,46	0,019	ATPase, Na+/K+ transporting, alpha 3 polypeptide	Atp1a3
Rn.10035	rc_AI228669_at	-3,86	0,041	GABA transporter protein	Gabt1
Rn.10624	J04629_at	-2,49	0,022	ATPase, Na+/K+ transporting, beta 2 polypeptide	Atp1b2

Table 18: Stress

Unigene	GeneID	Fold	p-value	Title	Gene Symbol
Rn.25166	AB008807_g_at	2,28	0,032	glutathione S-transferase omega 1	Gsto1
Rn.3647	L24896_s_at	1,68	0,007	glutathione peroxidase 4	Gpx4
Rn.3904	rc_AI170685_g_at	1,77	0,003	DnaJ (Hsp40) homolog, subfamily A, member 2	Dnaja2
Rn.1438	U77933_at	-1,63	0,005	caspase 2	Casp2

Rn.44942	AF044201_at	3,6	0,005	lifeguard	Lfg
Rn.11183	U30186_at	4,58	0,003	DNA-damage inducible transcript 3	Ddit3
Rn.10562	U84410_s_at	-2,13	0,011	caspase 3	Casp3
Rn.44369	S67722_s_at	-3,01	0,021	prostaglandin-endoperoxide synthase 2	Ptgs2
Rn.98208	M55534mRNA_s_at	3,35	0,026	crystallin, alpha B	Cryab
Rn.2084	rc_H31665_at	2,36	0,001	hypoxia induced gene 1	Hig1
Rn.54397	rc_AI102562_at	2,47	0,009	Metallothionein	Mt1a
Rn.37805	rc_AI236601_at	2,05	0,029	Rattus norvegicus similar to heat shock protein 105 kDa alpha (LOC288444), mRNA	---
Rn.2011	rc_AA799650_at	2,18	0,005	peroxiredoxin 3	Prdx3
Rn.6173	M63901_g_at	2,26	0,001	secretory granule neuroendocrine protein 1	Sgne1
Rn.107266	AF030358_g_at	3,9	0,022	chemokine (C-X3-C motif) ligand 1	Cx3cl1
Rn.11400	J04488_at	4,1	0,002	prostaglandin D2 synthase	Ptgds

To verify the microarray data Real-Time PCR was performed to measure transcript levels of 10 genes (Figure 7) at DIV 7 and DIV 40. The ratios measured by Real-Time PCR analysis were similar to those measured by the microarray experiments.

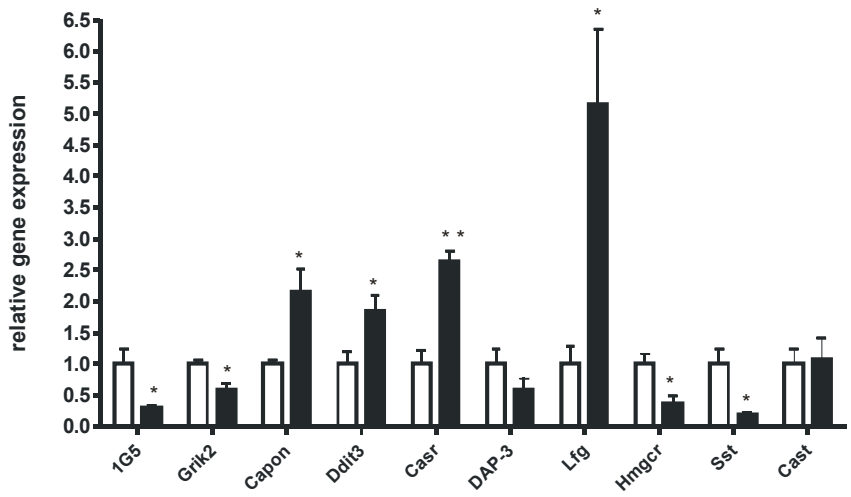

Figure 7: Real-time PCR confirmation of array results for select genes. For PCR, relative changes in gene expression (fold change) were calculated using the $2^{-\Delta\Delta C_T}$ method where C_T is threshold cycle. Also, the PCR fold change is relative to control cDNA while using GAPDH expression as a reference gene. Calpastatin (Cast) was selected as a gene whose expression was unchanged between groups based on array results. *p<0.05, **p<0.005 according to Student´s t-test. (1G5 - vesicle-associated calmodulin-binding protein; Grik2 - glutamate receptor, ionotropic, kainate 2; Capon - C-terminal PDZ domain ligand of neuronal nitric

oxide synthase; Ddit3 - DNA-damage inducible transcript 3; Casr - calcium-sensing receptor; DAP-3 - PSD-95/SAP90-associated protein-3; Lfg - lifeguard; Hmgcr - 3-hydroxy-3-methylglutaryl-Coenzyme A reductase; Sst – somatostatin; Cast – calpastatin).

4.4 Protein expression

To characterize the molecular properties of the long term culture, we evaluated the expression of proteins involved in differentiation, metabolism, oxidative stress response, and apoptosis (Figure 8). Total protein extracts collected from different time points (DIV 7, 20, 30, 40, 50) were analyzed by immunobloting.

Analysis of proteins involved in promoting or inhibiting cell death pathways revealed that three antiapoptotic proteins, Bcl-x_L, Bcl-2, and lifeguard increased their expression during the time in culture, while Bax, a proapoptotic protein, showed down-regulation with the time in culture (Figure 8 A,B). Lifeguard was also significantly upregulated in the microarray analysis (Table 18, Figure 7). The metabolic enzyme, glyceraldehyde-3-phosphate dehydrogenase (GAPDH), was also analyzed and it appeared to be stably expressed over the whole time *in vitro* (Figure 8 A,B). GAP-43, a common marker of differentiating neurons, is expressed at elevated levels by developing or regenerating neurons during axonal growth. We noticed down-regulation of this protein over time (Figure 8 A,B). This result was another conformation of our microarray analysis (Table 15). A presynaptic protein α-synuclein was also analyzed and showed to be stably expressed over the long term period of culturing. As the key cellular organelle responsible for transducing free energy from primary substrates into the ATP, the mitochondrion plays a central role in the majority of eukaryotic intracellular events. We further analysed two mitochondrial proteins. Cytochrome c is a redox protein, fourth in a row in respiratory chain and pro-apoptotic after release into the cytosol. Interestingly, we noticed upregulation of the expression of this protein at around DIV 20, which then stayed stable until DIV 50. MnSOD catalyzes the dismutation of two molecules of superoxide anion into water and

hydrogen peroxide. It is one of the cells primary defence against free radical mediated damage. Expression of this protein stayed stable over the whole period of *in vitro* culturing of cerebellar granule neurons. As a marker of glial contamination we analyzed expression of glial fibrilary acidic protein (GFAP). The expression increased from DIV 7 to DIV 20 and stayed constant until DIV 50.

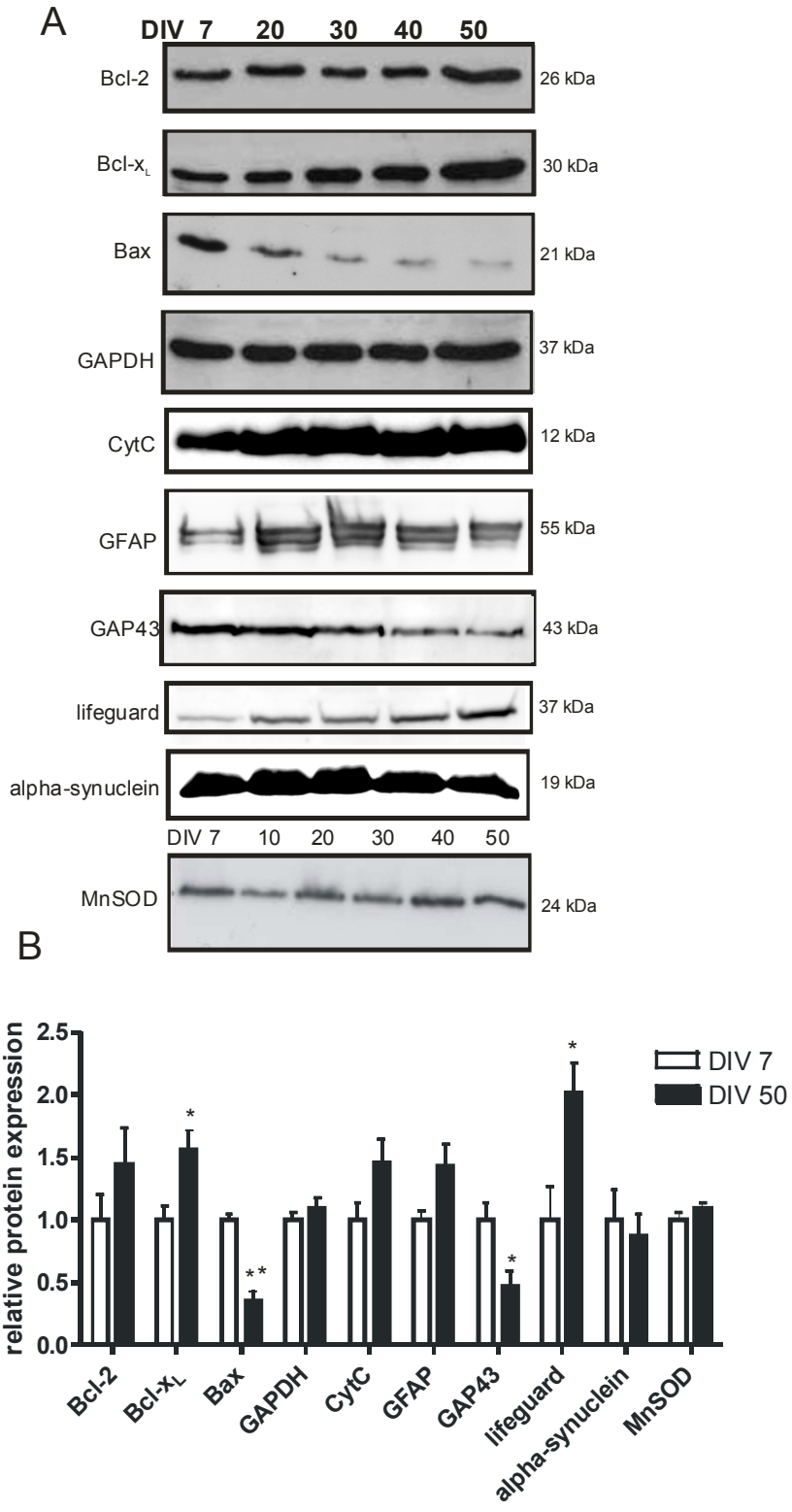

Figure 8: Maturation and aging of cerebellar granule neurons *in vitro*. (A) Total proteins were extracted from neuronal cultures at DIV 7, 10, 20, 30, 40 and 50.

Equal amount of protein (20 µg) was electrophoresed on 12-15% SDS-polyacrylamid gels, transferred to nitrocellulose membranes and then probed successively with specific monoclonal or polyclonal antibodies (see Materials and Methods). (B) The relative amount of each protein was quantified by densitometry as a ratio to actin. The values at DIV 7 were normalized to the value of 1. *p<0.05, **p<0.005 according to Student´s t-test. The values represent mean ± SD and are results from three independent cell cultures.

4.5 Reduced sensitivity to apoptosis in aged CGN

To investigate the functional consequences of aging in neurons, we compared cell death induced by different triggers at DIV 7 and DIV 50. Neuronal apoptosis is involved in brain development and is considered to play important role in neurodegenerative diseases. Mature cerebellar granule neurons deprived of depolarizing levels (25 mM) of extracellular potassium (K^+) undergo apoptosis characterized by chromatin condensation, pyknosis, and nucleosomal size DNA fragmentation in combination with serum withdrawal at DIV 7, whereas serum withdrawal alone only slightly reduces viability (D'Mello et al., 1993, Schulz et al., 1996; Armstrong et al., 1997; Gerhardt et al., 2001). After potassium deprivation for 24 h, ~50% of neurons die by apoptosis at DIV 7. The same experimental conditions did not induce apoptosis in old neurons at DIV 50 (Figure 9 A). These cells were resistant to the apoptotic stimulus of potassium withdrawal and no significant cell death occured. To test whether a different apoptotic stimulus would also result in a different response of old CGN compared with the vulnerability of young CGN, we treated neurons with staurosporine (1 µM), for 72 h. Staurosporine, a broad spectrum kinase inhibitor, decreased survival of CGN at DIV 7 cells, but not at DIV 50 (Figure 9 B).

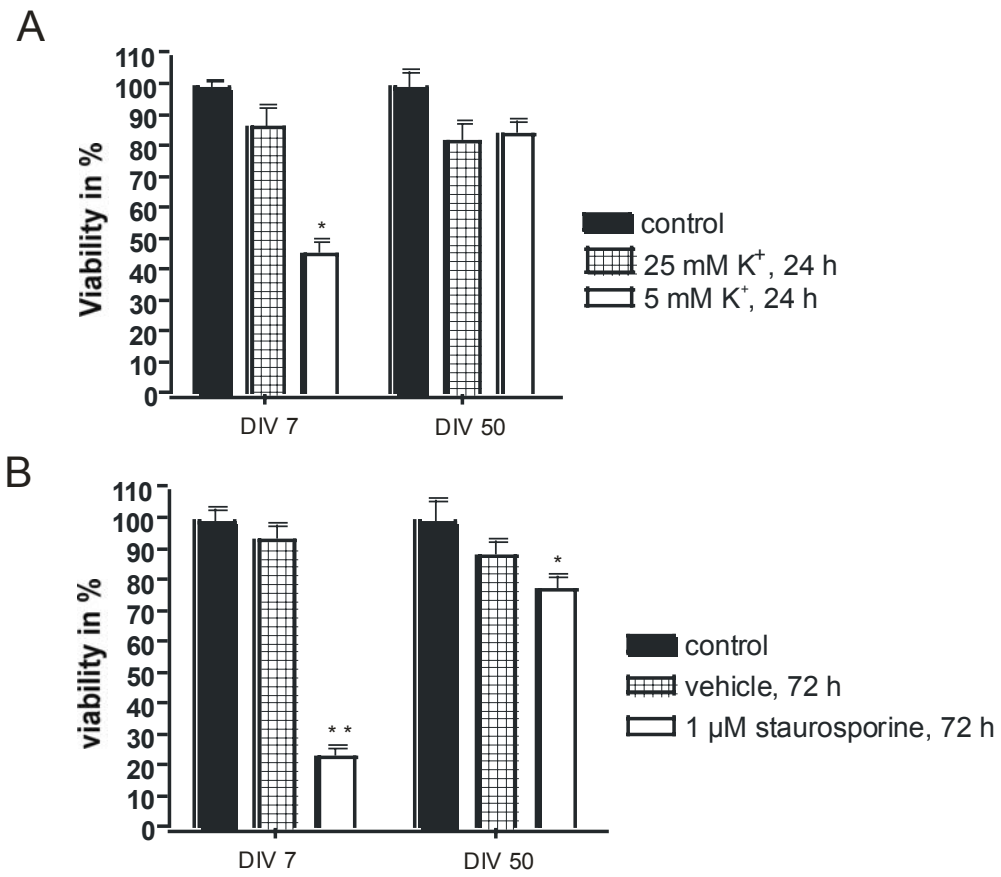

Figure 9: Differential sensitivity to apoptotic stimuli of young and old CGN. (A) DIV 7 and DIV 50 neurons were deprived from serum (25 mM K^+), or potassium and serum (5 mM K^+) and switched to serum free medium for 24 h. Controls were left untreated. At DIV 7, but not DIV 50, potassium deprivation induced cell death. (B) Young and old cells were treated with 1 µM staurosporine, or DMSO (as a vehicle) for 72 h. Survival was assessed by FDA viability staining. Values were normalized to controls that were set to 100%. **p<0.001, and *p<0.05, ANOVA followed by Bonferroni posthoc test. These experiments were performed at least three times with similar results.

4.5.1 Bax expression

Bcl-2 and related proteins from the same family are key regulators of apoptosis, the cell death suicide program which is critical for tissue development and homeostasis. The Bcl-2 family can roughly be divided into two groups: one which possess anti-apoptotic activity and one which promotes cell death. They have a property to make homodimers, but also heterodimers with different family members (Reed, 1996). Members of

both groups may neutralize each other. Pro- and anti-apoptotic Bcl-2 family members dimerize at the surface of mitochondria, where they compete to regulate cytochrome *c* exit by a still unclear process. Release of cytochrome *c* accompanies the activation of the caspase-3 via a mechanism involving the formation of the apoptosome (a protein complex comprising multimers of Apaf-1 and procapase-9) (Li et al., 1997).

We found a decrease of the protein level of Bax in culture (Figure 10 C) over time. To further explore the mechanisms of its downregulation we used Real-Time PCR to compare RNA expression of Bax in young and aged neurons. We observed no change of RNA level expression over time (Figure 10 D). Next we investigated whether the protein turn-over of Bax changed over 50 days in culture. According to Li and Dou (2000), Bax is under strong regulation of the ubiquitin/proteasome system in human cancer cells. Using two different inhibitors, calpain inhibitor 1 (10 µM), and MG132 (5 µM), we inhibited the proteasome in our cultures for 24 hours and made an immunoblot for Bax expression as well as for the ubiquitination of proteins. From our earlier analysis we knew already that cells at DIV 50 cells were more ubiqitinated then at DIV 7 (Figure 10 A). The inhibition of proteasome stopped protein degradation and increased overall ubiquitination of proteins in young cultures, but the level of Bax protein expression did not change (Figure 10 B). The ubiquitination in old cultures did not increase further with proteasomal inhibition (Figure 10 A,B). In order to investigate this phenomenon of age dependent Bax protein downregulation *in vivo*, we analyzed cerebellar protein extracts from young and old rats for bax expression (3 months and 24 months of age in three different samples for each age group). Interestingly, we noticed down-regulation of Bax protein in old animals as well (Figure 10 E, F).

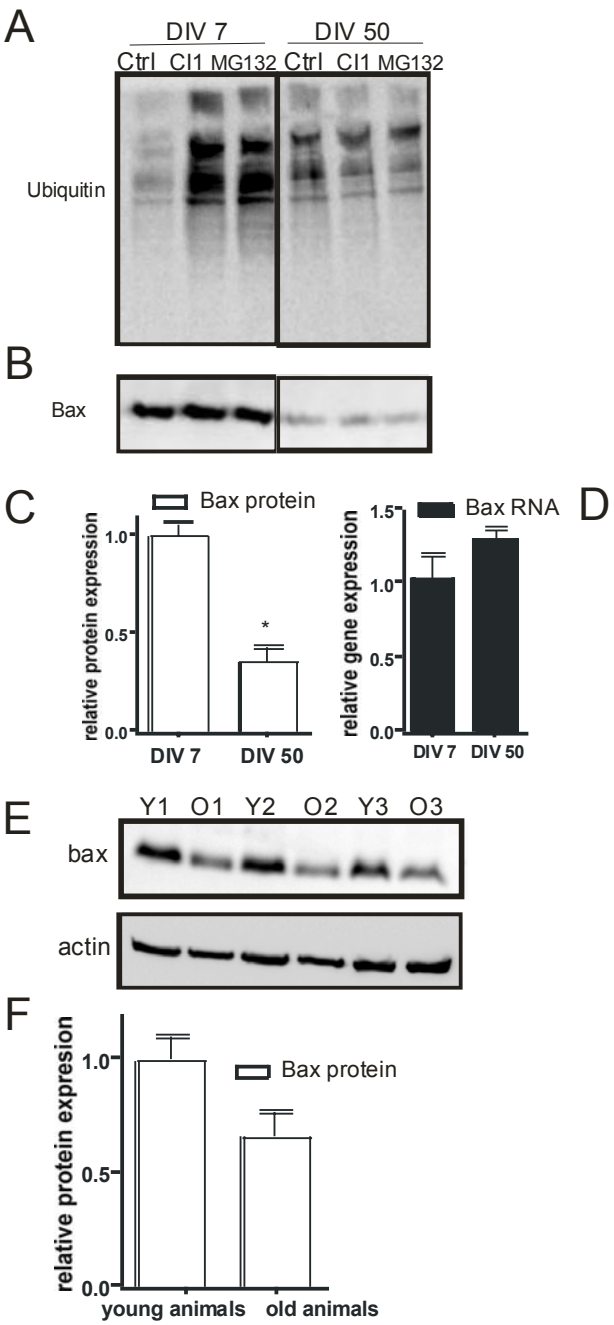

Figure 10: Bax protein expression after proteasomal inhibition. Young and old cultures were treated with MG132 (5 µM) and calpain inhibitor I – CI1 (10 µM) for 24h. (A) Proteasomal inhibition increases the amount of ubiquitinated proteins in young cultures but not old cultures. (B) Protein level of Bax does not change after proteasomal inhibition. (C) Bax protein expression decreases in aged cultures. The relative amount of protein was quantified by densitometry as ratios to actin. *p<0.05 according to Student´s t-test. The values of DIV 7 were assigned to 1. The values represent mean ± SD and are results from three independent cell cultures.

(D) Relative bax mRNA expression measured by real-time PCR. (E) Bax protein expression in cerebellar protein extracts of three young, 3 months (Y1, Y2, and Y3), and three old, 24 months (O1, O2, and O3) rats. The blot was stripped and reprobed with actin. (F) The relative amount of protein was quantified by densitometry as ratios to actin. Bax protein expression decreased, but not significantly.

4.5.2 Potassium withdrawal induces internucleosomal DNA cleavage of DNA at DIV 7 but not at DIV 50

Internucleosomal cleavage of DNA is caused by activation of caspase activated deoxyribonuclease (CAD) which pre-exists in living cells as an inactive complex with an inhibitory subunit (Nagata et al., 2000). Internucleosomal cleavage and is one of the biochemical characteristics of apoptosis. Activation of CAD occurs by cleaving the inhibitory subunit, which results in the release and activation of the catalytic subunit by caspase-3 (Enari et al.,1998). This fragmentation is easily evidenced by the electrophoretic migration of DNA into a ladder configuration. Potassium withdrawal from 25 mM to 5 mM in CGN causes DNA laddering pattern by random internucleosomal cleavage yielding different size multiplicates of 180 bp of DNA. Potassium withdrawal at DIV 7 leads to DNA fragmentation at 24 h and 48 h (Figure 11 A). At 72 h after potassium withdrawal, the laddering pattern is lost and the whole DNA is being degraded (Figure 11 A). The same treatment of CGN at DIV 50 produces no DNA fragmentation at any time point. When we treated cells with other cell death stimuli, such as glutamate (100 µM) or H_2O_2 (90 µM) for 24 h, we noticed DNA degradation in both ages (DIV 7 and DIV 50), but without characteristic apoptotic internucleosomal laddering pattern (Figure 11 B).

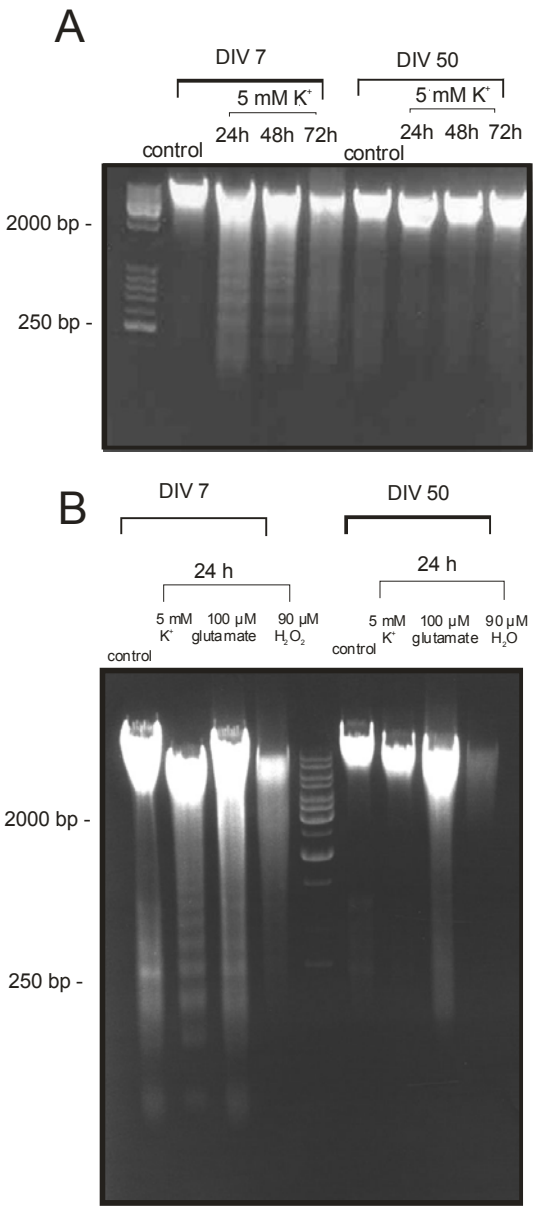

Figure 11: Internucleosomal cleavage as a marker of apoptosis does not occur after potassium withdrawal in old cultures. (A) After potassium withdrawal for 24h and 48h, characteristic DNA laddering pattern was visible, where at after 72h complete DNA degradation was noticed. In old cultures no DNA laddering pattern was visible at any time after potassium withdrawal. (B) At 24h, treatments such as potassium withdrawal, glutamate (100 µM) and H_2O_2 (90 µM) application caused apoptotic DNA laddering pattern in the young neuronal cultures only. However, DNA degradation into large fragments was noticeable in both conditions (DIV 7 and DIV 50) after treatment with glutamate and H_2O_2.

4.5.3 Caspase-3 expression and activity

To determine the cause of decreased sensitivity to apoptosis in old cerebellar granule neurons we first studied the expression of procaspase-3 as being the major executioner of this process. Caspases are highly conserved through evolution and also exist in simple model animals such as C. elegans (Yuan et al., 1993). The function of these enzymes is to cleave a restricted set of target proteins at specific points (after an aspartate residue) and activate or inactivate selected proteins. In order for this to happen, a caspase needs to be activated. Like many proteases they are synthesized as enzymatically inert zymogens. These zymogens are composed of three domains: an N-terminal prodomain, and the p20 and p10 domains. An active enzyme is a heterotetramer containing two p20/p10 heterodimers and two active sites (Earnshaw et al., 1999). There are three groups of caspases: caspases involved in inflammation (such as caspase-1, which is the interleukin1,3 converting enzyme), initiator and effector caspases. Effector caspases are usually activated proteolytically by an upstream caspase, whereas initiator caspases are activated through specific protein-protein interaction (Hengartner, 2000). Caspase-3 is an effector caspase in both, apoptosis induced by death-receptor and mitochondrial pathway. Studying its expression and activity in our model would give us useful information about the cell death mechanisms in young and old CGN.

We followed the expression of procaspase-3 in culture and noticed that it gradually decreases over time (Figure 12 A, B). Its expression is almost completely diminished at DIV 50. After potassium withdrawal for 6 h, at DIV 7 procaspase-3 was cleaved as shown by the occurrence of the p17 fragment, which indicates active form of caspase-3 (Figure 12 C). At DIV 50, hardly any procaspase-3 was expressed, and no active form of caspase-3 was noticed 6 h after switch (Figure 12 C).

Caspases selectively cleave a restricted set of target proteins after their activation, usually at one, or at most a few positions in the primary sequence. The caspase-3 assay is based on the hydrolysis of the peptide

substrate acetyl-asp-glu-val-asp-7-amido-4-methylcoumarin (Ac-DEVD-AMC), resulting in the release of the fluorescent 7-amido-4-methylcoumarin (Nicholson et al., 1995; Armstrong et al., 1996). Since different upstream pathways leading to apoptosis depend on caspase-3 induction for final apoptotic execution, eliminating caspase activity with pharmacological inhibitors or other means will slow down or even prevent apoptosis (Earnshaw et al., 1999). We measured caspase-3 activity six hours after potassium withdrawal and serum withdrawal at DIV 7 and DIV 50. Potassium withdrawal-induced caspase-3 activity was only detectable in CGN at DIV 7 but not DIV 50 (Figure 12 D). Peptide inhibitors of caspases have been shown to inhibit potassium withdrawal-induced apoptosis of CGN (Schulz et al., 1996). We tested the ability of zVAD-fmk, an irreversible pan-caspase inhibitor, to block caspase-3 activation after potassium deprivation. zVAD-fmk treatment (100 μM, 6 h) blocked caspase-3 activation in young cells as expected and was used as a control (Figure.12 D).

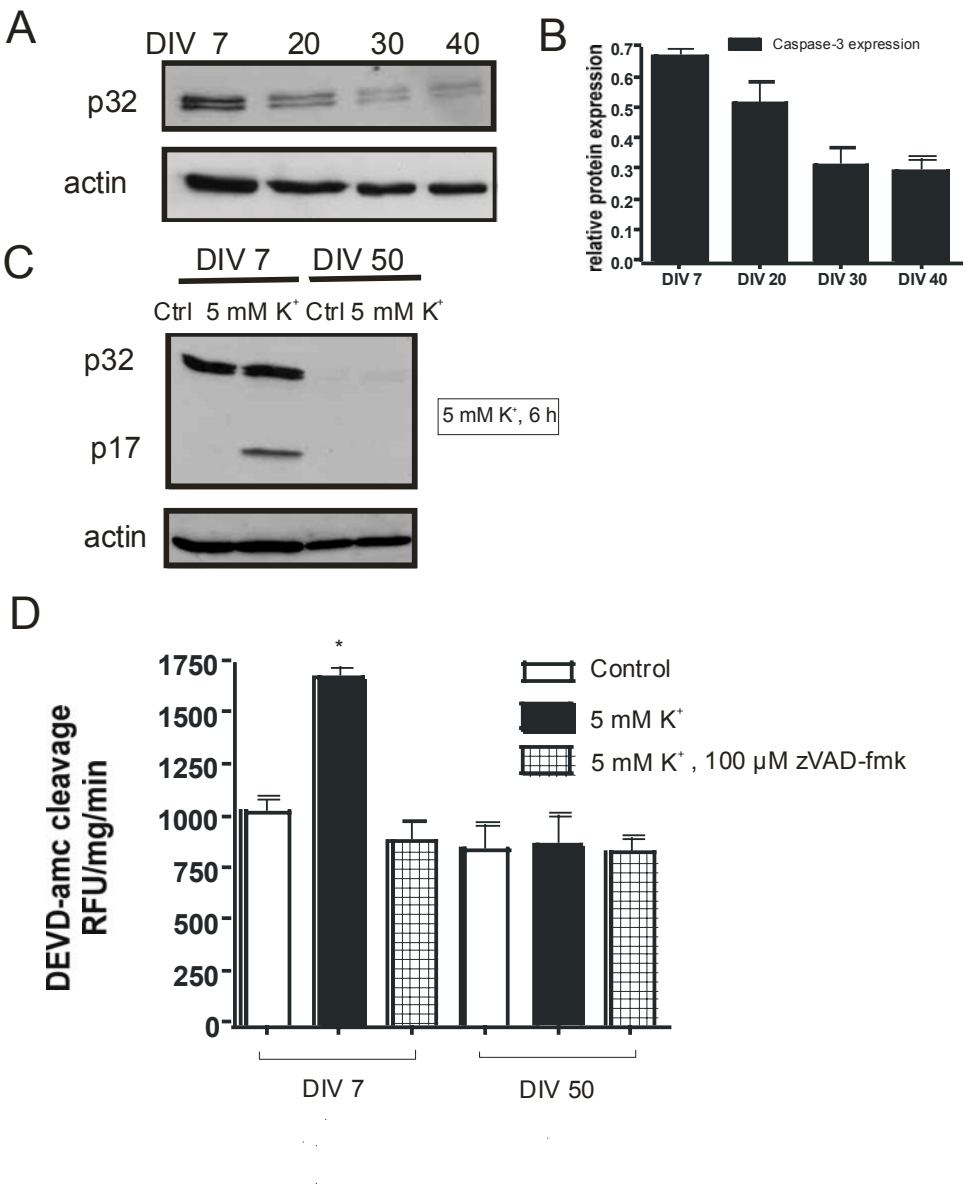

Figure 12: Caspase-3 expression and activity in young and old CGN. (A) Procaspase-3 expression decreases gradually with the time in culture. (B) Ratio between procaspase-3 expression and actin (bars represent SD and are results from three independent experiments) (C) Young and old CGN before and after potassium withdrawal (6 h). Active caspase-3 is visible at 17 kDa in young cultures after potassium deprivation. (D) Caspase-3 catalytic activity was determined by hydrolysis of the fluorogenic substrate Ac-DEVD-AMC in untreated cells and in potassium deprived cells in the absence or presence of the caspase inhibitor (zVAD-fmk). Data represent mean values ± SD of three independent experiments. *p<0.01, according to ANOVA and Bonferroni´s test. The activity was expressed as a relative fluorescence units/ mg of protein / min.

4.5.4 Tau protein expression

Tau protein is a microtubule associated protein (Weingarten et al., 1975) that is primarily restricted to neurons where it plays a role in stabilization of microtubules (Kanai et al., 1992). It has been proposed that phosphorylation of Tau regulates its binding to microtubules and its self aggregation in pathological conditions (Biernat et al., 1993; Goedert, 1996). To investigate whether hyperphosphorylation of Tau occurred during the aging process in vitro, total Tau protein was detected by the phosphorylation independent antibody K9JA or by monoclonal antibodies AT8 and PHF1, which selectively bind phospho-tau residues Ser202/Thr205 (Goedert et al., 1995) and Ser396/Ser404 (Otvos et al., 1994), respectively. Total Tau expression pattern was different between young and old neurons. Changes in Tau RNA splicing were demonstrated by Pizzi et al. (1995) who showed that CGN *in vitro* switch-on the exon containing four internal repeats by DIV 6 and switch-off of the mRNA containing three internal repeats after DIV 12.

As visualised by the shift of Tau to higher molecular weights using K9JA antibody, we found that old CGN use different RNA splicing mechanism as compared with young CGN (Figure 13). The phosphorylation of Tau at Ser202/Thr205 and Ser396/Ser404 did not seem to change with the time *in vitro*. However, there are other phosphorylation sites present on Tau protein which might be affected during the aging of CGN *in vitro*.

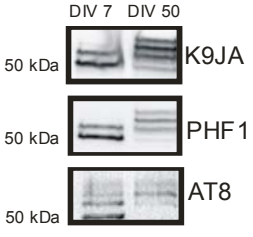

Figure 13: Expression and phosphorylation of Tau protein in young and old CGN *in vitro*. Expression and phosphorylation of tau proteins was analyzed in 20 µg of protein lysates from DIV 7 and DIV 50 neurons. Samples were incubated with either K9JA, phosphorylation independent antibody, or with PHF1, an antibody which recognizes phosphorylated epitope at Ser^{202}/Thr^{205}, or with AT8, an antibody which recognizes phosphorylated epitope at Ser^{396}/Ser^{404}.

4.5.5 Activation of the mitogen activated protein (MAP) kinase pathway

Mitogen activated protein kinases (MAPKs) are a family of related serine/threonine protein kinases that integrate diverse signals that direct cellular responses to proliferative cues or stressful stimuli (Davis, 1993). Extracellular-regulated protein kinase (ERK1/2) activation is typically associated with cell survival, proliferation, and differentiation given their activation by mitogens and cell survival factors (Xia et al., 1995). ROS contribute to cell death, in part, through effects on various cellular signalling pathways including the MAPK pathway (Bhat and Zhang, 1999; Guyton et al., 1996).

However, ERK1/2 activation may also contribute to neuronal cell death in some in vitro models of neurotoxicity (Murray et al., 1998, Lesuisse et al., 2002). Inhibition of the mitogen-activated protein kinase (MEK), the upstream activator of ERK1/2, protected albeit incompletely against apoptosis induced by nerve growth factor withdrawal of differentiated PC12 cells (Kummer et al., 1997). Also, it has been implicated that elevated calcium activates ERK1/2 (Grewal et al., 1999; Derkinderen et al., 1999).

We noticed that ERK1/2 is mildly phosphorylated in CGN, at DIV 50 but not at DIV 7 (Figure 14). Treatment with 100 µM glutamate led to a rapid, much stronger and sustained phosphorylation at DIV 50 but again not at DIV 7 neurons (Figure 14 B). Furthermore, potassium withdrawal did not activate ERK1/2 (Figure 14 C). When we treated cells with the MEK1/2 inhibitor, U0126 (10 µM), or NMDA receptor antagonist, MK801 (10 µM) for 24 h, we noticed an inhibition of phosphorylation of ERK1/2. However, viability assay did not show protection against glutamate-induced death in aged neurons after MEK1/2 inhibition, questioning the functional consenquences of ERK1/2 phosphorylation for the induction of cell death (Figure 14, E).

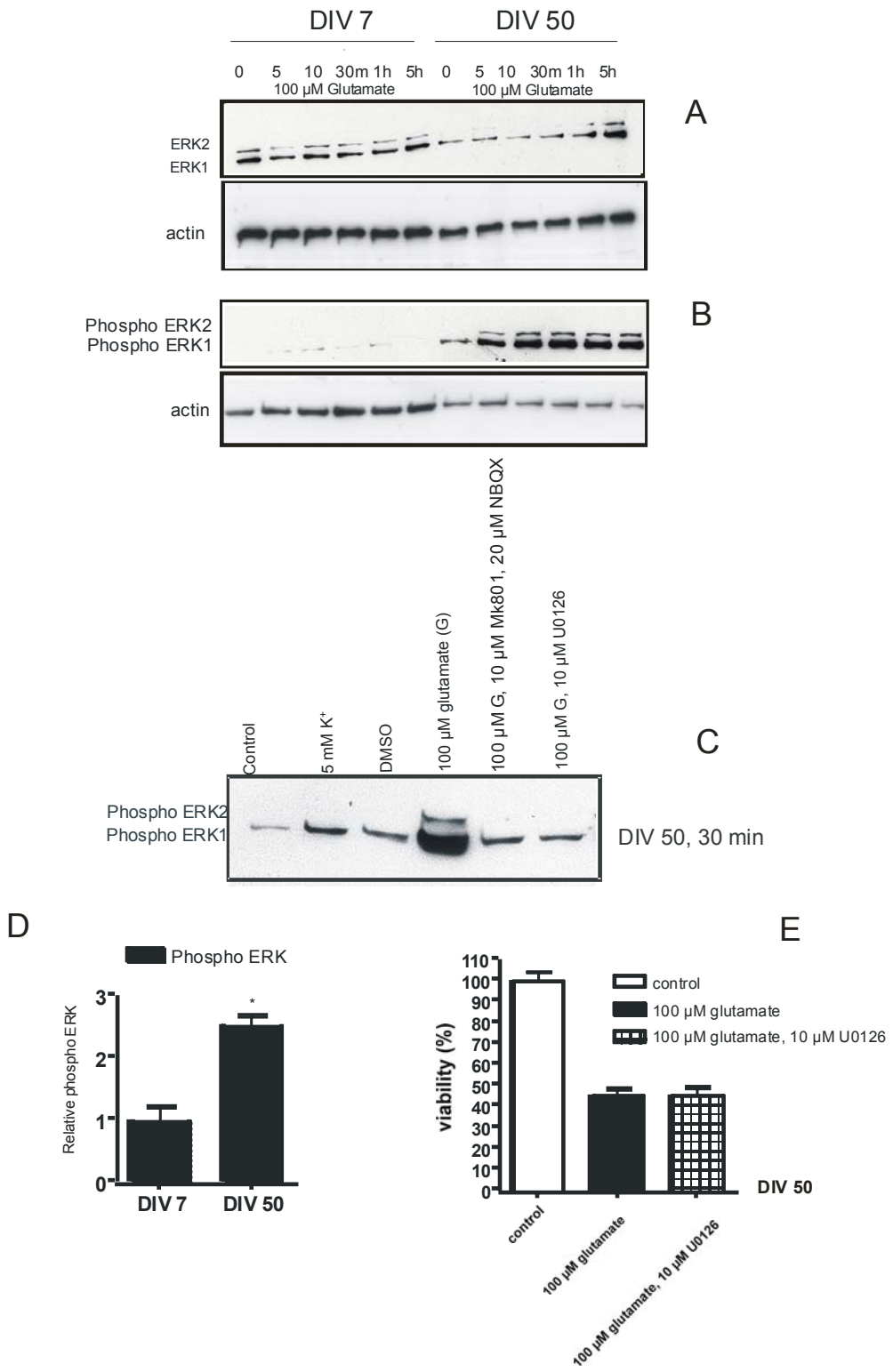

Figure 14: Extracellular-regulated protein kinase (ERK1/2) signalling in young and old cerebellar granule neurons. (A) Pan expression of ERK1/2 in young and old neurons after treatment with 100 µM glutamate for period from 0-5 h after treatment

and actin expression as internal loading control. (B) Phosphorylation of ERK1/2 after treatment with 100 µM glutamate for periods of 0, 5, 10, 30 minutes, 1 or 5 hours. (C) DIV 50 cultures were either switched to 5 mM K^+, or treated with DMSO, 100 µM glutamate, 100 µM glutamate together with 10 µM MK801 and 20 µM NBQX, or with 100 µM glutamate and 10 µM U0126 for 30 min and immunobloted with phospho-ERK1/2 antibody. Prominent phosphorylation only occurred when cells were treated with glutamate. (D) Relative phosphorylation of ERK1/2 in young and old neurons with no further treatment. Phosphorylation of ERK1/2 was increased in old cells compared with young ones (*p<0.05, Student´s t-test). (E) Treatment with 10 µM U0126 for 24 h did not protect cells against glutamate induced cell death.

4.5.6 Calpain activity

The calcium-dependent neutral cysteine protease, calpain, is present in virtually all vertebrate cells (Saido et al., 1994). Calpain is activated both in physiological states and also during various pathological conditions such as increased oxidative stress (Ray et al., 2000), Alzheimer's (Lee et al., 2000), and Parkinson's disease (Mouatt-Prigent et al., 1996). Under physiological conditions, the intracellular Ca^{2+} concentration is tightly regulated whereas under pathological conditions the intracellular Ca^{2+} concentration increases from extracellular pools through various channels and release from endoplasmatic reticulum stores. Excessive activation of calpain due to an increase in free Ca^{2+} leads to cytoskeletal protein breakdown, loss of structural integrity and disturbances of axonal transport and finally to neuronal death. Using a calpain assay kit, we measured its activity using Suc-LLVY-AMC as a fluorogenic substrate in the activation buffer (pH 7.4; with Ca^{2+} and reducing agent (TCEP)), as well as in inhibition buffer (containing calcium chelator BAPTA) for 1 h in dark at 37°C (Figure 15). The values from inhibition buffer were subtracted from the activation buffer and expressed as fluorogenic units (FU)/mg protein /min.

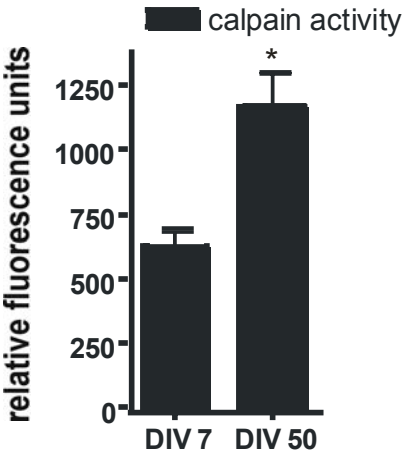

Figure 15 Calpain activity as a function of hydrolysis of Suc-LLVY-AMC. AMC was released upon cleavage with calpain and was measured fluorimetricaly at the excitation wavelength of 380 nm and the emission wavelength of 460 nm. The activity was expressed as the relative fluorescence units/ mg of protein / min. DIV 50 cells have significantly higher calpain activity (* $p<0.05$) according to Student's t-test.

4.5.7 Calpain substrates

Dozens of substrates for calpain have been identified and used to measure activation of the protease in the context of quantification of pathology. Many putative calpain substrates are cytoskeletal proteins especially those involved in cytoskeletal/plasma membrane interactions, kinases and phosphatases, membrane-associated proteins including some receptors and ion-channel proteins and some transcription factors (Goll et al., 2003).

Among the various substrate proteins for calpain, spectrin has been one of the most used markers of calpain activity, since this major cytoskeletal protein was the first to be described to undergo calpain-catalyzed protein lysis both in long-term potentiation and post ischemic degeneration (Saido et al., 1993). Spectrin is involved in keeping membrane mechanical properties and dynamic behaviour of integral membrane proteins (Bennett and Gilligan., 1993). It has been shown that both in apoptosis (Martin et al., 1995) and necrosis (Nath et al., 1996), spectrin is cleaved, giving

fragments of different sizes (120 and 150 kDa, respectively) depending on the activation of different proteases, caspases or calpains, respecitvely.

We analyzed by immunobloting if increased calpain activity would induce spectrin cleavage in old cells. At DIV 7, treatment with 100 µM glutamate for 12 h induced cleavage of spectrin and led to the detection of a 150 kDa fragment, typical for calpain cleavage (Figure 16 A). This cleavage was partially blocked by treatment with 5 µM calpeptin, a calpain inhibitor. In contrast, at DIV 50 spontaneous spectrin cleavage occurred that was not further augmentet by treatment with glutamate.

One other potential target of calpains is the sodium calcium exchanger, NCX3 (Bano et al., 2005). In the central nervous system, the Na^+/Ca^{2+} exchanger plays a fundamental role in controlling changes in the intracellular concentrations of Na^+ and Ca^{2+} ions that occur in physiologic conditions such as neurotransmitter release, cell migration and differentiation, gene expression, and neurodegeneration (Canitano et al., 2002). Two families of plasmalemmal Na^+/Ca^{2+} exchangers, K^+ - dependent (NCKX) and K^+ - independent (NCX), are expressed in the central nervous system (Philipson and Nicoll, 2000). The NCX family includes NCX1, NCX2, and NCX3 genes, which are all expressed in cerebellum (Canitano et al., 2002). Bano and colleagues (Bano et al., 2005) showed that NCX3 is a substrate of calpains and is cleaved after glutamate insult in CGN, causing excessive increase of calcium in cytoplasm and consequently cell death.

We wanted to know, if increased calpain activity in old neurons would affect NCX3 pump cleavage and performed immunoblot analysis for NCX3 expression of CGN at DIV 7 and DIV 50 (Figure 16 B). Uncleaved NCX3 is visualised with a molecular weight of about 100 kDa, and at around 58-60 kDa when it is cleaved by calpains (Bano et al., 2005). We observed a cleavage in lysates from CGN at DIV 50 (Figure 16 B).

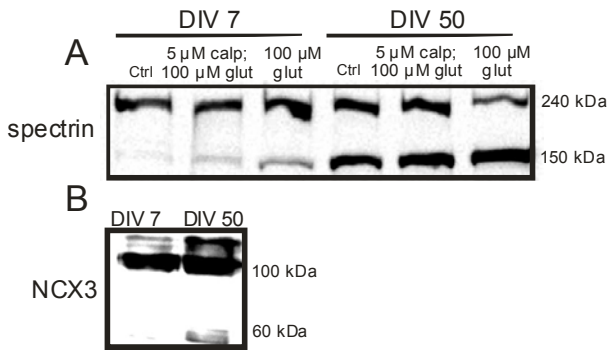

Figure 16: Calpain activity induces cleavage of spectrin and NCX3 pump in old cultures. (A) Cerebellar granule neurons were incubated with 5 µm calpeptin and 100 µM glutamate, or only with glutamate for 12 h. Cleavage of spectrin was analyzed using monoclonal antibody against nonerythroid spectrin. Non cleaved spectrin was visualized at the height of 240 kDa, and calpain cleaved fragment was visualized at around 150 kDa. (B) Protein lysates from young and old cultures were immunobloted with antibody against NCX3 pump. Full size fragment is visualized at around 100 kDa, and two bands cleavage products can be visualized at around 58-60 kDa.

4.5.8 Reduced ATP content in old cells

A decline in mitochondrial oxidative function and an increase in the incidence of mitochondrial DNA oxidative damage have been shown to occur in various tissues with age (Drew et al., 2003; Conley et al., 2000). Damage of mtDNA by reactive oxidative species may have more dramatic effects then damage to nuclear DNA, because mitochondria are lacking histones, have less repair mechanisms, and are closer to the ROS source – the inner mitochondrial membrane (Cadenas and Davies, 2000). The accumulation of mtDNA modification and mutations with age can interfere with the synthesis of proteins and pathways that are responsible for the transfer of electrons along respiratory chain, as well as with the production of ATP (Ramakrishna et al., 2001). Decreased energy production (Sohal and Weindruch, 1996) has been implicated in the reduction of cell viability as well as an increase in cell necrosis and/or apoptosis (Phaneuf and Leeuwenburgh, 2002) with age.

We measured ATP content using an ATP bioluminescence assay kit based on the light-emitting oxidation of luciferin by luciferase in the

presence of low levels of ATP and normalized it for the same amount of protein. Old neurons seem to have ATP level significantly lower compared with young cells before and after treatment with glutamate (30 min, 100 µM), (Figure 17).

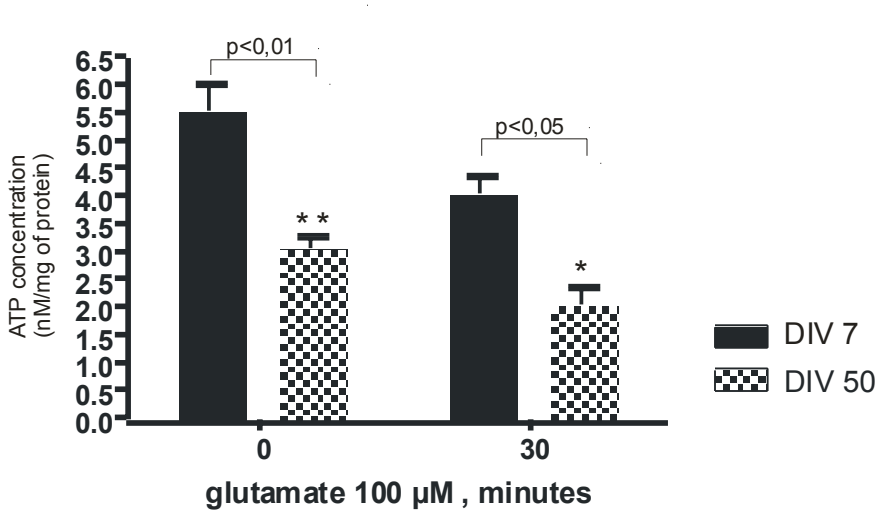

Figure 17: ATP concentration at DIV 7 and DIV 50, before and after glutamate insult. The cells were exposed to 100 µM glutamate for 30 min. Neuronal ATP concentration was assessed as described (see material and methods). Data were obtained from three different experiments, normalized for mg of proteins and expressed as nmol/mg cell protein. ANOVA and Bonferroni's test: * p< 0.05; ** p< 0.01

4.5.9 Increased sensitivity to excitotoxic stimulus

Glutamate is the major excitatory neurotransmitter in the mammalian central nervous system and if released in uncontrolled fashion can be a potent neurotoxin. On the other hand glutamate is the key mediator in cell to cell communication, plasticity, growth, and differentiation. Glutamatergic receptors are classified into two major groups, ionotropic and metabotropic (Nakanishi, 1992).The ionotropic receptors are ligand gated ion channels and are characterized by their affinity toward specific agonists N-methyl-D-aspartate (NMDA), α-amino-3-hydroxy-5-methylisoxazole-4-propionic acid (AMPA) and kainic acid (KA) (Monaghan et al., 1989). The metabotropic receptors (mGluR) are G-protein coupled and are subdivided into three groups by amino acid sequence, agonist sensitivity and signal

transduction mechanisms (Masu et al., 1991). Group I (mGluR 1 and 5) are coupled to phospholipase C-mediated polyphosphoinositide hydrolysis. Group II (mGluR 2 and 3) and group III (mGluR 4, 6, 7, and 8) are either negatively coupled to adenyl cyclase or linked to ion channels (Pin and Duvoisin, 1995). Overstimulation of glutamatergic receptors leads to dysfunction of downstream signalling systems and is called excitotoxicity.

In excitotoxicity, two processes can be distinguished depending on time and ionic characteristics (Choi, 1992). The first involves swelling of the cell bodies and dendrites, because of the Na^+ influx and passive Cl^- influx as well as water. The second, delayed process is marked by Ca^{2+} influx.

Excitotoxicity is a receptor mediated event and can be blocked by glutamate receptor antagonists such as MK801 (NMDA receptor antagonist) or NBQX (AMPA and kainate receptor antagonist).

To test the sensitivity of young and old CGN to excitotoxic stimuli we treated cells (DIV 7 and DIV 50) for 24 h with glutamate (100 µM) and then measured viability. Old neurons were significantly more sensitive to excitotoxic stimuli (Figure 18). In order to further explore the receptor subtype responsible for the increased sensitivity to excitotoxicity, we treated CGN with glutamate receptor agonists for 24 h (AMPA, 100 µM; kainic acid, 100 µM; NMDA, 500 µM). To try to block potential excitotoxicity on the level of receptor we used NMDA specific (MK801) or AMPA/kainate specific (NBQX) antagonists in combination with appropriate agonists or a mixture of both when treated with glutamate. We found that old neurons were more prone to all glutamate agonists (AMPA, kainic acid and NMDA), (Figure 18). Blocking the receptors protected DIV 50 neurons against cell death (Figure 18).

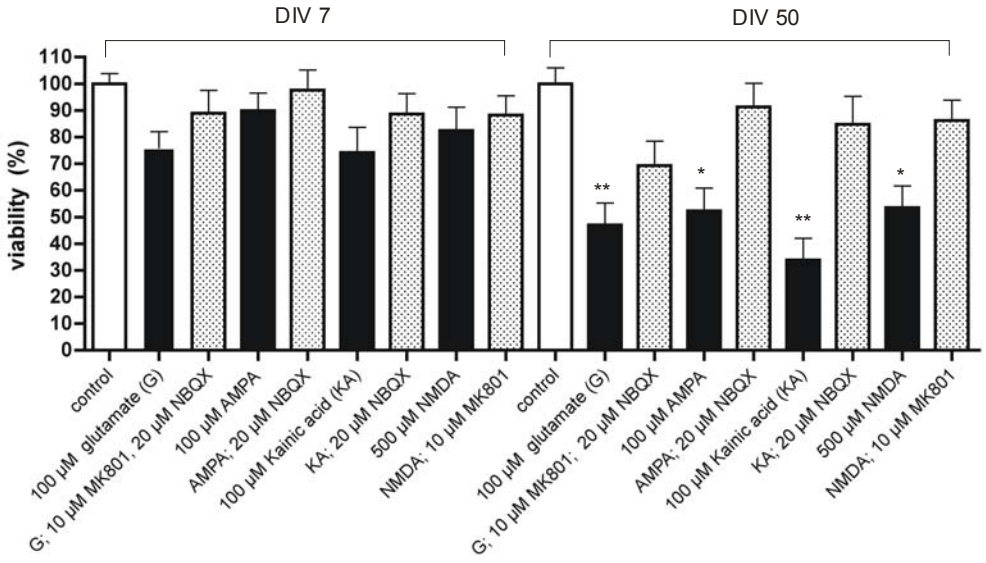

Figure 18: Different sensitivity to excitotoxic stimuli in young and old CGN *in vitro*. CGN were treated for 24 h with 100 µM glutamate or with its agonists (100 µM AMPA; 100 µM kainic acid, or 500 µM NMDA) or with glutamate, its agonists and specific antagonists (glutamate together with 10 µM MK801 and 20 µM NBQX, AMPA with NBQX, kainic acid with NBQX, and NMDA with MK801). * p< 0.01; ** p< 0.001, according to ANOVA and Bonferroni's test. Data represent mean values ± SD of at least three independent experiments.

In order to inhibit calpain activity, we started with treatment of fully differentiated CGN at DIV 7 with cell permeable calpain inhibitor calpeptin (Tsujinaka et al., 1988) on a regular basis. We applied this inhibitor two times per week until DIV 50. At this point we treated cells with 100 µM glutamate and noticed that cell having received calpeptin treatment only once, briefly before glutamate treatment in contrast to the cells that received long term celpaptin treatment, had significantly lower survival rate (Figure 19).

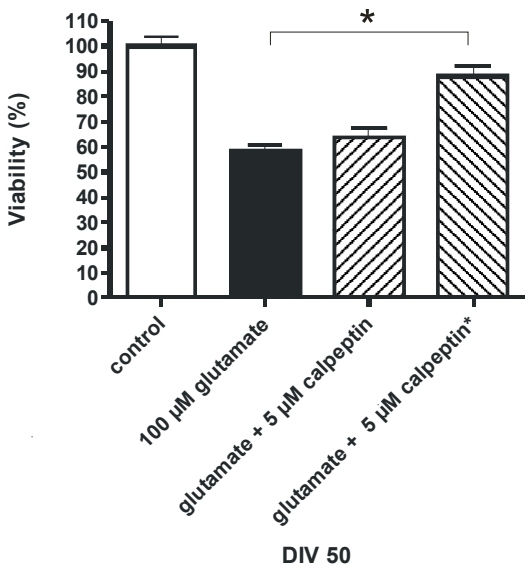

Figure 19: Old CGN can be saved by regular treatment with calpain inhibitor over longer period of time. CGN were treated two times per week with 5 µM calpeptin starting DIV 7 until DIV 50 (calpeptin*), and then treated with 100 µM glutamate for 24 h, or treated only once with 5 µM calpeptin, 30 min before glutamate application, or only treated with calpeptin two times per week starting at DIV 7 (control). * p< 0.001, according to ANOVA and Bonferroni's test.

4.6 Calcium homeostasis

Calcium is important secondary messenger and its signalling relies on transient elevations in intracellular Ca^{2+} ($[Ca^{2+}]_i$) concentration which are mediated by influx through membrane channels and/or release from intracellular Ca^{2+} sources, endoplasmatic reticulum (ER) and mitochondria (Toescu et al., 2004). An important feature of the aging neurons and neurodegeneration is the disturbance in Ca^{2+} homeostasis (Thibault et al., 1998). It proposes that the basal levels of $[Ca^{2+}]_i$ increase in aging neurons and that return to the baseline of $[Ca^{2+}]_i$ after stimulation is compromised (Thibault et al., 1996; Brewer et al., 2006).

Changes in intracellular calcium levels can be analyzed with the use of ion-sensitive indicators, whose light emission reflects the local concentration of the ion. By measuring the ratio of fluorescence intensity at two excitation wavelengths, the concentration ratio of the Ca^{2+}-bound

indicator to the Ca^{2+}-free indicator can be determined. Fura-2 is a widely used UV-excitable fluorescent calcium indicator. The indicator is typically excited at 340 nm and 380 nm respectively and the ratio of the fluorescent intensities corresponding to the two excitations is used in calculating the intracellular concentrations.

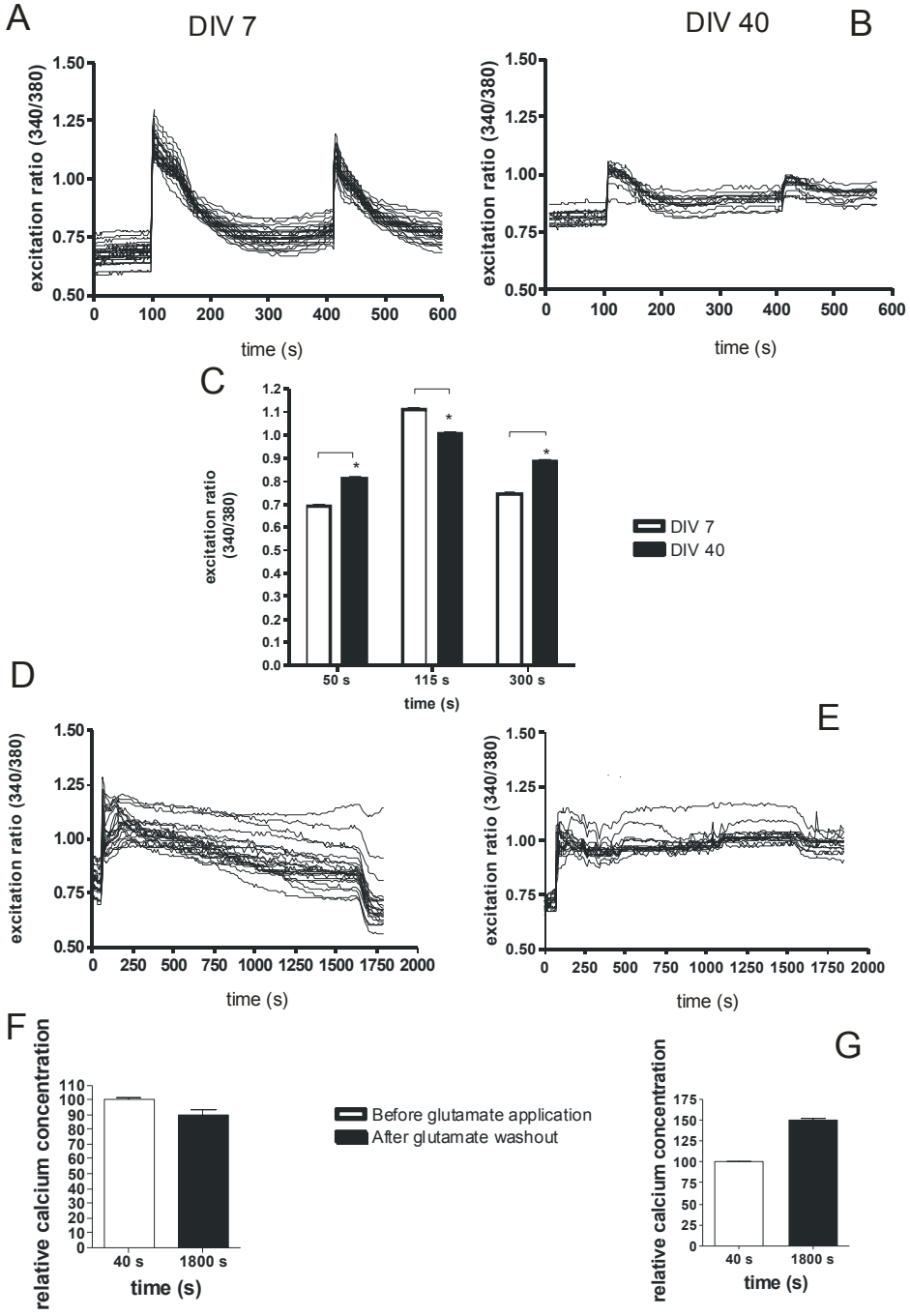

Figure 20: KCl and glutamate evoked calcium responses in young and old CGN. (A); (B) At the time 110 s and 420 s, CGN were exposed to bath perfusion with 25 mM KCl and immediately washed out. Each trace represents one cell. (A) DIV 7 CGN; (B) DIV 40 CGN; (C) The average $[Ca^{2+}]_i$ in young and old CGN, before (50 s), during (115 s), and after (300 s) exposure to 25 mM KCl. *p<0·001 according to Student's t-test. (D); (E) At the time 50 s, neurons were exposed to bath perfusion with 150 µM glutamate and washed out at the time 1600 s. (D) DIV 7 CGN; (E) DIV 40 CGN; (F), (G) Relative $[Ca^{2+}]_i$ concentration before and after glutamate application in young (F) and old (G) neurons.

In order to measure intracellular calcium levels of young and old CGN we loaded the cells with 2 µM Fura-2-AM in CSS-5 buffer for 20 minutes, applied 25 mM KCl (two times with immediate washout, 110 s and 420 s) to DIV 7 and DIV 40 CGN in a flow chamber with continuous ratiometric monitoring of intracellular Fura-2 fluorescence in order to determine the basic intracellular calcium concentration, intracellular calcium responses, and the ability to return to baseline (resting) calcium levels (Figure 20 A, B and C). We found that the basic intracellular calcium concentration in old cells was significantly increased (Figure 20 B, C). Old CGN were not able to depolarize as young ones after 25 mM KCl stimulus (Figure 20 B, C). In old neurons, after KCl washout, $[Ca^{2+}]_i$ level remains very high in comparison to young neurons (Figure 20, A, B, and C). By measuring $[Ca^{2+}]_i$ in CSS-5 buffer without Mg^{2+}, we monitored intracellular calcium concentration before and after glutamate application (Figure 20, D, E, and F). After glutamate application, calcium concentration increases almost momentarily after the stimuls, and then slowly returns to its basic level. This seems to be the case in young CGN (Figure 20 D, F) but not in the old CGN (Figure 20 E, F). After we washed out glutamate in the buffer containing Mg^{2+} (to block NMDA receptors), calcium concentration decreased, but was still very high in old compared with young neurons (Figure 20 D, E, F, G). We conclude that old CGN are not able to regulate the concentration of intracellular calcium as good as young ones, and that this might be one of the possible reasons for the increased vulnerability to excitotoxic stimuli.

5 Discussion

CGN as a primary neuronal culture are easy to prepare and to differentiate *in vitro*. However, only few studies have characterized CGN as a long term culture (Ishitani et al., 1996; Toescu and Verkhratsky, 2000) up to DIV 17 and 23, respectively. We were inspired by experiments from Ishitani et al. (1996) to further explore phenomena of aging in CGN *in vitro.* Thus, we were interested in assessing the question why CGN die after DIV 16-19. Ishitani and colleagues did not change any culture condition over the period of time and noticed an age-dependent increase in expression of GAPDH mRNA and protein. Our experimental paradigm, in contrast, consisted of adding 5 mM glucose every three days to the medium starting DIV 7. Neurons were rescued from cell death at this period (DIV 16-19) and survived for up to 60 days following this treatment. In order to confirm viability dependence on the resources from the culture media, we cultured CGN in three different densities (1 x 10^6/cm^2, 1.5 x 10^6/cm^2, and 2 x 10^6/cm^2 with or without regular glucose replenishment (5 mM, every three days). As expected, cultures with the highest number of neurons used all the nutrients from the medium faster then other two and were the first to die at DIV 16. The two cultures (1.5 x 10^6/cm^2, 1 x 10^6/cm^2) died with delay one to four days, respectively. Control cultures which had regular glucose supplement remained vital for at least 40 days. This result confirmed it was necessary to refresh the culture medium for assessing CGN cultures longitudinally and that only glucose was enough to keep neurons vital for up to 60 days. CGN are very sensitive to media change and complete media change results in neuronal cell death (Schramm et al., 1990). To eliminate acidification of the medium as a cause of cell death and to replenish nutrients other than glucose, we exchanged part of the medium two times per week by exchanging 25% of the medium starting the treatment at DIV 14. Substituting fetal cow serum with synthetic serum made this replacement possible and neurons were again vital for up to DIV 60. This outcome suggests that the state of cell medium was not the

cause for cell death of CGN after two months in culture (acidification of medium for example). So far there have been two other primary neuronal cultures characterized as long term cultures; primary hippocampal and cortical cultures (Aksenova et al., 1999; Lesuisse and Martin, 2002, respectively). The long-term viability of both cultures was similar to ours – up to DIV 60. Nevertheless, why neurons survive up to this time in culture and ddie thereafter is unknown.

In order to determine whether aging of isolated neurons can be compared with real physiological aging, our next goal was to characterise long term CGN culture morphologically and functionally during the two month viability period *in vitro*.

CGN is almost pure neuronal culture, with less then 5% contamination with astrocytes and some oligodendrocytes (Schulz et al., 1996; Nicoletti et al., 1986). This contamination cannot be avoided even with the regular AraC supplement, which acts as an inhibitor of mitosis and stops proliferation of nonneuronal cells. Astrocyte-rich neural cultures are beneficial for neurons because they increase neuronal viability and decrease glutamate-mediated neurotoxicity because of the ability to uptake glutamate from the synaptic cleft (Beaman-Hall et al., 1998). Astrogliosis is a progressive phenomenon occurring in the aging brain. There have been studies reporting age-related changes in the number of astrocytes (Jalenques et al., 1995) or increase in size without change in number (Geinisman et al., 1978). In our cultures astrocytes showed a significant increase in size. Our data are consistent with the findings of Geinisman et al. (1978) who found an increased volume fraction of astroglial processes in the supragranular zone of the dentate gyrus molecular layer in rats. Björklund et al. (1985) compared the cell area and the cell perimeter of astrocytes ranging from 1 to 30 months old rats and found as well a continuous increase in the cell size during the aging process. Since its description in 1995 (Dimri et al., 1995), β-galactosidase associated activity has been widely used as a marker of replicative senescence and organismal aging. In the present study we showed

increased β-gal activity in astrocytes corelating to increased time in culture. Age associated β-gal activity in senescent cells is not a specific marker of senescence *per se*, but rather a surrogate marker for increased lysosome activity (Sanchez-Martin and Cabezas, 1997; Gerland et al., 2003). Yang and Hu (2005) showed that β-gal activity increased not only in senescent cells but also in quiescent cells induced by serum starvation or confluence and that in this case β-gal activity can be reversed. We found that lipofuscin, another marker of aging, is also present in old astrocytes *in vitro*. Fluorescent pigment, consisting of undegradable oxidation products of lipids and proteins (Sitte et al., 2000b), was another conformation for senescence of astrocytes.

Protein carbonylation has been intensively studied because of it unrepairable nature and positive connection with increasing age (Starke-Reed and Oliver, 1989; Sohal et al., 1994b). Protein carbonyls can be determined by the reaction with a classical carbonyl reagent 2.4-dinitrophenylhydrazine (DNPH) (Levine et al., 1990). Our results show gradual overall increase of carbonylated proteins in culture with time using immunobloting methods. Aksenova et al. (1999) showed a similar effect on aging of hippocampal cells in culture by a immunocytochemical method. Carbonyl accumulation was more intense in the cell bodies then in the cell processes. Increase in protein carbonylation is most likely caused by increased oxidative stress. Increased oxidative stress can be further discussed as (I) a decline in the antioxidant defence system, (II) an increased production of ROS, (III) an incapability for normal removal of oxidized proteins, and/or (IV) an increased susceptibility of proteins to oxidative stress (from Nyström , (2005)). In order to gain a better understanding of CGN aging *in vitro* we analysed the activity of the cellular protease system, because it has been shown that in senescent fibroblast cultures the function of the proteasome decreases with aging (Sitte et al., 2000a). Increased ubiquitination of proteins and reduction of free ubiquitin in aged CGN in our study suggests that the proteasomal system is impaired. It has been proposed that decrease in proteolysis is a

consequence of the accumulated protein aggregates, 'aggresomes' which bind to the proteasome (Grune et al., 2004) and clog up the proteasome thereby blocking other proteins from degradation. By measuring the chymotrypsin-like activity we showed that the proteasomal activity was decreased during aging of CGN *in vitro* without changes in proteasomal protein expression over time. However, we were not able to determine whether the proteasomal system was damaged by itself and/or it was partially blocked by protein aggregates. In order to test this, the proteasome itself should be isolated and then tested for activity.

For studying molecular changes during aging *in vitro* in more detail, we performed a microarray analysis of CGN using the Affymetrix rat U34A chip. We compared differential gene expression between DIV 7 and DIV 40. Lee et al. (2000) performed gene profiling of the aging brain in mice investigating specifically the neocortex and cerebellum. Their view of the global transcriptional changes was major induction of inflammatory response and stress response followed by a decrease in protein turnover and a decrease in growth and trophic factors. Lu et al. (2004) performed microarray analysis of the aging brain in humans showing changes in genes involved in synaptic plasticity, vesicular transport, mitochondrial function, stress response and DNA repair genes. Aging in cell culture is a precisely defined system because of one cell type going through synchronous changes over time. Our findings were similar to the results from Lu et al. (2004) concerning changes at the level of synaptic function with the decrease in expression in neurotransmitter receptors such as metabotropic (mGluR3, mGluR4) and ionotropic (KA2, AMPA2, NMDAR1) glutamate receptors as well as gamma-aminobutyric acid (GABA-A) receptor. The expression of genes that mediate synaptic vesicle release and recycling such as synapsin 1, syntaxin 1a, and synaptosomal associated protein 25 were also down-regulated. Moreover, genes involved in vesicular/protein transport showed reduced expression in aged CGN including dynein, tubulin, and microtubule associated protein, member 1. GAP 43 on a RNA level also showed decrease in expression in

aging cultures which was confirmed by the protein analysis. This protein is considered to be involved in neuronal mechanisms underlying axonal growth, plasticity and regeneration (Benowitz and Routtenberg, 1987) as well as in outgrowth of neuronal processes (Zuber et al., 1989). All these changes are likely to contribute to the decrease of neuronal activity in aged CGN.. The aging of CGN was also associated with increased expression of genes that mediate stress responses such as chaperones (DnaJ (Hsp40) homologue 2, alpha B crystalline), oxidative stress (glutathione peroxidase 4; glutathione S transferase, omega 1; peroxiredoxin 3; DNA-damage inducible transcript 3), and metal ion homeostasis (metallothionein 1A). Pro-apoptotic genes, caspase-2 and caspase-3 were down-regulated. Xiao et al. (2001) reported that the levels of active forms of caspase-3, 8 and 9 are found to be considerably (60–80%) lower in the colonic mucosa of 22–24 month-old rats, compared to their younger counterparts. Decrease of pro-caspase-3 expression *in vitro* in senescent fibroblasts has been described by Marcotte et al. (2004). CGN as a cell culture model has been extensively used for studies of neuronal differentiation and apoptosis. Therefore we were interested in analyzing functional consequences of this change. In order to validate the results from microarray analysis and to further observe the state of apoptotic machinery of old CGN we analyzed protein expression by immunobloting methods. Our analysis of GAPDH expression showed stable expression of this protein up to DIV 50, which indicates that CGN up-regulated this protein due glucose deprivation in experiments from Ishitani et al. 1996, in order to support the glycolytic pathway. The expression of non-neuronal protein GFAP, as an astroglial marker, increased slightly expression from DIV 7 to DIV 20, and then remained stable. This could be explained from the increase in size of astrocytes and not from the increase in number of these cells. Cytochrome c showed the same trend. Manganese superoxide dismutase (MnSOD), another mitochondrial protein, which is involved in protection against oxidative stress, was stable on a protein level. Our results support an earlier finding

from van der Loo et al. (2005). They showed no change of MnSOD expression in the aging rat heart but additionally showed a decrease in function.

The analysis of proteins involved in apoptosis showed a trend of increase in pro-apoptotic proteins such as Bcl-2 (even though not significant), Bcl-x_L, lifeguard, and a decrease in expression of pro-apoptotic protein Bax and caspase-3. Real time analysis of Bax mRNA expression showed no difference between young and old CGN in contrast to caspase-3 expression, which was decreased. Li and Dou (2000) showed that decreased levels of Bax protein correlated with an increase of Bax degradation by the ubiquitin/proteasome system in advanced human prostate cancer. In aged CGN, Bax protein may not be degraded by the proteasome, because, we did not see increase in Bax protein levels after proteasomal inhibition. Furthermore, the proteasomal system in old cells was impaired as compared with young CGN. Another explanation comes from the discovery that Bax protein was down-regulated under hypoxic conditions (Erler et al., 2004; Sasabe et al., 2005). Erler and colleagues showed that under hypoxic conditions, tumor cells down-regulate Bax not by increasing its proteasomal degradation but rather by decreasing translational efficiency. The microarray analysis demonstrated an up-regulation of mRNA of hypoxia induced gene 1. We can not rule-out if aged CGN are hypoxic, because Gstraunthaler et al. (1999) showed the difference in tissue culture oxygenation of static monolayer cells compared with the ones that are under constant rocking prepared by using the technique of roller bottle cultures. We did not have the technical ability to have cultures grown in this way and even if we did it is unclear if they would have survived under these conditions.

Cerebellar granule neurons deprived of extracellular, depolarizing 25 mM KCl, undergo apoptosis characterized by caspase-3 activation, chromatin condensation, pyknosis, and nucleosomal size DNA fragmentation (D'Mello et al., 1993; Schulz et al., 1996). Staurosporine (1 µM), a broad-spectrum kinase inhibitor also causes apoptosis of cerebellar granule

neurons but in contrast to potassium deprivation (Schulz et al., 1996) is independent of new protein synthesis (Taylor et al., 1997). Using these two apoptotic stimuli we showed that DIV 50 CGN were almost resistant to apoptosis as compared with DIV 7 neurons. In contrast to the effects in young cells, we detected no caspase-3 activity in old CGN after potassium deprivation as well as no DNA fragmentation. Other stimuli such as treatment with glutamate or H_2O_2 killed neurons and degraded DNA of both ages, showing that old cells were sensitive to necrotic stimuli, but not to apoptotic. There are at least two possible explanations:: cytochrome c never exited mitochondria and activated pro-caspase-3 because of the decreased level of Bax and increased levels of Bcl-x_L and Bcl-2 or the level of pro-caspase-3 was too low for the execution of apoptosis or a combination or both. Anyway, apoptosis was significantly reduced after different apoptotic stimuli in old CGN compared with CGN. It would be interesting to allocate the molecular mechanism of down-regulation of caspase-3 in order to protect neurons from neurodegenerative diseases in which apoptosis is discussed as an important factor for neuronal cell death (Anderson et al., 1996; Giambarella et al., 1997; Mozhizuki et al., 1996, Schulz et al., 1999).

In contrast, we showed that old CGN (DIV 50) when challenged with excitotoxic stimuli (glutamate, NMDA, AMPA, or kaininc acid) were more vulnerable than young CGN (DIV 7). CGN grown in high potassium concentration (25 mM), are resistant to an excitotoxic insult at DIV 7 (Marini et al., 1999). Marks et al. (2000) showed that NMDA-induced cell death increases drastically in hippocampal neurons cultured from mature animals vs. the ones cultured from a newborn rat. Liu et al. (1996) injected glutamate into the hippocampus of rats at different postnatal days and showed that glutamate neurotoxicity in the hippocampus was highly age-dependent. A simple explanation of this phenomenon would be an increase in the number of excitatory neurotransmitter receptors (Wenk et al., 1989) or certain receptor subunits such as the NMDA receptor subunit NR2B (Cheng et al., 1999). This hypothesis is opposite to the results from

our microarray analysis (down-regluation of metabotropic mGluR3, mGluR4, and ionotropic (KA2, AMPA2, NMDAR1) glutamate receptors). Supporting our data, Lu et al. (2004) showed a decrease in GLUR1 and NMDA 2A in the aging brain. Thus, another mechanism must be involved in the increased sensitivity to glutamate insult of aged CGN *in vitro*.

Glutamate receptor activation is followed by a rapid increase in cytosolic Ca^{2+} concentration (Choi, 1992) which needs to be restored to the resting, prestimulation levels for the normal neuronal function and excitability and for the avoidance of cytotoxic effects of a potential prolonged exposition to high calcium levels. Our analyses revealed marked age-related differences in $[Ca^{2+}]_i$ homeostasis. Compared with young CGN, old CGN had an elevated baseline $[Ca^{2+}]_i$. They also had significantly smaller Ca^{2+} responses than young neurons during both glutamate and depolarizing KCl conditions followed by failure to restore resting $[Ca^{2+}]_i$. Toescu and Verkhratsky (2000) did not detect the significant difference in resting $[Ca^{2+}]_i$ between young (DIV 9) and old (DIV 23) CGN, but they measured a decreased amplitude of the Ca^{2+} signal during KCl-evoked depolarization and significant prolongation in the recovery phase of the Ca^{2+} response. From our results, we can conclude that the reason for increased neurotoxicity of glutamate and its agonists in old CGN comes from the inability of cells to restore the resting $[Ca^{2+}]_i$. Xiong et al. (2004) have shown that mitochondria in CGN cultures (DIV 22) are chronically depolarised and have an impaired repolarization profile following stimulation. According to the same authors, chronic mitochondrial depolarisation might lead to a chronic increase in resting $[Ca^{2+}]_i$, which might explain the increase in baseline $[Ca^{2+}]_i$ in the *in vitro* model of aging that we present .

We showed that ATP is significantly decreased in old CGN (DIV 50) compared with young CGN (DIV 7). In order to maintain resting $[Ca^{2+}]_i$, ATP is important for the activities of the Ca^{2+} pumps and the Na^+-K^+ ATPase. Calabresi et al. (1995) showed that impairment of the activity of Na^+-K^+ ATPase sensitizes striatal neurons to glutamate, lowering the

threshold for the excitotoxic event. From our microarray data we found that Na^+-K^+ ATPase mRNA was down-regulated in old CGN. This change might have also contributed to the increased vulnerability to glutamate and its agonists.

We showed that old CGN have increased calpain activity. Calpains are a family of calcium-activated cysteine proteases believed to be important in cell differentiation, migration and cell death (Suzuki and Sorimachi, 1998). Consistent with our observation of increased intracellular calcium it has been shown that calpain activity also increases during aging (Benuck et al., 1996; Sureda et al., 2006). We ruled-out a decrease in the expression of calpastatin, an endogenous inhibitor of calpains, by real-time PCR which has been shown to occur in old erythrocytes (Schwarz-Benmeier et al., 1994). An increase in calpain activity disturbs cellular homeostasis by cleaving for example a chaperone - α-crystallin (Kelley et al., 1993), a cytoskeletal protein - spectrin (Siman et al., 1984), and the sodium-calcium exchanger 3 – NCX3 (Bano et al., 2005). We found strong α-spectrin breakdown detected by an increase of a 150 kDa protein fragment, typical for α-spectrin cleavage by calpains. Our results are consistent with the results from *in vivo* analysis of aged rat brain (Bernath et al., 2006). Bernath and colleagues reported strong calpain cleavage of α-spectrin, but no caspase-3 mediated α-spectrin breakdown. It is interesting that they also noticed moderate reduction in pro-caspase-3 protein expression and its hydrolytic activity in the cortex of old animals. Cleavage of α-spectrin in old CGN contributes to loss of integrity of plasma membrane and is probably one of the factors that influence vulnerability of the cells to excitotoxic stimuli, and perhaps the maximum lifespan (around DIV 60 *in vitro)*. The other protein which showed degradation by calpains in old CGN was NCX3. The NCX is a family of transporters which catalyze the influx of 3 Na^+ for efflux of 1 Ca^{2+} and has three isoforms (NCX1, NCX2, and NCX3). Ca^{2+} extrusion via the exchanger, following neuronal stimulation, contributes to the maintenance of Ca^{2+} balance in neurons (Bano et al., 2005). Bano and colleagues showed that due to calcium influx and calpain

activation after glutamate stimulus, NCX3 is cleaved by calpains and inactivated. We detected calpain cleavage of NCX3 in old CGN, which did not occur in young neurons. When calpain activity was inhibited with calpeptin over a period of few weeks, CGN were significantly more resistant to excitotoxic stimulus. We conclude that *in vitro* aged CGN have impaired function to extrude calcium from the cytosol because NCX3 is cleaved by calpains and thereby cannot pump out calcium out of the cell.

In our study we observed markedly increased phosphorylation of extracellular signal-regulated protein kinase (ERK1/2) in old CGN. ERK plays prominent role in the regulation of cell proliferation, differentiation and adaptation. Moreover, Subramaniam et al., (2003) pointed importance of ERK activation after potassium deprivation in apoptotic cell death paradigm in CGN. We observed that the activity was strongly regulated by glutamate challenge. The age-related increase in ERK1/2 activity has been described in rats with a corresponding increase in ROS in contrast to calorie restricted rats that also had ROS levels decreased (Kim et al., 2002). Senescent human fibroblasts (Kim et al., 2003) and DIV 30 human mouse cortical neurons (Lesuisse and Martin, 2002) also show increased ERK1/2 activity compared with their younger counterparts. It would be important to investigate the mechanism and the functional consequences of this activation. ERK activity is tightly regulated by phosphorylation and dephosphorylation. Kim et al. (2003) showed that senescence-associated induction of ERK1/2 was associated with increased ROS concentration which inhibited phosphatases responsible for the dephosphorylation of ERK1/2. Based on these data we suggest that due to increased oxidative stress followed by a deregulation of the phosphorylation/dephosphorylation homeostasis, ERK phosphorylation was increased in old CGN. We were not able to conclude on the functional consequence of ERK activation in CGN after glutamate insult. Depending on the cell type and conditions it has been shown that ERK phosphorylation can be either protective (Hetman, et al., 1999) or deletoriuos (Lesuisse and Martin, 2002; Satoh et al., 2000) in different cell

death paradigms. Hetman et al. (1999) reported that ERK, when induced by brain-derived neurotrophic factor (BDNF), saved cortical neurons from camptothecin-induced cell death. Our microarray analysis showed that in old CGN, BDNF was up-regulated. That might explain the constitutive up-regulation of ERK in old CGN. However, we noticed no protection or increase in vulnerability, in glutamate induced cell death, when we inhibited ERK by MEK1/2 inhibitor U0126. Perhaps, this question should be answered using slightly younger cells, in which reparatory and protective mechanisms are in better conditions. If, in that case, there would also be no protection or increased cell death, this would lead to the conclusion that ERK1/2 signalling is not involved in cell death mechanisms of aging CGN *in vitro*.

Microtubule associated protein tau is a phosphoprotein that functions to stabilize microtubules and is abnormally phosphorylated in Alzheimer's disease. We found that old CGN have different splicing isoforms of tau compared with the young ones. Pizzi et al. (1995) showed that CGN *in vitro* switch on the exon containing four internal repeats by DIV 6 and switch off of the mRNA containing three internal repeats after DIV 12.

In sum, the data reported here show a new methodological approach to study aging of cerebellar granule neurons *in vitro*. During long term culturing, CGN accumulate oxidative damage which most likely causes disturbance in calcium homeostasis and eventually death after approximately two months *in vitro*. Increased $[Ca^{2+}]_i$ leads to the activation of calpains which inactivate Na^+/Ca^{2+} exchanger 3 and disturb calcium homeostasis even further making them extremely vulnerable to excitotoxic stimuli. In contrast, aging CGN *in vitro* gain high level of resistance toward apoptotic stimuli due to down-regulation of pro-apoptotic and increase of anti-apoptotic proteins. Numerous studies of neurodegeneration *in vivo* point to apoptosis as a cause of cell death. Therefore, we propose use of old animals for *in vivo* studies of neurodegeneration, because age factor might strongly affect predisposition to specific cell death pathways.

Because any mammalian aging studies are time consuming, having a model that would save time and simplify the conditions in order to answer crucial questions concerning aging related neurodegenerative diseases and aging processes would be very useful. One has to be cautious and keep in mind that neurons grown *in vitro* are aged in artificial physiological conditions. In order for our model to be completely accepted, an *in vivo* study of aging cerebellar granule neurons should be performed.

6 Summary

Aging is slow and cumulative process and is experimentally difficult to access. Neurodegenerative diseases such as Alzheimer's disease and Parkinson's disease are considered to be at high risk with increasing age. The molecular mechanisms by which they occur are not completely understood. Aim of the present study was to construct and investigate an *in vitro* model of neuronal aging. To this purpose we used rat primary cerebellar granule neurons which are a good characterized *in vitro* model for various paradigms of neuronal cell death, e.g. potassium deprivation or glutamate excitotoxicity.

We prepared CGN to a purity of 95% and kept them in culture for either 7 days or up to 60 days. To validate our *in vitro* model for aging, we tested whether known molecular changes associated with aging occur over time. Moreover, by using DNA microarray analysis we examined how aging *in vitro* influences the pattern of gene expression. In the end, we studied mechanisms of cell death signalling cascades in young vs. old CGN.

Old CGN had increased protein carbonylation and ubiquitination. Proteasomal activity was significantly lower in old CGN even though protein expression of proteasomal subunits did not change over the time.

Morphological changes in astrocytes included increase in size, accumulation of autofluorescent, undegradable pigment lipofuscine, and senescence-associated beta -galactosidase activity.

Aging *in vitro* caused increased expression of genes involved in stress response. Down-regulated genes were mostly responsible for control of synaptic function.

Young neurons favoured apoptosis over necrosis in contrast to old neurons. DIV 50 neurons were much less vulnerable as compared to DIV 7 neurons to classical apoptotic paradigms such as potassium deprivation, or staurosporine treatment. Old CGN had up-regulated anti-apoptotic proteins Bcl-$_{xL}$ and lifeguard, and down-regulated caspase-3 and Bax. On

the other hand, old neurons exhibited enhanced sensitivity to glutamate excitotoxicity. Aging *in vitro* caused ATP depletion, failure of intracellular Ca^{2+} homeostasis, increase in calpain activity, and changes in ERK signalling. Increased calpain activity caused cleavage of calcium pump NCX3 and blocked pumping excessive Ca^{2+} outside of the cell. This made old neurons extremely sensitive glutamate insult. When calpains were inhibited over longer period of time by regular application of calpeptin, sensitivity to excitotoxic stimulus was significantly reduced.

These data show that cerebellar granule neurons can successfully be cultured over period of 60 days *in vitro* and may represent a valuable tool for modelling aging and neurodegenerative diseases.

7 References

Aksenova MV, Aksenov MY, Markesbery WR, Butterfield DA. Aging in a dish: age-dependent changes of neuronal survival, protein oxidation, and creatine kinase BB expression in long-term hippocampal cell culture. J Neurosci Res. (1999) 58:308-17.

Amici A, Levine RL, Tsai L, Stadtman ER. Conversion of amino acid residues in proteins and amino acid homopolymers to carbonyl derivatives by metal-catalyzed oxidation reactions. J Biol Chem. (1989) 264:3341-6.

Anderson AJ, Su JH, Cotman CW. DNA damage and apoptosis in Alzheimer's disease: colocalization with c-Jun immunoreactivity, relationship to brain area, and effect of postmortem delay. J Neurosci. (1996) 16:1710-9.

Aoyama K, Matsubara K, Fujikawa Y, Nagahiro Y, Shimizu K, Umegae N, Hayase N, Shiono H, Kobayashi S. Nitration of manganese superoxide dismutase in cerebrospinal fluids is a marker for peroxynitrite-mediated oxidative stress in neurodegenerative diseases. Ann Neurol. (2000) 47:524-7.

Armstrong RC, Aja T, Xiang J, Gaur S, Krebs JF, Hoang K, Bai X, Korsmeyer SJ, Karanewsky DS, Fritz LC, Tomaselli KJ. Fas-induced activation of the cell death-related protease CPP32 Is inhibited by Bcl-2 and by ICE family protease inhibitors. J Biol Chem. (1996) 271:16850-5.

Armstrong RC, Aja TJ, Hoang KD, Gaur S, Bai X, Alnemri ES, Litwack G, Karanewsky DS, Fritz LC, Tomaselli KJ. Activation of the CED3/ICE-related protease CPP32 in cerebellar granule neurons undergoing apoptosis but not necrosis. J Neurosci. (1997) 17:553-62.

Artal-Sanz M, Tavernarakis N. Proteolytic mechanisms in necrotic cell death and neurodegeneration. FEBS Lett. (2005) 579:3287-96.

Ballesteros M, Fredriksson A, Henriksson J, Nystrom T. Bacterial senescence: protein oxidation in non-proliferating cells is dictated by the accuracy of the ribosomes. EMBO J. (2001) 20:5280-9.

Bano D, Young KW, Guerin CJ, Lefeuvre R, Rothwell NJ, Naldini L, Rizzuto R, Carafoli E, Nicotera P. Cleavage of the plasma membrane Na+/Ca2+ exchanger in excitotoxicity. Cell. (2005) 120:275-85.

Beaman-Hall CM, Leahy JC, Benmansour S, Vallano ML. Glia modulate NMDA-mediated signaling in primary cultures of cerebellar granule cells. J Neurochem. (1998) 71:1993-2005.

Bennett V, Gilligan DM. The spectrin-based membrane skeleton and micron-scale organization of the plasma membrane. Annu Rev Cell Biol. (1993) 9:27-66.

Benowitz LI, Routtenberg A. GAP-43: an intrinsic determinant of neuronal development and plasticity. Trends Neurosci. (1997) 20:84-91.

Benuck M, Banay-Schwartz M, DeGuzman T, Lajtha A. Changes in brain protease activity in aging. J Neurochem. (1996) 67:2019-29.

Bernath E, Kupina N, Liu MC, Hayes RL, Meegan C, Wang KK. Elevation of cytoskeletal protein breakdown in aged Wistar rat brain. Neurobiol Aging. (2006) 27:624-32.

Bhat NR, Zhang P. Hydrogen peroxide activation of multiple mitogen-activated protein kinases in an oligodendrocyte cell line: role of extracellular signal-regulated kinase in hydrogen peroxide-induced cell death. J Neurochem. (1999) 72:112-9.

Biernat J, Gustke N, Drewes G, Mandelkow EM, Mandelkow E. Phosphorylation of Ser262 strongly reduces binding of tau to

microtubules:distinction between PHF-like immunoreactivity and microtubule binding. Neuron. (1993) 11:153-63.

Bjorklund H, Eriksdotter-Nilsson M, Dahl D, Rose G, Hoffer B, Olson L. Image analysis of GFA-positive astrocytes from adolescence to senescence. Exp Brain Res. (1985) 58:163-70.

Blackburn EH. The end of the (DNA) line. Nat Struct Biol. (2000) 7:847-50.

Bonifati V, Rizzu P, van Baren MJ, Schaap O, Breedveld GJ, Krieger E, Dekker MC, Squitieri F, Ibanez P, Joosse M, van Dongen JW, Vanacore N, van Swieten JC, Brice A, Meco G, van Duijn CM, Oostra BA, Heutink P. Mutations in the DJ-1 gene associated with autosomal recessive early-onset parkinsonism. Science. (2003) 299:256-9.

Brewer GJ, Reichensperger JD, Brinton RD. Prevention of age-related dysregulation of calcium dynamics by estrogen in neurons. Neurobiol Aging. (2006) 27:306-17.

Butterfield DA, Castegna A, Lauderback CM, Drake J. Evidence that amyloid beta-peptide-induced lipid peroxidation and its sequelae in Alzheimer's disease brain contribute to neuronal death. Neurobiol Aging. (2002) 23:655-64.

Cadenas E, Davies KJ. Mitochondrial free radical generation, oxidative stress, and aging. Free Radic Biol Med. (2000) 29:222-30.

Calabresi P, De Murtas M, Pisani A, Stefani A, Sancesario G, Mercuri NB, Bernardi G. Vulnerability of medium spiny striatal neurons to glutamate: role of Na+/K+ ATPase. Eur J Neurosci. (1995) 7:1674-83.

Campisi, J. Cancer, aging and cellular senescence. In Vivo (2000) 14:183–188.

Canitano A, Papa M, Boscia F, Castaldo P, Sellitti S, Taglialatela M, Annunziato L. Brain distribution of the Na+/Ca2+ exchanger-encoding genes NCX1, NCX2, and NCX3 and their related proteins in the central nervous system. Ann N Y Acad Sci. (2002) 976:394-404.

Carrard G, Bulteau AL, Petropoulos I, Friguet B. Impairment of proteasome structure and function in aging. Int J Biochem Cell Biol. (2002) 34:1461-74.

Carrell, A., On the permanent life of tissues outside of the organism. J. Exp. Med. (1912) 15, 516-528.

Cheng C, Fass DM, Reynolds IJ. Emergence of excitotoxicity in cultured forebrain neurons coincides with larger glutamate-stimulated [Ca(2+)](i) increases and NMDA receptor mRNA levels. Brain Res. (1999) 849:97-108.

Chiu CP, Harley CB. Replicative senescence and cell immortality: the role of telomeres and telomerase. Proc Soc Exp Biol Med. (1997) 214:99-106.

Choi DW. Excitotoxic cell death. J Neurobiol. 1992 Nov;23(9):1261-76.

Citron M. Strategies for disease modification in Alzheimer's disease. Nat Rev Neurosci. (2004) 5:677-85.

Conley KE, Jubrias SA, Esselman PC. Oxidative capacity and ageing in human muscle. J Physiol. (2000) 1:203-10.

Contestabile A. Cerebellar granule cells as a model to study mechanisms of neuronal apoptosis or survival in vivo and in vitro. Cerebellum. (2002) 1:41-55.

Cryns V, Yuan J. Proteases to die for. Genes Dev. (1998) 12:1551-70.

Cutler RG. Peroxide-producing potential of tissues: inverse correlation with longevity of mammalian species. Proc Natl Acad Sci U S A. (1985) 82:4798-802.

Davis RJ. The mitogen-activated protein kinase signal transduction pathway. J Biol Chem. (1993) 268:14553-6.

Dawson T, Mandir A, Lee M. Animal models of PD: pieces of the same puzzle? Neuron. (2002) 35:219-22.

Dawson TM, Dawson VL. Neuroprotective and neurorestorative strategies for Parkinson's disease. Nat Neurosci. (2002) 5 Suppl:1058-61.

Dawson TM, Dawson VL. Rare genetic mutations shed light on the pathogenesis of Parkinson disease. J Clin Invest. (2003) 111:145-51.

Denham Harman, Aging: A Theory Based on Free Radical and Radiation Chemistry. J. Gerontol. (1956) 11, 298-300

Derkinderen P, Enslen H, Girault JA. The ERK/MAP-kinases cascade in the nervous system. Neuroreport. (1999) 10:R24-34.

Dexter DT, Carter CJ, Wells FR, Javoy-Agid F, Agid Y, Lees A, Jenner P, Marsden CD. Basal lipid peroxidation in substantia nigra is increased in Parkinson's disease. J Neurochem. (1989) 52:381-9.

Dimri GP, Lee X, Basile G, Acosta M, Scott G, Roskelley C, Medrano EE, Linskens M, Rubelj I, Pereira-Smith O, et al. A biomarker that identifies senescent human cells in culture and in aging skin in vivo. Proc Natl Acad Sci U S A. (1995) 92:9363-7.

D'Mello SR, Galli C, Ciotti T, Calissano P. Induction of apoptosis in cerebellar granule neurons by low potassium:inhibition of death by insulin-like growth factor I and cAMP. Proc Natl Acad Sci U S A. (1993) 90:10989-93.

Drew B, Leeuwenburgh C. Method for measuring ATP production in isolated mitochondria: ATP production in brain and liver mitochondria of Fischer-344 rats with age and caloric restriction. Am J Physiol Regul Integr Comp Physiol. (2003) 285:R1259-67.

Duan W, Guo Z, Mattson MP. Brain-derived neurotrophic factor mediates an excitoprotective effect of dietary restriction in mice. J Neurochem. (2001) 76:619-26.

Duffy PH, Feuers RJ, Leakey JA, Nakamura K, Turturro A, Hart RW. Effect of chronic caloric restriction on physiological variables related to energy metabolism in the male Fischer 344 rat. Mech Ageing Dev. (1989) 48:117-33.

Earnshaw WC, Martins LM, Kaufmann SH. Mammalian caspases: structure, activation, substrates, and functions during apoptosis. Annu Rev Biochem. (1999) 68:383-424.

Enari M, Sakahira H, Yokoyama H, Okawa K, Iwamatsu A, Nagata S. A caspase-activated DNase that degrades DNA during apoptosis, and its inhibitor ICAD. Nature. (1998) 391:43-50.

Erler JT, Cawthorne CJ, Williams KJ, Koritzinsky M, Wouters BG, Wilson C, Miller C, Demonacos C, Stratford IJ, Dive C. Hypoxia-mediated down-regulation of Bid and Bax in tumors occurs via hypoxia-inducible factor 1-dependent and -independent mechanisms and contributes to drug resistance. Mol Cell Biol. (2004) 24:2875-89.

Forno LS. Neuropathology of Parkinson's disease. J Neuropathol Exp Neurol. (1996) 55:259-72.

Friguet B, Bulteau AL, Chondrogianni N, Conconi M, Petropoulos I. Protein degradation by the proteasome and its implications in aging. Ann N Y Acad Sci. (2000) 908:143-54.

Gage FH. Mammalian neural stem cells. Science. (2000) 287:1433-8.

Gallo V, Ciotti MT, Coletti A, Aloisi F, Levi G. Selective release of glutamate from cerebellar granule cells differentiating in culture. Proc Natl Acad Sci U S A. (1982) 79:7919-23.

Geinisman Y, Bondareff W, Dodge JT. Hypertrophy of astroglial processes in the dentate gyrus of the senescent rat. Am J Anat. (1978) 153:537-43.

Gerhardt E, Kugler S, Leist M, Beier C, Berliocchi L, Volbracht C, Weller M, Bahr M, Nicotera P, Schulz JB. Cascade of caspase activation in potassium-deprived cerebellar granule neurons: targets for treatment with peptide and protein inhibitors of apoptosis. Mol Cell Neurosci. (2001) 17:717-31.

Gerland LM, Peyrol S, Lallemand C, Branche R, Magaud JP, Ffrench M. Association of increased autophagic inclusions labeled for beta-galactosidase with fibroblastic aging. Exp Gerontol. (2003) 38:887-95.

Giambarella U, Yamatsuji T, Okamoto T, Matsui T, Ikezu T, Murayama Y, Levine MA, Katz A, Gautam N, Nishimoto I. G protein betagamma complex-mediated apoptosis by familial Alzheimer's disease mutant of APP. EMBO J. (1997) 16:4897-907.

Goedert M, Jakes R, Spillantini MG, Hasegawa M, Smith MJ, Crowther RA. Assembly of microtubule-associated protein tau into Alzheimer-like filaments induced by sulphated glycosaminoglycans. Nature. (1996) 383:550-3.

Goedert M, Jakes R, Vanmechelen E. Monoclonal antibody AT8 recognises tau protein phosphorylated at both serine 202 and threonine 205. Neurosci Lett. (1995) 189:167-9.

Goldberg AL. Protein degradation and protection against misfolded or damaged proteins. Nature. (2003) 426:895-9.

Goll DE, Thompson VF, Li H, Wei W, Cong J. The calpain system. Physiol Rev. (2003) 83:731-801.

Good PF, Hsu A, Werner P, Perl DP, Olanow CW. Protein nitration in Parkinson's disease. J Neuropathol Exp Neurol. (1998) 57:338-42.

Grewal SS, York RD, Stork PJ. Extracellular-signal-regulated kinase signalling in neurons. Curr Opin Neurobiol. (1999) 9:544-53.

Grune T, Jung T, Merker K, Davies KJ. Decreased proteolysis caused by protein aggregates, inclusion bodies, plaques, lipofuscin, ceroid, and 'aggresomes' during oxidative stress, aging, and disease. Int J Biochem Cell Biol. (2004) 36:2519-30.

Gstraunthaler G, Seppi T, Pfaller W. Impact of culture conditions, culture media volumes, and glucose content on metabolic properties of renal epithelial cell cultures. Are renal cells in tissue culture hypoxic? Cell Physiol Biochem. (1999) 9:150-72.

Guyton KZ, Liu Y, Gorospe M, Xu Q, Holbrook NJ. Activation of mitogen-activated protein kinase by H2O2. Role in cell survival following oxidant injury. J Biol Chem. (1996) 271:4138-42.

Haldane, J. B. S., New Paths in Genetics. Allen & Unwin, London. (1941)

Harman, D. Aging: a theory based on free radical and radiation chemistry. J. Gerontol. (1956) 11, 298-300.

Harrison RG The outgrowth of the nerve fiber as a mode of protoplasmic movement. J Exp Zool (1910) 9: 787–846

Hayflick L, Moorhead PS. The serial cultivation of human diploid cell strains. Exp Cell Res. (1961) 25:585-621.

Hengartner MO. Apoptosis: corralling the corpses. Cell. (2001) 104:325-8.

Hengartner MO. The biochemistry of apoptosis. Nature. (2000) 407:770-6.

Hetman M, Kanning K, Cavanaugh JE, Xia Z. Neuroprotection by brain-derived neurotrophic factor is mediated by extracellular signal-regulated kinase and phosphatidylinositol 3-kinase. J Biol Chem. (1999) 274:22569-80.

Huang TL, O'Banion MK. Interleukin-1 beta and tumor necrosis factor-alpha suppress dexamethasone induction of glutamine synthetase in primary mouse astrocytes. J Neurochem. (1998) 71:1436-42.

Ishitani R, Sunaga K, Hirano A, Saunders P, Katsube N, Chuang DM. Evidence that glyceraldehyde-3-phosphate dehydrogenase is involved in age-induced apoptosis in mature cerebellar neurons in culture. J Neurochem. (1996) 66:928-35.

Jalenques I, Albuisson E, Despres G, Romand R. Distribution of glial fibrillary acidic protein (GFAP) in the cochlear nucleus of adult and aged rats. Brain Res. (1995) 686:223-32.

Jin LW, Saitoh T. Changes in protein kinases in brain aging and Alzheimer's disease. Implications for drug therapy. Drugs Aging. (1995) 6:136-49.

Kanai Y, Chen J, Hirokawa N. Microtubule bundling by tau proteins in vivo: analysis of functional domains. EMBO J. (1992) 11:3953-61.

Kanduc D, Mittelman A, Serpico R, Sinigaglia E, Sinha AA, Natale C, Santacroce R, Di Corcia MG, Lucchese A, Dini L, Pani P, Santacroce S, Simone S, Bucci R, Farber E. Cell death: apoptosis versus necrosis (review). Int J Oncol. (2002) 21:165-70.

Kelley MJ, David LL, Iwasaki N, Wright J, Shearer TR. alpha-Crystallin chaperone activity is reduced by calpain II in vitro and in selenite cataract. J Biol Chem. (1993) 268:18844-9.

Kim HJ, Jung KJ, Yu BP, Cho CG, Chung HY. Influence of aging and calorie restriction on MAPKs activity in rat kidney. Exp Gerontol. (2002) 37:1041-53.

Kim HS, Song MC, Kwak IH, Park TJ, Lim IK. Constitutive induction of p-Erk1/2 accompanied by reduced activities of protein phosphatases 1 and 2A and MKP3 due to reactive oxygen species during cellular senescence. J Biol Chem. (2003) 278:37497-510.

Kim JH, Auerbach JM, Rodriguez-Gomez JA, Velasco I, Gavin D, Lumelsky N, Lee SH, Nguyen J, Sanchez-Pernaute R, Bankiewicz K, McKay R. Dopamine neurons derived from embryonic stem cells function in an animal model of Parkinson's disease. Nature. (2002) 418:50-6.

Kitada T, Asakawa S, Hattori N, Matsumine H, Yamamura Y, Minoshima S, Yokochi M, Mizuno Y, Shimizu N. Mutations in the parkin gene cause autosomal recessive juvenile parkinsonism. Nature. (1998) 392:605-8.

Kordower JH, Emborg ME, Bloch J, Ma SY, Chu Y, Leventhal L, McBride J, Chen EY, Palfi S, Roitberg BZ, Brown WD, Holden JE, Pyzalski R, Taylor MD, Carvey P, Ling Z, Trono D, Hantraye P, Deglon N, Aebischer P. Neurodegeneration prevented by lentiviral vector delivery of GDNF in primate models of Parkinson's disease. Science. (2000) 290:767-73.

Koubova J, Guarente L. How does calorie restriction work? Genes Dev. (2003) 17:313-21.

Kummer JL, Rao PK, Heidenreich KA. Apoptosis induced by withdrawal of trophic factors is mediated by p38 mitogen-activated protein kinase. J Biol Chem. (1997) 272:20490-4.

Kurz DJ, Decary S, Hong Y, Erusalimsky JD. Senescence-associated (beta)-galactosidase reflects an increase in lysosomal mass during replicative ageing of human endothelial cells. J Cell Sci. (2000) 113:3613-22.

Lang AE, Lozano AM. Parkinson's disease. First of two parts. N Engl J Med. (1998) 339:1044-53.

LeBel CP, Bondy SC. Oxidative damage and cerebral aging. Prog Neurobiol. (1992) 38:601-9.

Lee CK, Weindruch R, Prolla TA. Gene-expression profile of the ageing brain in mice. Nat Genet. 2000 Jul;25(3):294-7.

Lee MS, Kwon YT, Li M, Peng J, Friedlander RM, Tsai LH. Neurotoxicity induces cleavage of p35 to p25 by calpain. Nature. (2000) 405:360-4.

Leist M, Jaattela M. Four deaths and a funeral: from caspases to alternative mechanisms. Nat Rev Mol Cell Biol. (2001) 2:589-98.

Lesuisse C, Martin LJ. Immature and mature cortical neurons engage different apoptotic mechanisms involving caspase-3 and the mitogen-activated protein kinase pathway. J Cereb Blood Flow Metab. (2002) 22:935-50.

Levine RL, Garland D, Oliver CN, Amici A, Climent I, Lenz AG, Ahn BW, Shaltiel S, Stadtman ER. Determination of carbonyl content in oxidatively modified proteins. Methods Enzymol. (1990) 186:464-78.

Li B, Dou QP. Bax degradation by the ubiquitin/proteasome-dependent pathway: involvement in tumor survival and progression. Proc Natl Acad Sci U S A. (2000) 97:3850-5.

Li D, Sun F, Wang K. Caloric restriction retards age-related changes in rat retina. Biochem Biophys Res Commun. (2003) 309:457-63.

Li P, Nijhawan D, Budihardjo I, Srinivasula SM, Ahmad M, Alnemri ES, Wang X. Cytochrome c and dATP-dependent formation of Apaf-1/caspase-9 complex initiates an apoptotic protease cascade. Cell. (1997) 91:479-89.

Liu Z, Stafstrom CE, Sarkisian M, Tandon P, Yang Y, Hori A, Holmes GL. Age-dependent effects of glutamate toxicity in the hippocampus. Brain Res Dev Brain Res. (1996) 97:178-84.

Lu T, Pan Y, Kao SY, Li C, Kohane I, Chan J, Yankner BA. Gene regulation and DNA damage in the ageing human brain. Nature. (2004) 429:883-91.

Marcotte R, Lacelle C, Wang E. Senescent fibroblasts resist apoptosis by downregulating caspase-3. Mech Ageing Dev. (2004) 125:777-83.

Marini AM, Ueda Y, June CH. Intracellular survival pathways against glutamate receptor agonist excitotoxicity in cultured neurons. Intracellular calcium responses. Ann N Y Acad Sci. 1999 890:421-37.

Marks JD, Bindokas VP, Zhang XM. Maturation of vulnerability to excitotoxicity: intracellular mechanisms in cultured postnatal hippocampal neurons. Brain Res Dev Brain Res. (2000) 124:101-16.

Martin SJ, O'Brien GA, Nishioka WK, McGahon AJ, Mahboubi A, Saido TC, Green DR. Proteolysis of fodrin (non-erythroid spectrin) during apoptosis. J Biol Chem. (1995) 270:6425-8.

Masu M, Tanabe Y, Tsuchida K, Shigemoto R, Nakanishi S. Sequence and expression of a metabotropic glutamate receptor. Nature. (1991) 349:760-5.

Mattson MP. Calcium as sculptor and destroyer of neural circuitry.Exp Gerontol. (1992) 27:29-49.

Mattson MP. Cellular actions of beta-amyloid precursor protein and its soluble and fibrillogenic derivatives. Physiol Rev. (1997) 77:1081-132.

Mattson MP. Gene-diet interactions in brain aging and neurodegenerative disorders. Ann Intern Med. (2003)139:441-4.

McCay, C., Crowell, M. & Maynard, L. The effect of retarded growth upon the length of life span and upon the ultimate body size. J. Nutr. (1935) 10: 63–79.

Micheau O, Tschopp J. Induction of TNF receptor I-mediated apoptosis via two sequential signalling complexes. Cell. (2003) 114:181-90.

Milgram NW, Head E, Zicker SC, Ikeda-Douglas C, Murphey H, Muggenberg BA, Siwak CT, Tapp PD, Lowry SR, Cotman CW. Long-term treatment with antioxidants and a program of behavioral enrichment reduces age-dependent impairment in discrimination and reversal learning in beagle dogs. Exp Gerontol. (2004) 39:753-65.

Mochizuki H, Goto K, Mori H, Mizuno Y. Histochemical detection of apoptosis in Parkinson's disease. J Neurol Sci. (1996) 137:120-3.

Monaghan DT, Bridges RJ, Cotman CW. The excitatory amino acid receptors: their classes, pharmacology, and distinct properties in the function of the central nervous system. Annu Rev Pharmacol Toxicol. (1989) 29:365-402.

Morley A. Somatic mutation and aging. Ann N Y Acad Sci. (1998) 854:20-2.

Mouatt-Prigent A, Karlsson JO, Agid Y, Hirsch EC. Increased M-calpain expression in the mesencephalon of patients with Parkinson's disease but not in other neurodegenerative disorders involving the mesencephalon: a role in nerve cell death? Neuroscience. (1996) 73:979-87.

Murray B, Alessandrini A, Cole AJ, Yee AG, Furshpan EJ. Inhibition of the p44/42 MAP kinase pathway protects hippocampal neurons in a cell-culture model of seizure activity. Proc Natl Acad Sci U S A. (1998) 95:11975-80.

Nagata S. Apoptotic DNA fragmentation. Exp Cell Res. (2000) 256:12-8.

Nakanishi S. Molecular diversity of glutamate receptors and implications for brain function. Science. (1992) 258:597-603.

Nath R, Raser KJ, Stafford D, Hajimohammadreza I, Posner A, Allen H, Talanian RV, Yuen P, Gilbertsen RB, Wang KK. Non-erythroid alpha-spectrin breakdown by calpain and interleukin 1 beta-converting-enzyme-like protease(s) in apoptotic cells: contributory roles of both protease families in neuronal apoptosis. Biochem J. (1996) 319:683-90.

Nicholson DW, Ali A, Thornberry NA, Vaillancourt JP, Ding CK, Gallant M, Gareau Y, Griffin PR, Labelle M, Lazebnik YA, et al. Identification and inhibition of the ICE/CED-3 protease necessary for mammalian apoptosis. Nature. (1995) 376:37-43.

Nicoletti F, Wroblewski JT, Novelli A, Alho H, Guidotti A, Costa E. The activation of inositol phospholipid metabolism as a signal-transducing system for excitatory amino acids in primary cultures of cerebellar granule cells. J Neurosci. (1986) 6:1905-11.

Nystrom T. Role of oxidative carbonylation in protein quality control and senescence. EMBO J. (2005) 24:1311-7.

Oddo S, Billings L, Kesslak JP, Cribbs DH, LaFerla FM. Abeta immunotherapy leads to clearance of early, but not late, hyperphosphorylated tau aggregates via the proteasome. Neuron. (2004) 43:321-32.

Oppenheim RW. Cell death during development of the nervous system. Annu Rev Neurosci. (1991);14:453-501.

Orgel LE. The maintenance of the accuracy of protein synthesis and its relevance to aging. Proceedings of the National Academy of Science USA (1963) 49: 517-21.

Orlowski M. The multicatalytic proteinase complex, a major extralysosomal proteolytic system. Biochemistry. (1990) 29:10289-97.

Otvos L Jr, Feiner L, Lang E, Szendrei GI, Goedert M, Lee VM. Monoclonal antibody PHF-1 recognizes tau protein phosphorylated at serine residues 396 and 404. J Neurosci Res. (1994) 39:669-73.

Pappolla MA, Omar RA, Kim KS, Robakis NK. Immunohistochemical evidence of oxidative [corrected] stress in Alzheimer's disease. Am J Pathol. (1992) 140:621-8.

Partridge L, Gems D. Mechanisms of ageing: public or private? Nat Rev Genet. (2002) 3:165-75.

Pedersen WA, Fu W, Keller JN, Markesbery WR, Appel S, Smith RG, Kasarskis E, Mattson MP. Protein modification by the lipid peroxidation product 4-hydroxynonenal in the spinal cords of amyotrophic lateral sclerosis patients. Ann Neurol. (1998) 44:819-24.

Phaneuf S, Leeuwenburgh C. Cytochrome c release from mitochondria in the aging heart: a possible mechanism for apoptosis with age. Am J Physiol Regul Integr Comp Physiol. (2002) 282:R423-30.

Philipson KD, Nicoll DA, Ottolia M, Quednau BD, Reuter H, John S, Qiu Z. The Na+/Ca2+ exchange molecule: an overview. Ann N Y Acad Sci. (2002) 976:1-10.

Pin JP, Duvoisin R. The metabotropic glutamate receptors: structure and functions. Neuropharmacology. (1995) 34:1-26.

Pizzi M, Valerio A, Belloni M, Arrighi V, Alberici A, Liberini P, Spano P, Memo M. Differential expression of fetal and mature tau isoforms in primary cultures of rat cerebellar granule cells during differentiation in vitro. Brain Res Mol Brain Res. (1995) 34:38-44.

Polymeropoulos MH, Lavedan C, Leroy E, Ide SE, Dehejia A, Dutra A, Pike B, Root H, Rubenstein J, Boyer R, Stenroos ES, Chandrasekharappa S, Athanassiadou A, Papapetropoulos T, Johnson WG, Lazzarini AM, Duvoisin RC, Di Iorio G, Golbe LI, Nussbaum RL. Mutation in the alpha-synuclein gene identified in families with Parkinson's disease. Science. (1997) 276:2045-7.

Ramakrishna R, Edwards JS, McCulloch A, Palsson BO. Flux-balance analysis of mitochondrial energy metabolism: consequences of systemic stoichiometric constraints. Am J Physiol Regul Integr Comp Physiol. (2001) 280:R695-704.

Rao MS, Mattson MP. Stem cells and aging: expanding the possibilities. Mech Ageing Dev. (2001) 122:713-34.

Ray SK, Fidan M, Nowak MW, Wilford GG, Hogan EL, Banik NL. Oxidative stress and Ca2+ influx upregulate calpain and induce apoptosis in PC12 cells. Brain Res. (2000) 852:326-34.

Reed JC, Zha H, Aime-Sempe C, Takayama S, Wang HG. Structure-function analysis of Bcl-2 family proteins. Regulators of programmed cell death. Adv Exp Med Biol. (1996) 406:99-112.

Rego AC, Areias FM, Santos MS, Oliveira CR. Distinct glycolysis inhibitors determine retinal cell sensitivity to glutamate-mediated injury. Neurochem Res. (1999) 24:351-8.

Romero PJ, Salas V, Hernandez C. Calcium pump phosphoenzyme from young and old human red cells. Cell Biol Int. (2002) 26:945-9.

Roth GS, Ingram DK, Lane MA. Calorie restriction in primates: will it work and how will we know? J Am Geriatr Soc. (1999) 47:896-903.

Saido TC, Sorimachi H, Suzuki K. Calpain: new perspectives in molecular diversity and physiological-pathological involvement. FASEB J. (1994) 8:814-22.

Saido TC, Yokota M, Nagao S, Yamaura I, Tani E, Tsuchiya T, Suzuki K, Kawashima S. Spatial resolution of fodrin proteolysis in postischemic brain. J Biol Chem. (1993) 268:25239-43.

Sanchez-Martin MM, Cabezas JA. Evaluation of the activities of eight lysosomal hydrolases in sera of humans, rats and pigs of different ages. Mech Ageing Dev. (1997) 99:95-107.

Sasabe E, Tatemoto Y, Li D, Yamamoto T, Osaki T. Mechanism of HIF-1alpha-dependent suppression of hypoxia-induced apoptosis in squamous cell carcinoma cells. Cancer Sci. (2005) 96:394-402.

Satoh T, Nakatsuka D, Watanabe Y, Nagata I, Kikuchi H, Namura S. Neuroprotection by MAPK/ERK kinase inhibition with U0126 against oxidative stress in a mouse neuronal cell line and rat primary cultured cortical neurons. Neurosci Lett. (2000) 288:163-6.

Schramm M, Eimerl S, Costa E. Serum and depolarizing agents cause acute neurotoxicity in cultured cerebellar granule cells: role of the glutamate receptor responsive to N-methyl-D-aspartate. Proc Natl Acad Sci U S A. (1990) 87:1193-7.

Schulz JB, Weller M, Klockgether T. Potassium deprivation-induced apoptosis of cerebellar granule neurons: a sequential requirement for new mRNA and protein synthesis, ICE-like protease activity, and reactive oxygen species. J Neurosci. (1996) 16:4696-706.

Schulz JB, Weller M, Moskowitz MA. Caspases as treatment targets in stroke and neurodegenerative diseases. Ann Neurol. (1999) 45:421-9.

Schwarz-Benmeir N, Glaser T, Barnoy S, Kosower NS. Calpastatin in erythrocytes of young and old individuals. Biochem J. (1994) 304:365-70.

Sherer TB, Betarbet R, Greenamyre JT. Environment, mitochondria, and Parkinson's disease. Neuroscientist. (2002) 8:192-7.

Shikama N, Ackermann R, Brack C. Protein synthesis elongation factor EF-1 alpha expression and longevity in Drosophila melanogaster. Proc Natl Acad Sci U S A. (1994) 91:4199-203.

Siman R, Baudry M, Lynch G. Brain fodrin: substrate for calpain I, an endogenous calcium-activated protease. Proc Natl Acad Sci U S A. (1984) 81:3572-6.

Sitte N, Huber M, Grune T, Ladhoff A, Doecke WD, Von Zglinicki T, Davies KJ. Proteasome inhibition by lipofuscin/ceroid during postmitotic aging of fibroblasts. FASEB J. (2000b) 14:1490-8.

Sitte N, Merker K, Von Zglinicki T, Davies KJ, Grune T. Protein oxidation and degradation during cellular senescence of human BJ fibroblasts: part II--aging of nondividing cells. FASEB J. (2000a) 14:2503-10.

Smith MA, Richey Harris PL, Sayre LM, Beckman JS, Perry G. Widespread peroxynitrite-mediated damage in Alzheimer's disease. J Neurosci. (1997) 17:2653-7.

Sohal RS, Agarwal S, Candas M, Forster MJ, Lal H. Effect of age and caloric restriction on DNA oxidative damage in different tissues of C57BL/6 mice.Mech Ageing Dev. (1994a) 76:215-24.

Sohal RS, Ku HH, Agarwal S, Forster MJ, Lal H. Oxidative damage, mitochondrial oxidant generation and antioxidant defenses during aging and in response to food restriction in the mouse. Mech Ageing Dev. (1994b) 74:121-33.

Sohal RS, Weindruch R. Oxidative stress, caloric restriction, and aging. Science. (1996) 273:59-63.

Stadtman ER. Protein oxidation and aging. Science. (1992) 257:1220-4.

Starke-Reed PE, Oliver CN. Protein oxidation and proteolysis during aging and oxidative stress. Arch Biochem Biophys. (1989) 275:559-67.

Subramaniam S, Strelau J, Unsicker K. Growth differentiation factor-15 prevents low potassium-induced cell death of cerebellar granule neurons by differential regulation of Akt and ERK pathways. J Biol Chem. (2003) 278:8904-12.

Sugihara S, Mihara K, Marunouchi T, Inoue H, Namba M. Telomere elongation observed in immortalized human fibroblasts by treatment with 60Co gamma rays or 4-nitroquinoline 1-oxide. Hum Genet. (1996) 97:1-6.

Sureda FX, Gutierrez-Cuesta J, Romeu M, Mulero M, Canudas AM, Camins A, Mallol J, Pallas M. Changes in oxidative stress parameters and

neurodegeneration markers in the brain of the senescence-accelerated mice SAMP-8. Exp Gerontol. (2006) 41:360-7.

Suzuki K, Sorimachi H. A novel aspect of calpain activation. FEBS Lett. (1998) 433:1-4.

Tatar M, Bartke A, Antebi A. The endocrine regulation of aging by insulin-like signals. Science. (2003) 299:1346-51.

Taylor J, Gatchalian CL, Keen G, Rubin LL. Apoptosis in cerebellar granule neurones: involvement of interleukin-1 beta converting enzyme-like proteases. J Neurochem. (1997) 68:1598-605.

Terman A, Brunk UT. Lipofuscin. Int J Biochem Cell Biol. (2004) 36:1400-4.

Thibault O, Landfield PW. Increase in single L-type calcium channels in hippocampal neurons during aging. Science. (1996) 272:1017-20.

Thibault O, Porter NM, Chen KC, Blalock EM, Kaminker PG, Clodfelter GV, Brewer LD, Landfield PW. Calcium dysregulation in neuronal aging and Alzheimer's disease: history and new directions. Cell Calcium. (1998) 24:417-33.

Toescu EC, Verkhratsky A, Landfield PW. Ca2+ regulation and gene expression in normal brain aging. Trends Neurosci. (2004) 27:614-20.

Toescu EC, Verkhratsky A. Neuronal ageing in long-term cultures: alterations of Ca2+ homeostasis. Neuroreport. (2000) 11:3725-9.

Tsujinaka T, Kajiwara Y, Kambayashi J, Sakon M, Higuchi N, Tanaka T, Mori T. Synthesis of a new cell penetrating calpain inhibitor (calpeptin). Biochem Biophys Res Commun. (1988) 153:1201-8.

Valente EM, Abou-Sleiman PM, Caputo V, Muqit MM, Harvey K, Gispert S, Ali Z, Del Turco D, Bentivoglio AR, Healy DG, Albanese A, Nussbaum

R, Gonzalez-Maldonado R, Deller T, Salvi S, Cortelli P, Gilks WP, Latchman DS, Harvey RJ, Dallapiccola B, Auburger G, Wood NW. Hereditary early-onset Parkinson's disease caused by mutations in PINK1. Science. (2004) 304:1158-60.

van der Loo B, Bachschmid M, Labugger R, Schildknecht S, Kilo J, Hahn R, Palacios-Callender M, Luscher TF. Expression and activity patterns of nitric oxide synthases and antioxidant enzymes reveal a substantial heterogeneity between cardiac and vascular aging in the rat. Biogerontology. (2005) 6:325-34.

Weindruch R, Walford RL, Fligiel S, Guthrie D. The retardation of aging in mice by dietary restriction: longevity, cancer, immunity and lifetime energy intake. J Nutr. (1986) 116:641-54.

Weingarten MD, Lockwood AH, Hwo SY, Kirschner MW. A protein factor essential for microtubule assembly. Proc Natl Acad Sci U S A. (1975) 72:1858-62.

Weismann A Essays upon Heredity and Kindred Biological Problems. Oxford, UK: Clarendon. (1891)

Wenk GL, Pierce DJ, Struble RG, Price DL, Cork LC. Age-related changes in multiple neurotransmitter systems in the monkey brain. Neurobiol Aging. (1989) 10:11-9.

Williams RW, Herrup K. The control of neuron number. Annu Rev Neurosci. (1988) 11:423-53.

Wright WE, Shay JW. Historical claims and current interpretations of replicative aging. Nat Biotechnol. (2002) 20:682-8.

Xia Z, Dickens M, Raingeaud J, Davis RJ, Greenberg ME. Opposing effects of ERK and JNK-p38 MAP kinases on apoptosis. Science. (1995) 270:1326-31.

Xiao ZQ, Moragoda L, Jaszewski R, Hatfield JA, Fligiel SE, Majumdar AP. Aging is associated with increased proliferation and decreased apoptosis in the colonic mucosa. Mech Ageing Dev. (2001) 122:1849-64.

Xiong J, Camello PJ, Verkhratsky A, Toescu EC. Mitochondrial polarisation status and [Ca2+]i signalling in rat cerebellar granule neurones aged in vitro. Neurobiol Aging. (2004) 25:349-59.

Yang NC, Hu ML. The limitations and validities of senescence associated-beta-galactosidase activity as an aging marker for human foreskin fibroblast Hs68 cells. Exp Gerontol. (2005) 40:813-9.

Yuan J, Shaham S, Ledoux S, Ellis HM, Horvitz HR. The C. elegans cell death gene ced-3 encodes a protein similar to mammalian interleukin-1 beta-converting enzyme. Cell. (1993) 75:641-52.

Zeng BY, Medhurst AD, Jackson M, Rose S, Jenner P. Proteasomal activity in brain differs between species and brain regions and changes with age. Mech Ageing Dev. (2005) 126:760-6.

Zimprich A, Biskup S, Leitner P, Lichtner P, Farrer M, Lincoln S, Kachergus J, Hulihan M, Uitti RJ, Calne DB, Stoessl AJ, Pfeiffer RF, Patenge N, Carbajal IC, Vieregge P, Asmus F, Muller-Myhsok B, Dickson DW, Meitinger T, Strom TM, Wszolek ZK, Gasser T. Mutations in LRRK2 cause autosomal-dominant parkinsonism with pleomorphic pathology. Neuron. (2004) 44:601-7.

Zuber MX, Goodman DW, Karns LR, Fishman MC. The neuronal growth-associated protein GAP-43 induces filopodia in non-neuronal cells. Science. (1989) 244:1193-5.